SECOND AND THIRD VIRIAL COEFFICIENTS FOR LINEAR FLEXIBLE POLYMERS

A Doctoral Thesis

by

YO NAKAMURA

Submitted to the Faculty

of Science, Osaka University

February, 1992

SECOND AND THIRD VIRIAL COEFFICIENTS FOR LINEAR FLEXIBLE POLYMERS

A Doctoral Thesis

by

YO NAKAMURA

Submitted to the Faculty of Science,

Osaka University

February, 1992

Approvals

February, 1992

This thesis is approved as to

style and content by

寺本明夫

Member-in-chief

小林雅通

Member

小高忠男

Member

則末尚志

Member

足立柱一郎

Member

Acknowledgments

This work has been performed under the direction of Professor Akio Teramoto at the Department of Macromolecular Science, Faculty of Science, Osaka University. I thank Professor Akio Teramoto and Associate Professor Takashi Norisuye for their guidance, valuable discussions, and encouragement throughout the course of this work.

I wish to express my sincere thanks to Dr. Takahiro Sato for his valuable comments and also to my colleagues Kenichi Katayama and Kazutomo Akasaka for their help in experiments on polyisobutylene solutions. Thanks are extended to all the members of Teramoto's laboratory for their encouragement and friendship.

中村 洋

Yo Nakamura

Toyonaka, Osaka

February, 1992

Contents

Chapter I	Introduction	
I.1	Purposes of This Work	1
I.2	Previous Experimental Studies of A_3	4
I.3	Scope of This Work	7
Chapter II	Experimental	
II.1	Polymer Samples	11
II.2	Preparation of Solutions	14
II.3	Light Scattering Photometry	14
II.4	Specific Refractive Index Increment	17
II.5	Methods of Data Analysis	20
Chapter III	Good Solvent Systems	
III.1	Introduction	28
III.2	Results for Polystyrene in Benzene	28
III.3	Results for Polyisobutylene in Cyclohexane	40
III.4	Discussion	50

Chapter IV Theta Solvent Systems

IV.1 Introduction 60

IV.2 Results for Polystyrene in Cyclohexane 60

IV.2.1 Data Analysis 60

IV.2.2 Second Virial Coefficient and Theta Temperature 68

IV.2.3 Third Virial Coefficient 70

IV.2.4 Some Remarks 74

IV.3 Results for Polystyrene in trans-Decalin 76

IV.3.1 Second Virial Coefficient and Theta Temperature 76

IV.3.2 Third Virial Coefficient 87

IV.4 Discussion 89

Appendix A 99

Appendix B 101

Chapter V Remarks on Smoothed-Density Theories for Flexible Chains with Three-Segment Interactions

V.1 Introduction 104

V.2 Second Virial Coefficient 105

V.3 End-Distance Expansion Factor 111

V.4 Discussion 114

Appendix C 118

Chapter VI Summary and Conclusions 123

References 128

List of Abbreviations and Symbols 140

List of Publications 146

Chapter I

Introduction

I.1 Purposes of This Work

Since the pioneering work of Flory,[1] numerous studies have been made to explain the dilute-solution behavior of linear flexible polymers in terms of monomer-monomer or segment-segment interactions.[2,3] The mean-square radius of gyration $\langle S^2 \rangle$ and the second virial coefficient A_2 have been the main subjects in those investigations. The former is concerned with the interactions among segments in one chain and the latter with those among segments belonging to two different chains as well as in each chain. The current theoretical framework called two-parameter theory[2] invokes the binary cluster approximation in which any types of segment interaction are pairwise additive and thus represented by the binary cluster integral β_2:[2]

$$\beta_2 = \int (1 - e^{-W(R_{12})/k_B T}) \, dR_{12} \qquad (1.1)$$

Here, $W(R_{12})$ is the potential of mean force acting on segments 1 and 2 belonging to either one chain or

different chains, R_{12} the distance vector between the two segments, k_B the Boltzmann constant, and T the absolute temperature. The two-parameter theory further assumes that any chains obey the Gaussian statistics when $\beta_2 = 0$.[2] Experimental data for A_2 and $\langle S^2 \rangle$ accumulated before the early 1970s lent support to this theory.[2]

However, further elaboration[3] in the last two decades disclosed some experimental facts for A_2 that can hardly be explained by the two-parameter theory. Typical examples are (1) the molecular weight independent behavior[4-6] of A_2 below the theta point Θ where $A_2 = 0$ and (2) positive A_2 values[7-9] for very low molecular weight samples at the temperature at which A_2 for high molecular weight samples vanishes. For their explanation, suggestions[7,10] were given to take into account the non-Gaussian nature or stiffness of actual polymer chains and the ternary cluster integral β_3 representing the residual interaction among three segments 1, 2, and 3, where β_3 is defined by[2]

$$\beta_3 = \int (1 - e^{-W(R_{12})/k_B T})(1 - e^{-W(R_{23})/k_B T}) \times (1 - e^{-W(R_{31})/k_B T})\, dR_{12}\, dR_{23} \qquad (1.2)$$

with $R_{12} + R_{23} + R_{31} = 0$. Effects of chain stiffness

must be nontrivial for relatively short chains, but may be considered less important for long flexible chains.[3] On the other hand, little is known about the magnitude of β_3 for actual polymers, though effects of three-segment interactions on dilute-solution properties were theoretically investigated in the early days by Orofino and Flory[11] and Yamakawa[12] and recently by several groups.[13-17]

Under these circumstances, it seems significant to measure some property relating most closely to three-segment interactions and to see whether the property can be explained by the two-parameter theory. To this end, the third virial coefficient A_3 is most appropriate in that it reflects the interactions among three segments belonging to three different molecules.[18] In particular, data of A_3 at Θ may be expected to give decisive information about the validity of the binary cluster approximation, since according to this approximation, A_3 must vanish at Θ.[2,3] Thus, the present work was undertaken to determine A_3 for two typical flexible polymers, polystyrene (PS) and polyisobutylene (PIB), in good and theta solvents by precise light scattering measurements. The data of A_3 as well as those of A_2 obtained were used to check the validity or consistency of the two-parameter theories of the virial

coefficients. In connection with the experimental study of A_3, the following remarks are in order.

It was early recognized that information on A_3 is important for accurate determination of A_2.[19] Besides this practical importance, A_3 is a key parameter for understanding thermodynamic behavior of polymer solutions, especially in the crossover concentration region between dilute and concentrated solutions.[20,21] Nonetheless, its experimental determination has long been left as a challenge to the capability of experimentalists, because very accurate measurements of scattering intensities or osmotic pressures are required. In fact, as mentioned below, systematic experimental data on A_3 are limited only to those reported by Kniewske and Kulicke[22] for PS in toluene, a good solvent, and our understanding of A_3 remains far from satisfactory despite its basic as well as practical importance.

I.2 Previous Experimental Studies of A_3

Good Solvents

In the early 1950s, Bawn et al.[23] and Stockmayer and Casassa[24] attempted to estimate A_3 from their own or published osmotic pressure data of PS and PIB solu-

tions. Further attempt was made by Casassa and Stockmayer,[25] who evaluated A_3 for poly(methyl methacrylate) samples in butanone and nitroethane from light scattering measurements. It is probably fair to say that the A_3 data from these early studies have only historical value because of insufficient characterization of samples and large experimental uncertainties. A point to note is that Bawn et al. and Stockmayer and Casassa presented methods for determining A_3 from osmotic pressure or scattering intensity data.

As mentioned above, Kniewske and Kulicke[22] were the first to report systematic A_3 data. They analyzed light scattering data for toluene solutions (25°C) of PS ranging in weight-average molecular weight M_w from 5 x 10^4 to 2 x 10^7 by a curve-fitting method, with the result that $A_3 \propto M_w^{0.58}$. They also found that the reduced third virial coefficient g defined by

$$g \equiv A_3/A_2^2 M_w \qquad (1.3)$$

was about 0.33 regardless of M_w.

Very recently, Sato et al.,[26] analyzing light scattering data by the method of Bawn et al.[23] (see Chapter II), evaluated A_3 for three PS samples ($M_w \simeq 4$ x 10^4, 4 x 10^5, and 4 x 10^6) in benzene. The molecu-

lar weight dependence of A_3 they determined was similar to that reported by Kniewske and Kulicke.[22] However, Sato et al. obtained g which increased appreciably with increasing M_w, in contrast to the finding of Kniewske and Kulicke. Whether g in a given good solvent system depends on M_w or not remains to be seen.

Theta Solvents

Experimental information about A_3 at Θ was first given by Flory and Daoust[27] in 1957. These authors analyzed their osmotic pressure data for PIB in benzene in terms of the Flory-Huggins theory.[28,29] The result suggested that $A_3(\Theta)$ (A_3 at Θ) is positive but negligibly small. Two years later, Krigbaum and Geymer[30] concluded from osmotic pressure measurements that $A_3(\Theta)$ for PS in cyclohexane is essentially zero. Undoubtedly, these early thermodynamic studies played an important role in the later development of two-parameter theories.

In the mid 1970s, Vink[31] analyzed his osmotic pressure data for cyclohexane solutions of PS by the method of Stockmayer and Casassa[24] (see Chapter II), and obtained measurable $A_3(\Theta)$ values of 3×10^{-4} to 7×10^{-4} mol g^{-3} cm^6. He also showed that the theta temperature depends on molecular weight in a region

from 3.7 x 10^4 to 4.1 x 10^5. However, this was at variance with most experimental results for the PS + cyclohexane system.[32,33] Another report of non-vanishing $A_3(\Theta)$ was given by Murakami et al.,[34] who estimated $A_3(\Theta)$ for poly(chloroprene) in butanone to be 6 x 10^{-4} mol g^{-3} cm^6 by applying the Stockmayer-Casassa method to sedimentation equilibrium data.

The previous A_3 data at Θ mentioned above are at variance with one another and do not allow any definitive conclusion to be derived on the validity of the binary cluster approximation. In the previous studies, osmotic pressure was mostly used, but generally, light scattering is more appropriate to obtain accurate data.

I.3 Scope of This Work

In this work, we used PS and PIB fractions covering a broad range of molecular weight from 2 x 10^4 to 2 x 10^7. The solvent systems investigated and their qualities (i.e., good or theta solvent) are shown in Table I-1.

Chapter II following this introductory chapter describes experimental details, i.e., the preparation of PS and PIB fractions, light scattering measurements,

Table I-1

Polymer + Solvent Systems Studied
in the Present Work

System		Solvent Quality
PS[a] in benzene	(25°C)	good solvent
PIB[b] in cyclohexane	(25°C)	good solvent
PS in cyclohexane	(27 - 45°C)	theta solvent
PS in trans-decalin	(13 - 55°C)	theta solvent

[a]polystyrene, [b]polyisobutylene

and methods of data analysis for evaluating M_w, A_2, and A_3. Light scattering measurements for two good solvent systems, PS + benzene and PIB + cyclohexane, were made at 25°C, and those for theta solvent systems, PS + cyclohexane and PS + trans-decahydronaphthalene (trans-decalin), at different temperatures encompassing the theta point. For the good solvent systems, z-average mean-square radii of gyration $\langle S^2 \rangle_z$ were also determined. In this connection, we note that $\langle S^2 \rangle_z$ for PIB was studied only by Matsumoto et al.[35] twenty years ago, although that for PS was extensively studied by Yamamoto et al.,[36] Fukuda et al.,[37] and Miyaki et al.[33,38] over a very wide range of molecular weight.

Chapter III is concerned with the two good solvent systems mentioned above. First, we determine the molecular weight dependence of A_2, A_3, g, and $\langle S^2 \rangle_z$ for PS and PIB. The data of A_2 are then compared with the latest two-parameter theory of Barrett.[39] Finally, we compare the data for g with the existing two-parameter theories[24,40,41] and recently developed renormalization group theories,[42-44] and check the validity of the binary cluster approximation to g in good solvents.

The core of this thesis lies in examining whether, as the two-parameter theory requires, A_3 vanishes at Θ. Experimental results for A_2 and A_3 of the two theta solvent systems, PS in cyclohexane and trans-decalin, are presented in Chapter IV. It is shown that for both systems, A_3 and hence β_3 remain positive at the theta temperature. This demonstrates the breakdown of the binary cluster approximation and suggests that the contribution of β_3 to A_2 must be carefully considered. Thus, with the A_2 data near Θ we critically test the available theories of A_2 based on the smoothed-density model[11] and the first-order cluster expansion,[12,15] both taking β_3 into account.

Long ago, Yamakawa[12] pointed out that the smoothed-density and perturbation theories for A_2 are inconsistent unless β_3 is zero. This turned out very

serious, in that the two types of theory give different interpretations of Θ. The origin of the inconsistency is therefore investigated in Chapter V. It is shown theoretically that a few approximations widely accepted lead to serious errors. This thesis ends with Chapter VI in which the major conclusions and remarks derived from the present study are summarized.

Chapter II

Experimental

II.1 Polymer Samples

Polystyrene

Standard "monodisperse" polystyrene (PS) samples with appropriate molecular weights were chosen from our stock. They were Tosoh's F1, F4, F20, F80, F128, and F288 and Pressure Chemical's 2b and 4a. These samples were each divided into three parts by fractional precipitation with benzene as the solvent and methanol as the precipitant. The central fractions, designated below as F1-B, F4-B, F20-B, F80-B, F128-B, F288-B, 2b-B, and 4a-B, were used for the present study.

In addition to these samples, the fraction F-40B prepared by Sato et al.[26] and the ultra-high-molecular weight fractions BK2500-4, BK2500-3, and BK2500-2 prepared by Miyaki et al.[38] were also used. The weight-average molecular weights of the last three fractions determined in this work were systematically smaller than those reported by Miyaki et al.[38] (2 to 3% for fractions BK2500-4 and BK2500-3 and 15% for frac-

tion BK2500-2). The discrepancy suggested that these fractions degraded slightly during storage in a freezer. In this thesis, Miyaki's fractions BK2500-4, BK2500-3, and BK2500-2 are designated as BK2500-4', BK2500-3', and BK2500-2', respectively, to denote the difference in M_w.

Polyisobutylene

Two polyisobutylene (PIB) samples, Enjay's Vistanex L-80 and L-300, and one sample (designated here as SPP-85) obtained from Scientific Polymer Products Co. were used. The viscosity-average molecular weights M_v (in benzene at 25°C) for L-80 and L-300 were 5.8×10^5 and 3.9×10^6, respectively, and that for SPP-85 was 8.5×10^4.

Samples L-80 and L-300 were fractionated two times by the Θ column elution technique with benzene as the solvent. The column used was 120 cm in height and 6.8 cm in inner diameter. It was packed with glass beads of diameter 0.1 - 0.3 mm. From many fractions eluted, fractions designated A-22, A-42, and A-62 (from L-80), P-32, P-53, and P-62 (from L-300) were chosen. The first three fractions were further fractionally precipitated with benzene as the solvent and methanol as the precipitant to remove lower and higher molecular weight

portions. The fractions thus obtained were designated A-22B4, A-42B3, and A-62B1, and used for the present study, along with fractions P-32, P-53, and P-62. These fractions were reprecipitated from benzene solutions into acetone and dried in vacuo for about a week.

Sample SPP-85 was fractionated by the column method with a benzene-methanol mixture instead of pure benzene as the eluent; the composition of methanol in the mixture was adjusted so that the solution became turbid at about 23°C. However, a larger portion of the polymer tended to elute at a lower temperature, and the column method seemed less effective for a lower molecular weight sample. Thus, after this method had been repeated, the fractions obtained were subjected to fractional precipitation in benzene-methanol mixtures. In this way, four fractions, designated below as S-111B, S-112B, S-114B, and S-14B, were prepared. They were freeze-dried from cyclohexane solutions after being reprecipitated from benzene solutions into methanol.

Fractions S-112B, S-114B, S-14B, A-22B4, and A-42B3 were investigated by gel permeation chromatography with chloroform as the eluent. The M_w/M_n values estimated were in the range 1.08 - 1.10. Here, as usual M_n denotes the number-average molecular weight.

II.2 Preparation of Solutions

As mentioned in Chapter I, benzene (good solvent), cyclohexane (theta solvent), and trans-decalin (theta solvent) were used for PS, and cyclohexane (good solvent) for PIB. A given polymer sample and a solvent were mixed in a ground-glass-stoppered Erlenmeyer flask. The mixture was stirred for two to seven days; for high molecular weight fractions ($M_w > 5 \times 10^6$) of either PS or PIB, very gentle stirring was applied to prevent the polymer from degradation. After complete dissolution, the solution was diluted with the solvent to prepare serial solutions of six or seven different concentrations.

The benzene and cyclohexane used were refluxed over sodium for about 5 h and then fractionally distilled. The trans-decalin (manufactured by Tokyo Kasei) was similarly distilled under a reduced nitrogen atmosphere after being refluxed over calcium hydride for about 5 h. Its trans content was 99.7% when determined by gas chromatography.

II.3 Light Scattering Photometry

Intensities of light scattered from PS or PIB

solutions were measured on a Fica 50 light scattering photometer using cylindrical cells in an angular range from 12.5 to 150° with no analyzer. Vertically polarized incident light of 436 or 546 nm wavelength was used. With pure benzene as the reference liquid, the instrument constant Φ was determined from the measured scattering intensity $I_{90,Uv}$ for vertically polarized incident light at scattering angle 90°, according to the relation

$$\Phi = \frac{2R_{b,Uu}}{I_{90,Uv}\, n_b^2 (1 + \rho_u)} \qquad (2.1)$$

Here, n_b is the refractive index of benzene and $R_{b,Uu}$, its Rayleigh ratio at 90° for unpolarized incident light. For the latter, the literature values[45] 46.5 x 10^{-6} cm^{-1} and 16.1 x 10^{-6} cm^{-1} were used for 436 and 546 nm, respectively. The depolarization ratio ρ_u of benzene for unpolarized incident light was determined to be 0.41 for 436nm and 0.40 for 546nm by the method of Rubingh and Yu.[46]

The reduced scattering intensity $R_{\theta,Uv}(c)$ for a given solution with a polymer mass concentration c at scattering angle θ was calculated from

$$R_{\theta,Uv}(c) = \Phi\, I_{\theta,Uv}\, n^2 \sin\theta \qquad (2.2)$$

and the excess reduced scattering intensity R_θ was obtained as the difference in $R_{\theta,\mathrm{Uv}}(c)$ between the solution and the solvent, i.e., $R_{\theta,\mathrm{Uv}}(c) - R_{\theta,\mathrm{Uv}}(0)$. In eq. 2.2, n denotes the refractive index of the solution.

Test solutions were made optically clean by centrifugation at about 3×10^4 gravities for 1.5 h. Each of them was transferred into a light scattering cell using a pipet. The cell and the pipet had been rinsed with refluxing acetone vapor for about 6 h.

For PS in benzene and PIB in cyclohexane, both good solvent systems, c in each solution was calculated from the polymer weight fraction w, with the solution density ρ approximated by the solvent density ρ_0. This approximation introduced errors less than 1% in the values of A_2 and A_3 for any fractions.

It was anticipated, however, that the approximation ceases to be good for PS in cyclohexane and trans-decalin, theta solvents. Thus, c in each cyclohexane solution was calculated, using Scholte's data[47] for ρ; desired densities at different temperatures were obtained by interpolation or extrapolation of his data. On the other hand, no ρ data for trans-decalin solutions of PS were available in the literature, so that

we made density measurements at 21 and 35°C using a bicapillary picnometer of 30 cm^3 capacity. Use was made of fraction F-40B. Figure 2.1 illustrates the concentration dependence of ρ thus determined. The curves fitting the experimental points at the respective T are represented by

$$\rho = 0.86877 + 0.190c + 0.15c^2 \quad (21^{\circ}C) \qquad (2.3)$$

$$\rho = 0.85830 + 0.193c + 0.15c^2 \quad (35^{\circ}C) \qquad (2.4)$$

The necessary values of ρ at different T were obtained by interpolation or extrapolation.

II.4 Specific Refractive Index Increment

Excess refractive indices Δn for PS in benzene and PIB in cyclohexane, both at 25°C, and PS in trans-decalin at 21, 25, 35, and 45°C were measured as functions of w or c using a modified Schulz-Cantow type differential refractometer. The results for PS (F20-B) in benzene at 546 nm are illustrated in Figure 2.2. The indicated curve represents the empirical relation

$$\Delta n = 0.0931w + 0.015w^2 \qquad (w < 0.08) \qquad (2.5)$$

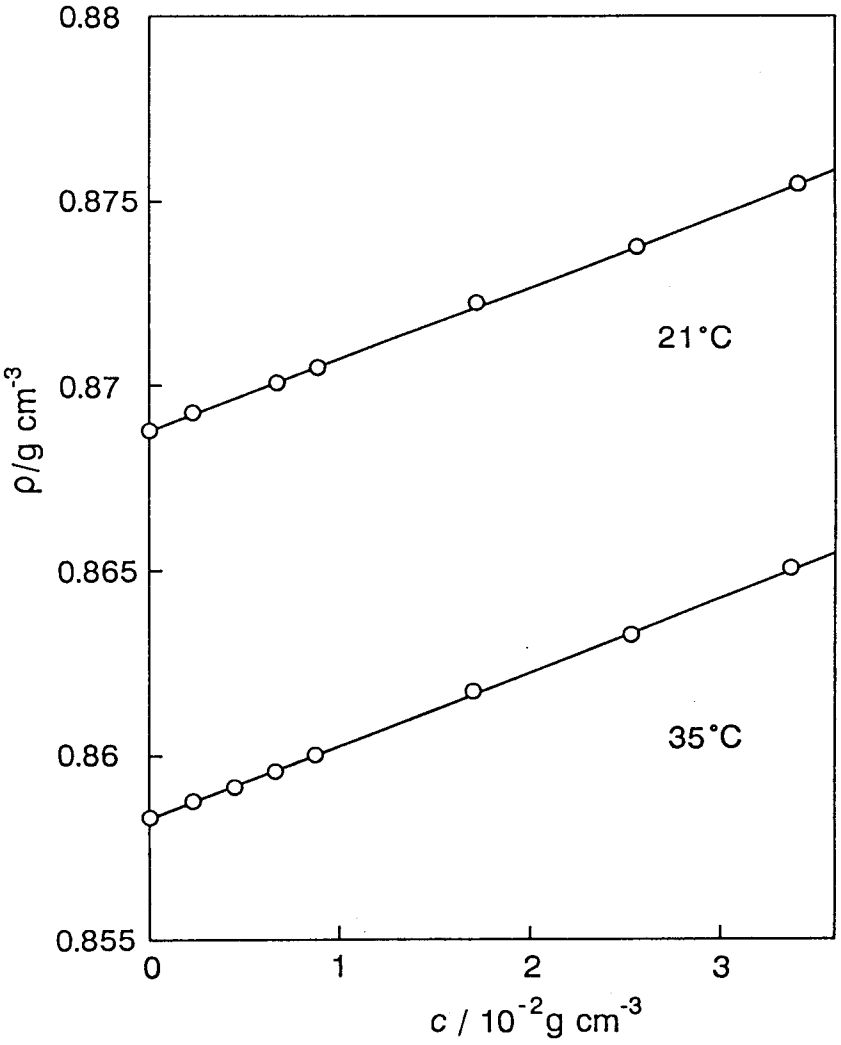

Figure 2.1 Concentration dependence of solution density ρ for PS in trans-decalin at indicated temperatures.

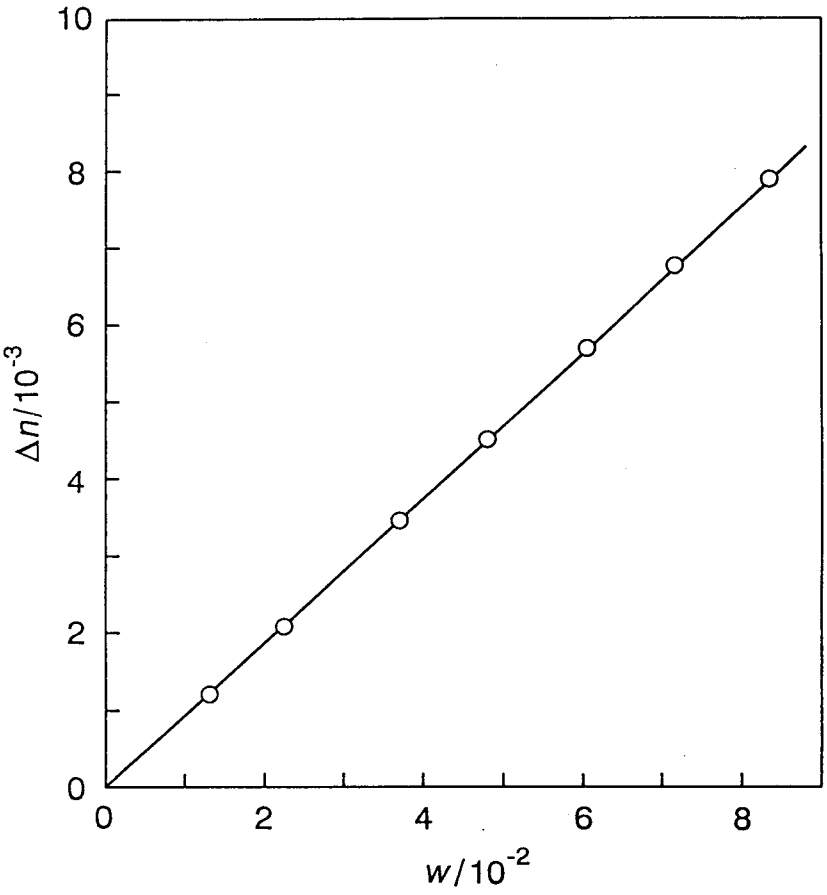

Figure 2.2 Concentration dependence of excess refractive index Δn for PS in benzene at 25°C and 546 nm.

which yields for the specific refractive index increment $\partial n/\partial c$ in units of cm^3g^{-1}

$$\partial n/\partial c = 0.1066 - 0.008c \qquad (2.6)$$

(PS in benzene at 25°C and 546 nm; $c < 0.07$ g cm^{-3})

when the literature values of 0.8737 g cm^{-3} and 0.917 cm^3 g^{-1} are used for ρ_0 and the partial specific volume[48] of PS in benzene at 25 °C, respectively.

The values of $\partial n/\partial c$ for PIB in cyclohexane at 25°C were similarly determined to be 0.0991 and 0.0966 cm^3 g^{-1} at 436 and 546 nm, respectively, regardless of c below 2 x 10^{-2} g cm^{-3}. These values agree closely with 0.0987 cm^3 g^{-1} (at 436 nm) and 0.0961 cm^3 g^{-1} (at 546 nm) obtained by Tong et al.[49]

The specific refractive index increment for PS in trans-decalin as a function of T in degree centigrade was found to be represented by

$$\partial n/\partial c = 1.50 \times 10^{-4} T + 0.1224 - 0.02c \qquad (2.7)$$

(PS in trans-decalin at 546nm; $c < 0.05$ g cm^{-3})

For $\partial n/\partial c$ of PS in cyclohexane, Scholte's data[47] were used.

II.5 Methods of Data Analysis

Some Basic Equations

According to the theory[50] of light scattering from dilute polymer solutions, R_θ is expressed by

$$\frac{Kc}{R_\theta} = \frac{1}{M_w P(\theta)} + 2A_2 Q_2(\theta) c + 3A_3 Q_3(\theta) c^2 + \ldots \qquad (2.8)$$

where $P(\theta)$ is the intramolecular interference factor or the particle scattering function, $Q_i(\theta)$ (i = 2,3) is the intermolecular interference factor associated with i polymer chains, and K is the optical constant defined by

$$K = \frac{4\pi^2 n^2}{N_A \lambda_0^4} (\partial n/\partial c)^2 \qquad (2.9)$$

with N_A and λ_0 being the Avogadro constant and the wavelength of incident light in vacuum. At infinite dilution, eq 2.8 becomes

$$\left(\frac{Kc}{R_\theta}\right)_{c=0} = \frac{1}{M_w P(\theta)}$$

$$= \frac{1}{M_w}\left[1 + \frac{1}{3}\left(\frac{4\pi}{\lambda}\right)^2 \langle S^2 \rangle_z \sin^2\frac{\theta}{2} + O\left(\sin^4\frac{\theta}{2}\right)\right] \qquad (2.10)$$

where λ is the wavelength of incident light in the scattering medium.

Experimental Determination of M_w, A_2, and A_3

At the limit of θ = 0, eq. 2.8 reduces to

$$\frac{Kc}{R_0} = \frac{1}{M_w} + 2A_2c + 3A_3c^2 + \ldots \qquad (2.11)$$

where R_0 denotes R_θ at zero scattering angle. With eq 1.3 for g, this equation is rewritten

$$\left(\frac{Kc}{R_0}\right)^{1/2} = \frac{1}{M_w{}^{1/2}} \left[1 + A_2M_wc + \frac{1}{2} A_2{}^2M_w{}^2(3g - 1)c^2 + \ldots \right] \qquad (2.12)$$

The values of $(Kc/R_0)^{1/2}$ can be obtained as a function of c by extrapolation of $(Kc/R_\theta)^{1/2}$ plotted against $\sin^2(\theta/2)$ at respective c to $\theta = 0$. Then, M_w and A_2 are evaluated from the intercept and initial slope of a square-root plot of $(Kc/R_0)^{1/2}$ vs. c according to eq 2.12. This procedure has widely been used to determine M_w and A_2 of a given polymer sample, but it does not allow A_3 to be estimated.

Three methods to determine A_3 from Kc/R_0 data are available. We outline them and discuss their advantages and disadvantages.

(1) Stockmayer-Casassa Plot

Defining $S(c)$ by

$$S(c) \equiv (Kc/R_0 - 1/M_w)/c \qquad (2.13)$$

we obtain from eq 2.11

$$S(c) = 2A_2 + 3A_3c + 4A_4c^2 + \ldots \qquad (2.14)$$

where we have explicitly shown the term associated with the fourth virial coefficient A_4 for convenience in the ensuing discussion. According to eq 2.14, A_2 and A_3 can be evaluated, respectively, from the intercept and initial slope of a plot of $S(c)$ versus c, which is called the Stockmayer-Casassa (SC) plot.[24]

As can be seen from the definition of $S(c)$, this plot requires for its application an M_w value to be known in advance. The above-mentioned square-root plot may be used for this purpose, but use of the M_w determined in a different solvent is desirable in order that the values of A_2 and A_3 estimated from the SC plot in a test solvent have no correlation with the input value of M_w. Further, the M_w value has to be accurate since, as may be anticipated from eq 2.13, $S(c)$ is very susceptible to the input M_w at low concentrations. In fact, Sato et al.[26] showed for a PS sample with M_w = 4.3×10^6 in benzene that an error of only 2% in M_w gives rise to considerable, systematic deviations of plotted points at low c from the linear relation of

$S(c)$ vs. c found at high c. Thus, the Stockmayer-Casassa method is not practical in determining A_2 and A_3.

(2) Bawn Plot

Defining $S(c_1, c_2)$ by

$$S(c_1, c_2) \equiv \frac{(Kc/R_0)_{c=c_2} - (Kc/R_0)_{c=c_1}}{c_2 - c_1} \qquad (2.15)$$

we get from eq 2.11

$$S(c_1, c_2) = 2A_2 + 3A_3(c_1 + c_2) + 4A_4(c_1^2 + c_1c_2 + c_2^2) + \ldots \qquad (2.16)$$

where $(Kc/R_0)_{c=c_2}$ and $(Kc/R_0)_{c=c_1}$ denote the values of Kc/R_0 at two different concentrations c_2 and c_1, respectively. Equation 2.16 shows that the intercept and initial slope of a plot of $S(c_1, c_2)$ vs. $c_1 + c_2$ give A_2 and A_3, respectively. This plot was originally proposed by Bawn et al.[23] for osmotic pressure. It is referred to here as the Bawn plot.

We again quote the above-mentioned work of Sato et al.[26] on a PS sample with $M_w = 4.3 \times 10^6$ in benzene. These authors, making additional measurements at higher

concentrations, found that either the SC or Bawn plot bends down significantly when c or $c_1 + c_2$ exceeds a certain value. This implies that there is a "critical" concentration above which contributions of A_4 and higher virial coefficients are significant. In other words, neither $S(c)$ nor $S(c_1, c_2)$ is substantially affected by A_4 below such a concentration, and thus both plots are equally useful in principle. However, the Bawn plot has a distinct advantage over the SC plot in that no M_w value is needed for its application.

Once A_2 and A_3 for a given sample are evaluated by the Bawn plot, the value of M_w may be determined in the following way.[26] First, an apparent molecular weight M_{app} defined by

$$M_{app} = [Kc/R_0 - 2A_2c - 3A_3c^2]^{-1} \qquad (2.17)$$

is calculated as a function of c. The M_{app} values obtained are then plotted against c and extrapolated to $c = 0$ to obtain the desired M_w.

(3) Curve-Fitting Method

The values of M_w, A_2, and A_3 may also be estimated by a trial-and-error or nonlinear least-square method, in which eq 2.11 truncated at the c^2 term is forced to

fit experimental values of Kc/R_0 over a range of c. This curve-fitting procedure may be carried out easily with the help of a computer. However, since Kc/R_0 vs. c plots are generally very monotonous, it is difficult to judge from them at what concentration the contribution of A_4 starts playing a significant role. This is a serious disadvantage of the curve-fitting procedure. In fact, Norisuye and Fujita[51] have recently warned against the use of this method by showing an example that an erroneous parameter set is obtained unless the upper bound c in the three-parameter fit is adequately found.

On the basis of the above discussion, we decided to adopt the Bawn plot for the present data analysis. It may be anticipated from the definition of $S(c_1, c_2)$ that for an actual application of this plot light scattering data have to be very accurate over the range of concentration covered. In particular, small errors in Kc/R_0 are magnified in the plot when c_1 and c_2 are close to each other. In this work, care was therefore taken to prepare a series of test solutions whose concentrations were almost evenly spaced.

Determination of $\langle S^2 \rangle_z$

We determined $\langle S^2 \rangle_z$ for PS fractions in benzene and PIB fractions in cyclohexane in the following way. First, values of $(Kc/R_\theta)_{c=0}^{1/2}$ for a given fraction were obtained by extrapolating $(Kc/R_\theta)^{1/2}$ at fixed θ to infinite dilution using the square-root plot[52] of $(Kc/R_\theta)^{1/2}$ vs. c. The values of $(Kc/R_\theta)_{c=0}^{1/2}$ were then plotted versus $\sin^2(\theta/2)$ according to the equation

$$\left(\frac{Kc}{R_\theta}\right)_{c=0}^{1/2} = \frac{1}{M_w^{1/2}} \left[1 + \frac{1}{6}\left(\frac{4\pi}{\lambda}\right)^2 \langle S^2 \rangle_z \sin^2 \frac{\theta}{2} + O\left(\sin^4 \frac{\theta}{2}\right)\right] \qquad (2.18)$$

and $\langle S^2 \rangle_z$ was evaluated from the initial slope of the plot. For low molecular weight PIB fraction S-114B, $\langle S^2 \rangle_z$ was determined, using the procedure proposed by Kitagawa et al.[53] In this method, an apparent mean-square radius of gyration at finite c, which is defined as the initial slope of a $(Kc/R_\theta)^{1/2}$ vs. $\frac{1}{6}(4\pi/\lambda)^2\sin^2(\theta/2)$ plot multiplied by $M_w^{1/2}$, is first evaluated and then extrapolated to $c = 0$.

Chapter III

Good Solvent Systems

III.1 Introduction

This chapter is concerned primarily with A_2 and A_3 for PS in benzene and PIB in cyclohexane, both good solvent systems. First, we present experimental results for A_2, A_3, g (defined by eq 1.3), and $\langle S^2 \rangle_z$ of the two polymers and then discuss their molecular weight dependence. Finally, the data of A_2 and A_3 (or g) are compared with the existing theories to check the validity of the binary cluster approximation in good solvents.

III.2 Results for Polystyrene in Benzene

Figure 3.1 illustrates square-root plots of $(Kc/R_\theta)^{1/2}$ vs. $\sin^2(\theta/2)$ at fixed concentrations for PS fraction BK2500-3' in benzene at 25°C. The curves fitting the data points at the respective c bend down for $\sin^2(\theta/2)$ above 0.07, but can be accurately extrapolated to zero scattering angle.

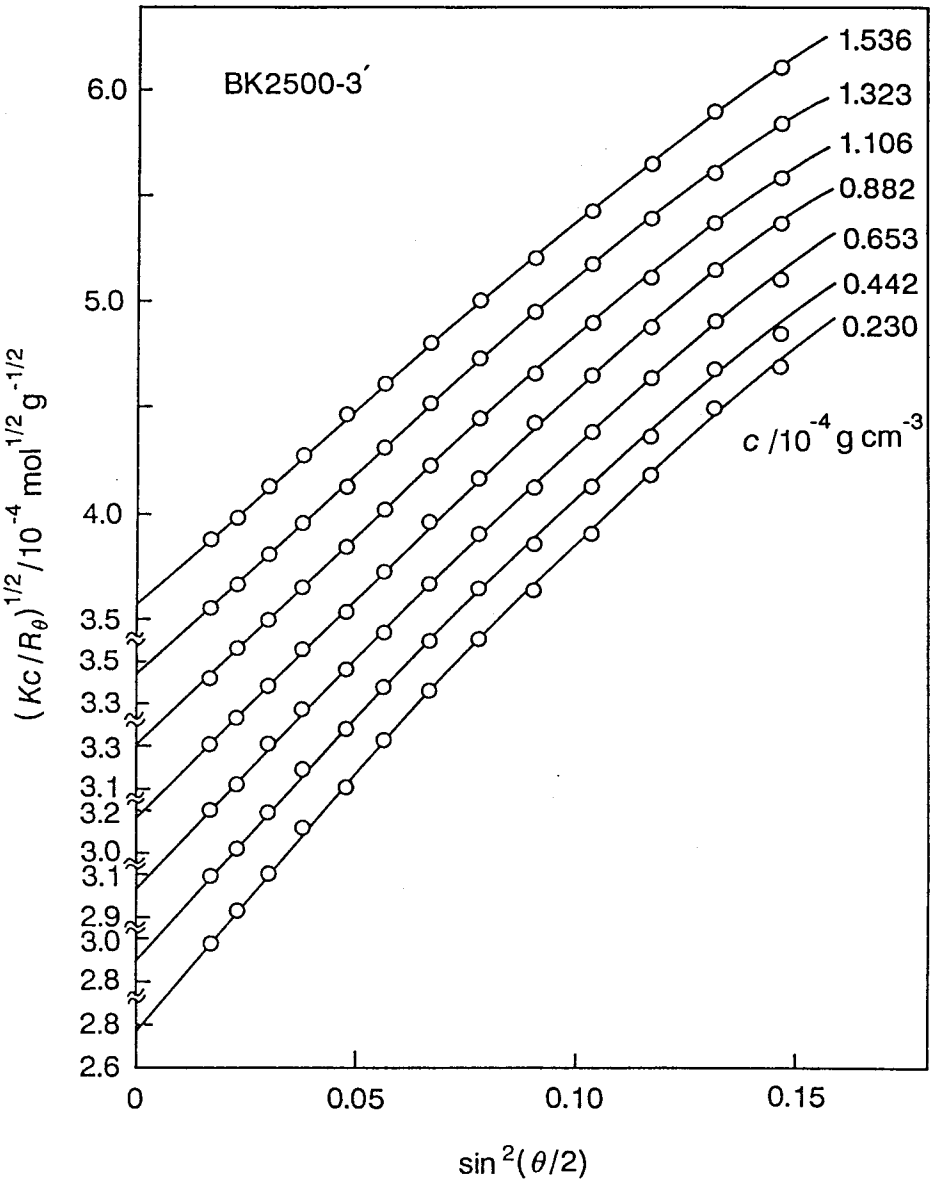

Figure 3.1 Plots of $(Kc/R_\theta)^{1/2}$ vs. $\sin^2(\theta/2)$ at indicated c for PS fraction BK2500-3' in benzene at 25°C.

The Bawn plots of $S(c_1, c_2)$ vs. $c_1 + c_2$ constructed from Kc/R_0 data for PS fractions according to eq 2.16 are shown in Figure 3.2. The plotted points for each fraction follow a straight line over the entire range of $c_1 + c_2$ studied. The intercept and slope of the line give A_2 and A_3, respectively.

We made additional measurements on fractions F80-B, F128-B, and BK2500-4' at higher concentrations. The Bawn plots constructed exhibited appreciable downward curvatures at high $c_1 + c_2$ (not shown here), as was found to be the case for a PS fraction (M_w = 4.3 x 10^6) by Sato et al.[26] These findings indicate that A_4 for polystyrene in benzene is negative. Very recently, Norisuye and Fujita,[51] analyzing the classical osmotic pressure data of Flory and Daoust,[27] found that A_4 for PIB in cyclohexane is also negative.

In Figure 3.3, values of the apparent molecular weight M_{app} defined by eq 2.17 are plotted against c. The plot for each fraction is horizontal, allowing accurate extrapolation of M_{app} to c = 0. The intercepts give the weight-average molecular weights of the respective fractions.

Numerical results for M_w, A_2, A_3, and the reduced third virial coefficient g defined by eq 1.3 are all summarized in Table III-1, where are included those for

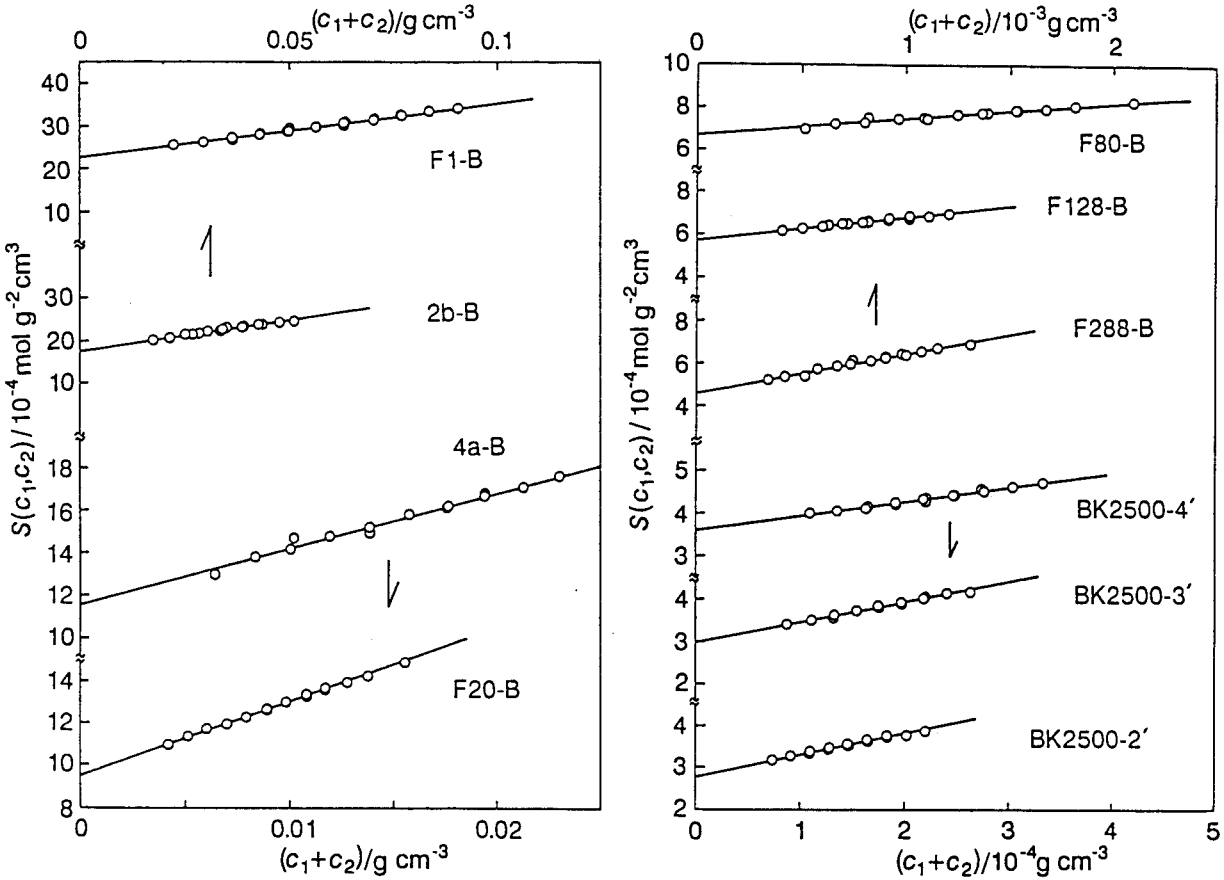

Figure 3.2 Bawn plots for the indicated PS fractions in benzene at 25°C.

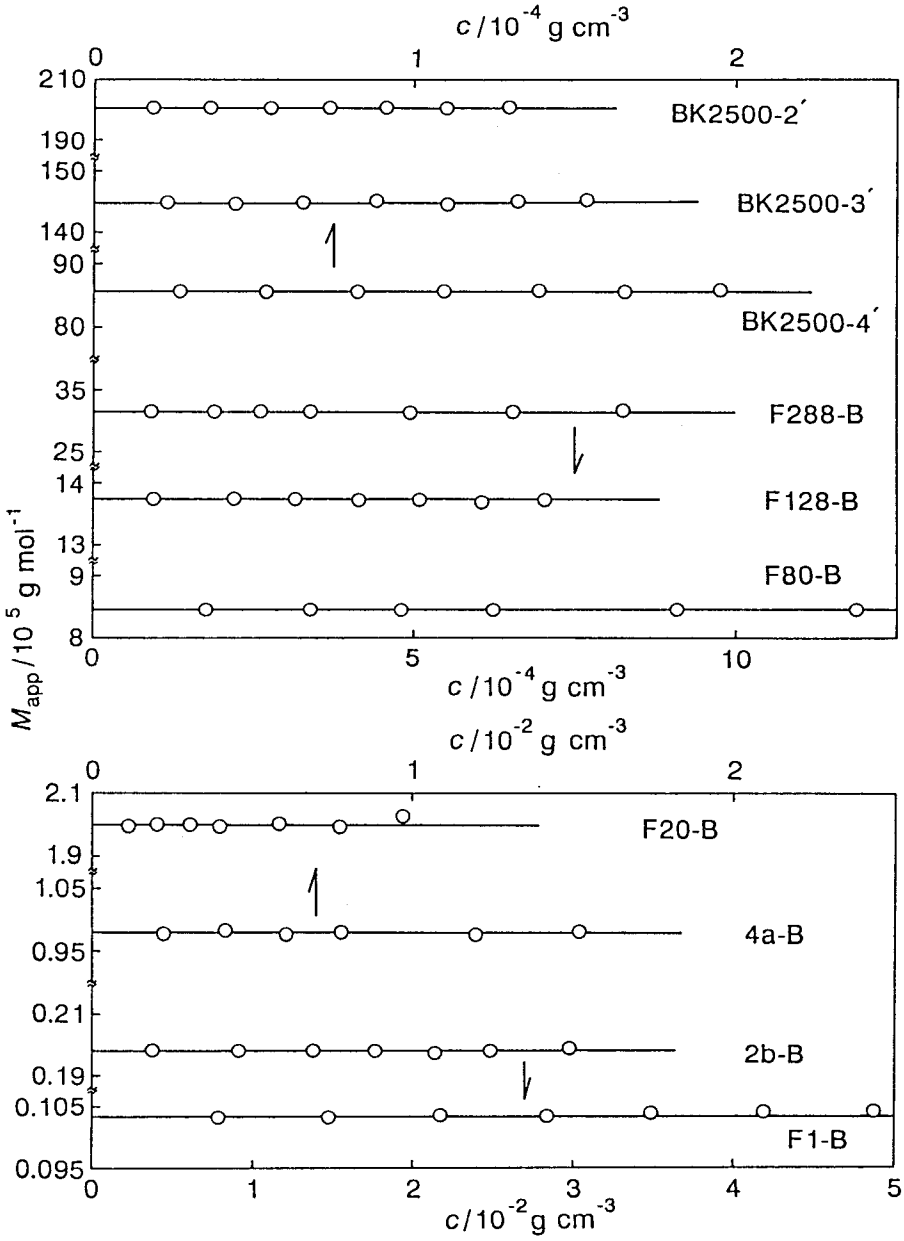

Figure 3.3 Plots of M_{app} vs. c for the indicated PS fractions in benzene at 25°C.

Table III-1

Numerical Results from Light Scattering Measurements on PS Fractions in Benzene at 25°C

Fraction	$M_w \times 10^{-5}$	$A_2 \times 10^4$ / mol g^{-2} cm^3	$A_3 \times 10^2$ / mol g^{-3} cm^6	g	$\langle S^2 \rangle_z^{1/2}$ / nm
F1-B	0.103	11.3	0.43	0.32	—
2b-B	0.198	8.80	0.48	0.31	—
F-4B[a]	0.447	7.40	0.61	0.25	—
4a-B	0.979	5.78	0.86	0.26	—
F20-B	2.00	4.72	1.1_8	0.27	17
F-40B[a]	3.79	4.10	1.9	0.30	24
F80-B	8.45	3.33	2.7	0.29	41
F128-B	13.8	2.85	3.8	0.34	54
F288-B	31.5	2.29	6.1	0.37	89
F-380B[a]	43.8	2.05	8.7	0.47	104
BK2500-4'	85.6	1.80	$11._2$	0.40	170
BK2500-3'	145	1.49	$15._8$	0.49	223
BK2500-2'	201	1.38	$17._9$	0.47	276

[a]Data of Sato et al.[26]

three fractions determined by Sato et al.[26] in the same way. The last column in the table presents the values for $\langle S^2 \rangle_z^{1/2}$.

The molecular weight dependence of A_2 is displayed by unfilled circles in Figure 3.4, in which the data of Sato et al.[26] (half-filled circles) in Table III-1 and those of Miyaki et al.[33,38] (filled circles) are also shown for comparison. The last group evaluated A_2 by the conventional square-root plot (see eq 2.12). All the data points are seen to fall on a single solid curve as indicated. Thus, we find that the two types of plot give consistent A_2 values.

The dashed line in Figure 3.4 is drawn to have a slope -0.2, which is the asymptotic exponent γ in the relation $A_2 \propto M_w^{\gamma}$ predicted by two-parameter theories[2] for long flexible chains in good solvents. The experimental curve appears to have this asymptotic slope only for $M_w > 10^7$.

The present A_3 data and those of Sato et al. in Table III-1 are plotted double-logarithmically against M_w in Figure 3.5. The data points for M_w above 10^5 are fitted by a straight line with a slope 0.6. Essentially the same slope was reported for PS in toluene by Kniewske and Kulicke,[22] who used a curve-fitting method to evaluate M_w, A_2, and A_3. The slope

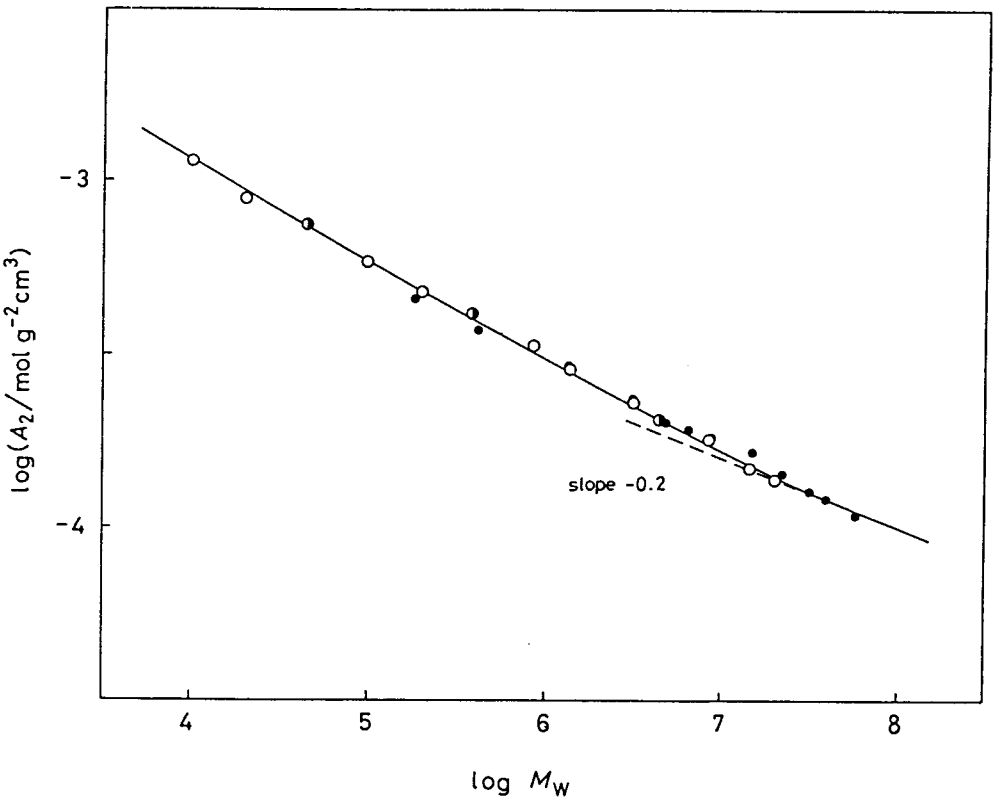

Figure 3.4 Molecular weight dependence of A_2 for PS in benzene at 25°C: (○) this work; (◑) Sato et al.;[26] (●) Miyaki et al.[33,38]

0.6 observed conforms to the asymptotic exponent for A_3 predictable from the two-parameter theory. However, it should be noted that the data points for the three lowest molecular weight fractions deviate upward from

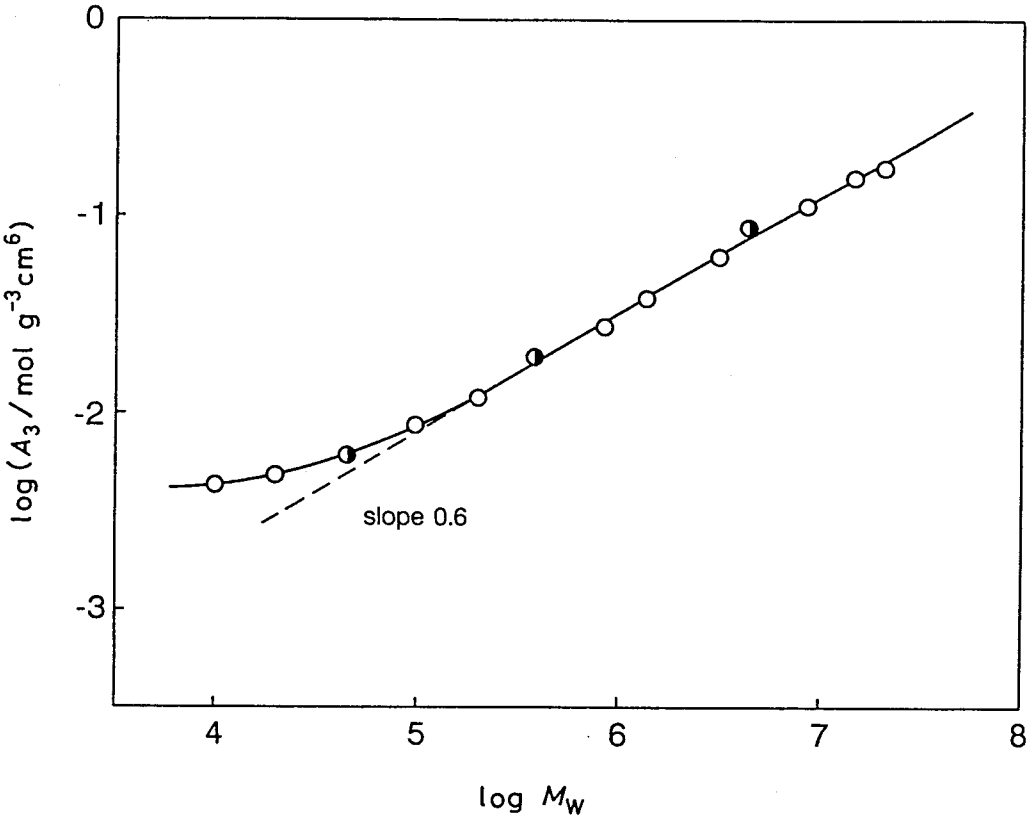

Figure 3.5 Molecular weight dependence of A_3 for PS in benzene at 25°C: (○) this work; (◑) Sato et al.[26]

the line with the slope 0.6.

The $M_W^{0.6}$ dependence of A_3 over a wide molecular weight range shown in Figure 3.5 leads us to conclude that A_3 for PS in benzene reaches the asymptotic region

at a relatively low M_w of 2 x 10^5. This is in contrast to the very slow approach of A_2 to the asymptotic relation. Because of these features of the experimental A_2 and A_3, g must increase toward an asymptotic value with increasing M_w above 2 x 10^5. In fact, our g values, which are plotted against log M_w in Figure 3.6, show this to be the case. The initial decline of the indicated curve at low M_w is due primarily to the upward deviation of A_3 from the asymptotic line with a slope 0.6 in Figure 3.5.

In contrast to the above finding, Kniewske and Kulicke[22] obtained a constant g of about 0.33 for toluene solutions of PS covering a broad range of M_w from 5 x 10^4 to 2 x 10^7. This result is consistent with their A_2 data that decreased in proportion to $M_w^{-0.21}$ in the M_w range. However, such molecular weight dependence of A_2 differs from what has been reported for flexible polymers in good solvents[3] as well as those shown in Figure 3.4. In addition, Berry's A_2 data[52] for PS in toluene vary as $M_w^{-0.25}$ throughout the range of M_w from 5.4 x 10^4 to 4.4 x 10^6 he studied.

Figure 3.7 shows that the present $\langle S^2 \rangle_z$ data for PS in benzene are consistent with those from well-documented previous studies.[26,33,36-38] All the plotted points fall on a single straight line with slope

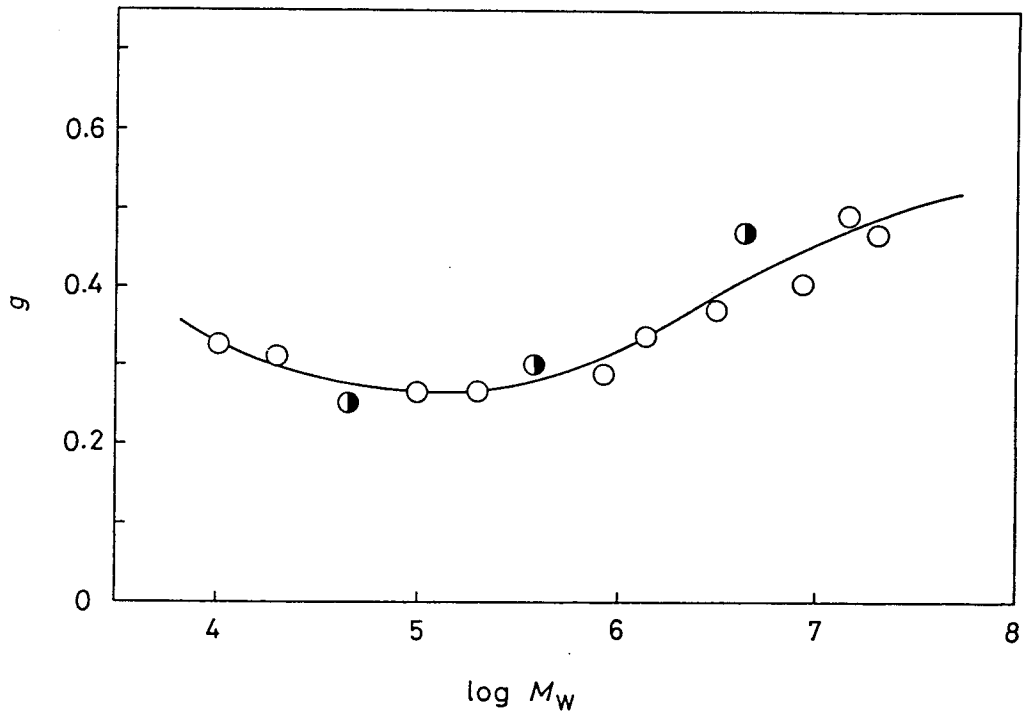

Figure 3.6 Molecular weight dependence of g for PS in benzene at 25°C. The symbols are the same as those used in Figure 3.5.

1.19 (± 0.01). This slope is just the one that has been determined by Miyaki et al.,[33,38] and is to be expected for long flexible chains with large excluded volume.[3]

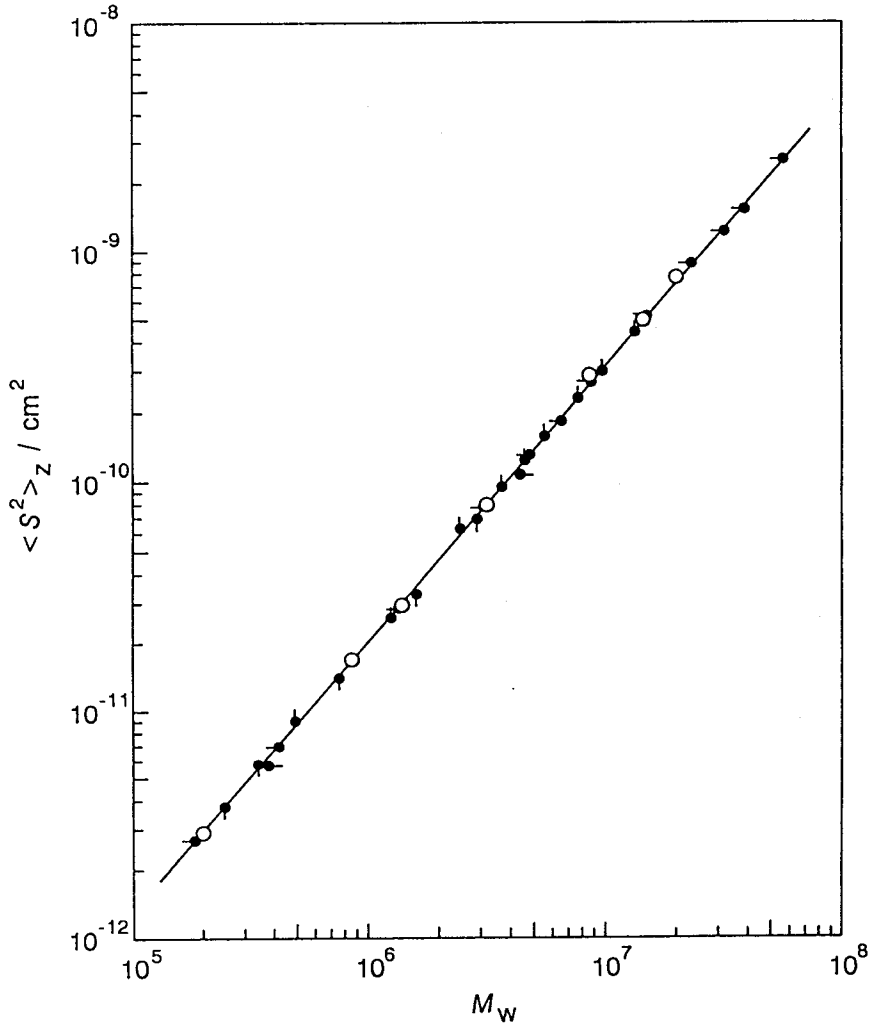

Figure 3.7 Molecular weight dependence of $\langle S^2 \rangle_z$ for PS in benzene at 25°C: (○) this work; (●) Yamamoto et al.;[36] (●) Fukuda et al.;[37] (●) Miyaki et al.;[33,38] (●) Sato et al.[26]

III.3 Results for Polyisobutylene in Cyclohexane

Analyses of light scattering data for polyisobutylene fractions in cyclohexane at 25°C are illustrated in Figures 3.8 through 3.10, and the numerical results for M_w, A_2, A_3, g, and $\langle S^2 \rangle_z^{1/2}$ are summarized in Table III-2.

Figure 3.11 shows the molecular weight dependence of A_2 for PIB in cyclohexane (the unfilled circles) in comparison with the data of Matsumoto et al.[35] (the half-filled circles) and Fetters et al.[54] (the triangles), who used the square-root plot of $(Kc/R_0)^{1/2}$ vs. c (eq 2.12) and the linear plot of Kc/R_0 vs. c (eq 2.11), respectively. The solid line fitting our data points bend slightly upward and merges with the indicated dashed line of slope -0.2 at $M_w \sim 3 \times 10^6$. The data of Matsumoto et al. are in substantial agreement with ours, but those of Fetters et al. appear slightly below them for $M_w < 4 \times 10^5$.

The molecular weight dependence of A_3 is shown in Figure 3.12. The straight line fitting the data points has a slope of 0.6, which is the same as that found above for PS in benzene for M_w above 2.5×10^5. The agreement strongly suggests that the exponent 0.6

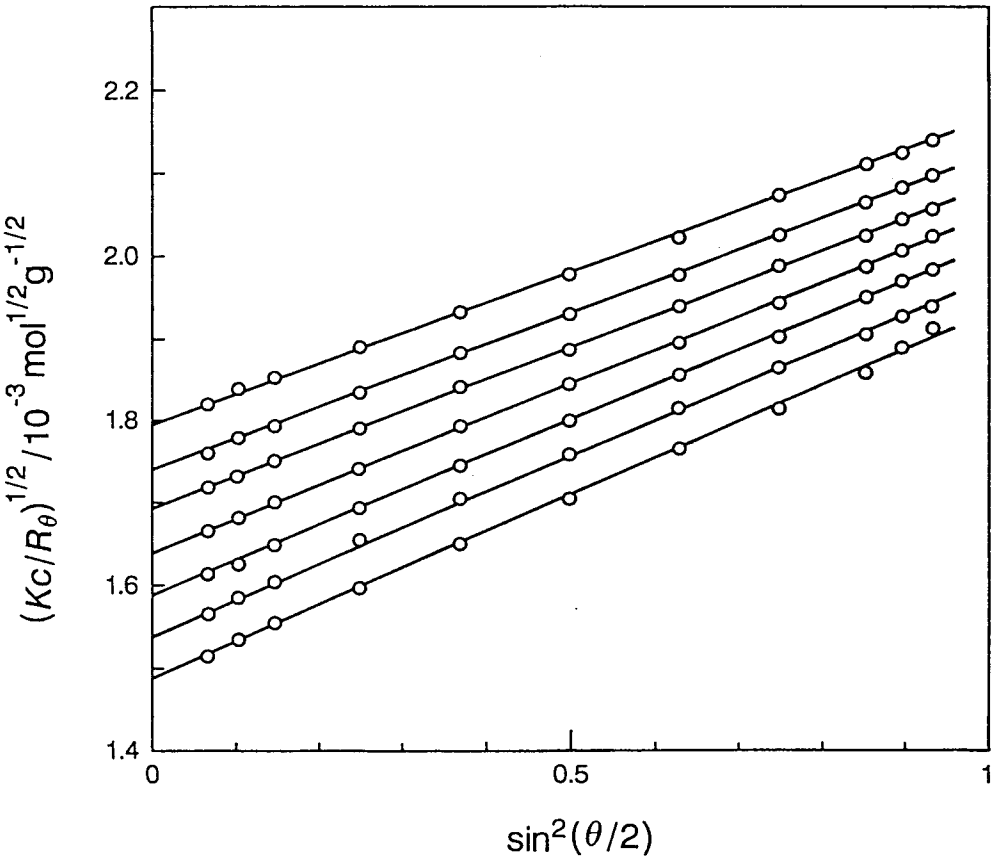

Figure 3.8 Plots of $(Kc/R_\theta)^{1/2}$ vs. $\sin^2(\theta/2)$ for PIB fraction A-22B4 in cyclohexane at 25°C. The polymer concentrations are 9.755×10^{-4}, 8.301×10^{-4}, 6.954×10^{-4}, 5.523×10^{-4}, 4.170×10^{-4}, 2.803×10^{-4}, and 1.440×10^{-4} g cm^{-3} from top to bottom.

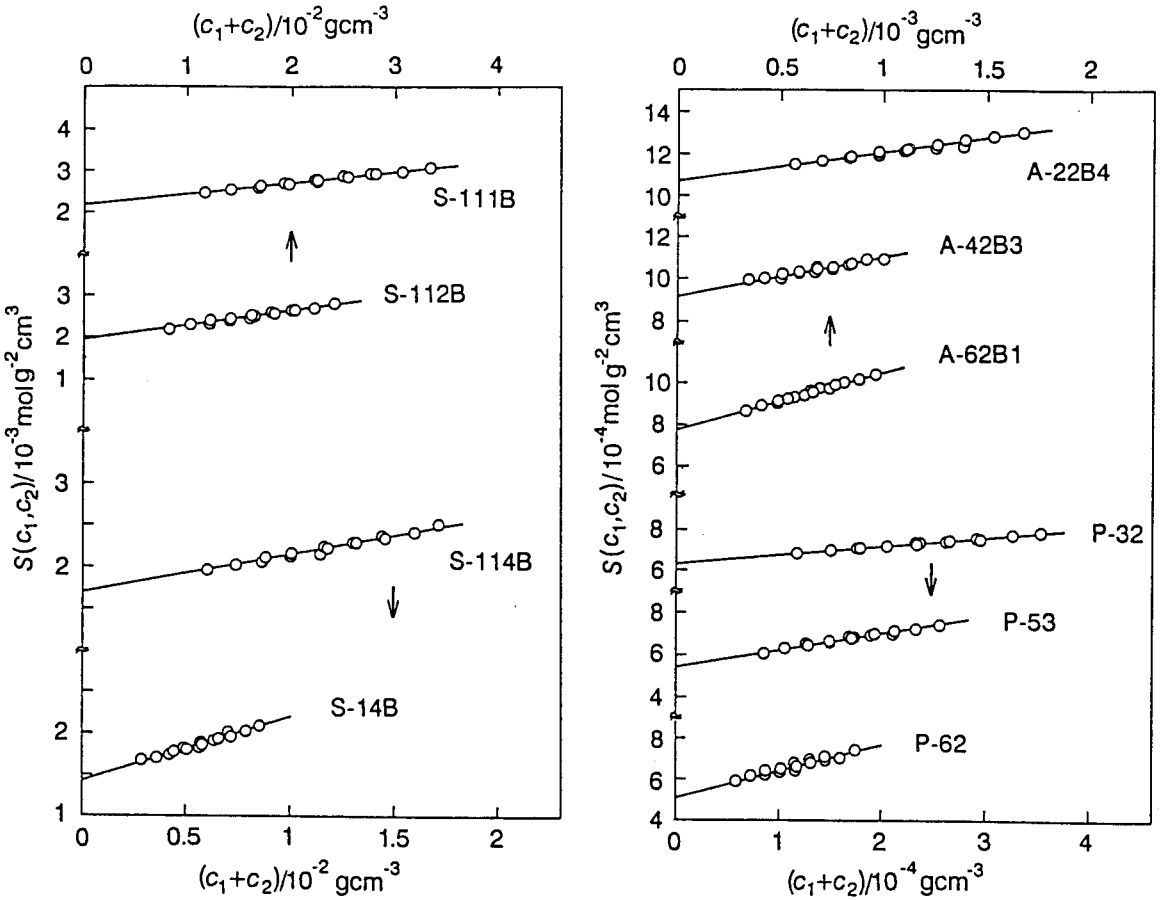

Figure 3.9 Bawn plots for the indicated PIB fractions in cyclohexane at 25°C. $S(c_1,c_2)$ data for pairs of neighboring c_1 and c_2 in a series of polymer concentrations are omitted, since they were not very accurate.

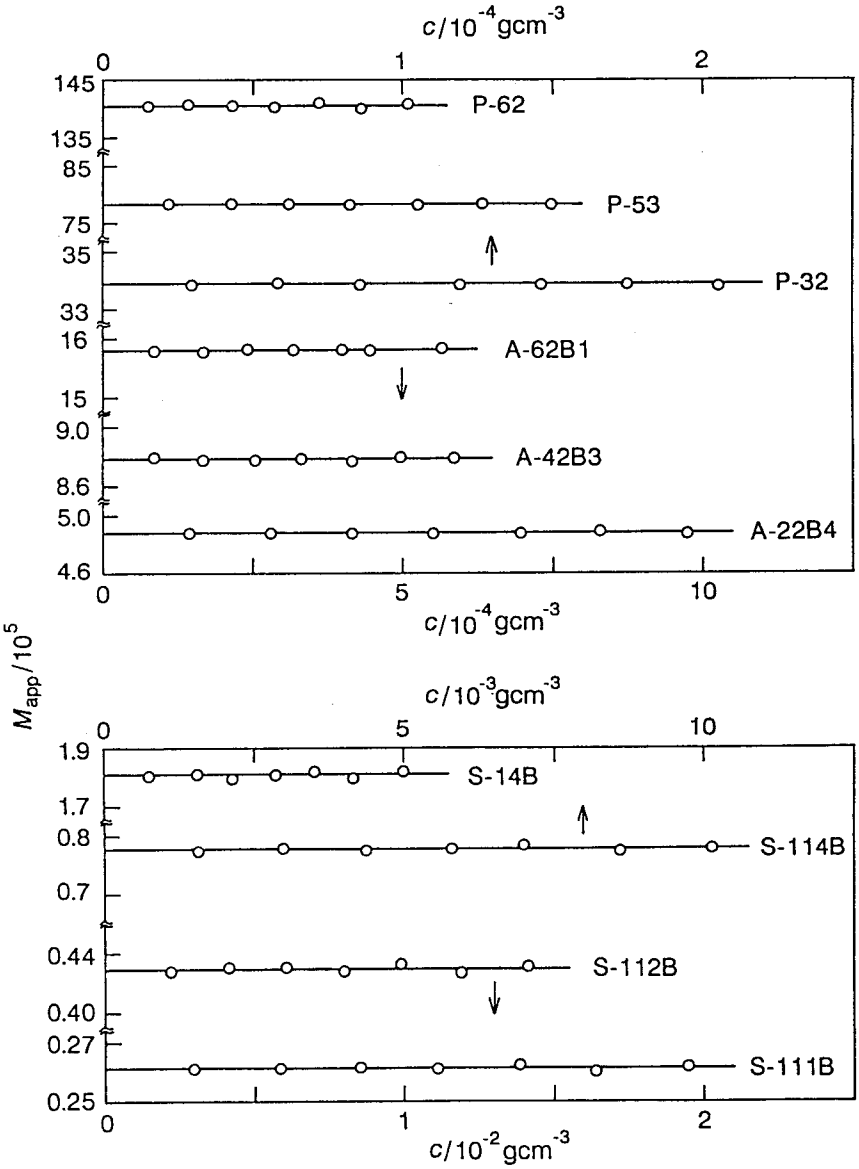

Figure 3.10 Plots of M_{app} vs. c for the indicated PIB fractions in cyclohexane at 25°C.

Table III-2

Numerical Results from Light Scattering Measurements on PIB Fractions in Cyclohexane at 25°C

Fraction	$M_w \times 10^{-5}$	$A_2 \times 10^4$ / mol g^{-2} cm^3	$A_3 \times 10^2$ / mol g^{-3} cm^6	g	$\langle S^2 \rangle_z^{1/2}$ / nm
S-111B	0.261	10.6	0.88	0.30	——
S-112B	0.429	9.55	1.1_5	0.29	——
S-114B	0.777	8.40	1.5_0	0.27	$11._6$
S-14B	1.81	7.05	2.6	0.29	18.7
A-22B4	4.88	5.30	4.7	0.34	33.4
A-42B3	8.78	4.55	6.3	0.35	47.6
A-62B1	15.8	3.85	9.2	0.39	66.8
P-32	33.9	3.13	$14._0$	0.42	107
P-53	78.3	2.68	27	0.48	177
P-62	141	2.54	42	0.46	252

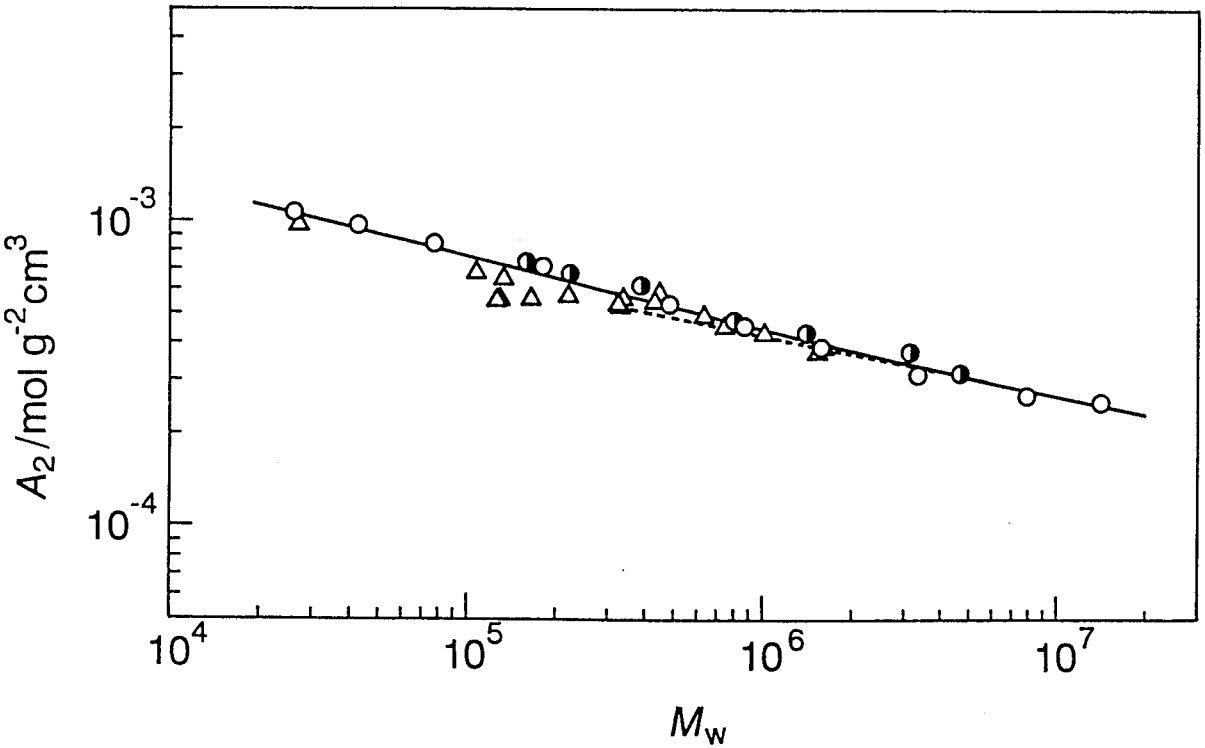

Figure 3.11 Molecular weight dependence of A_2 for PIB in cyclohexane at 25°C: (○) this work; (◑) Matsumoto et al.;[35] (△) Fetters et al.[54]

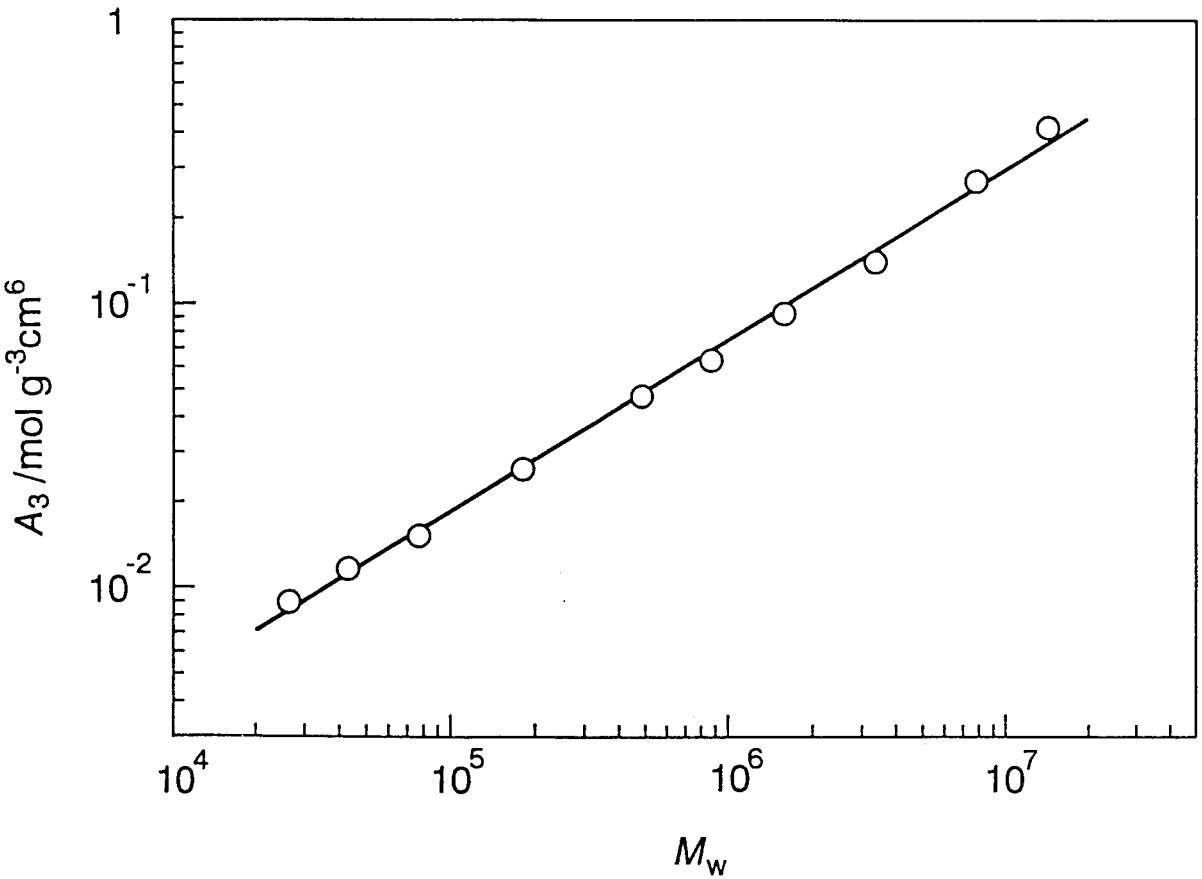

Figure 3.12 Molecular weight dependence of A_3 for PIB in cyclohexane at 25°C.

for A_3 is common to long flexible chains in good solvents. The PS data for $M_w < 10^5$ were found to deviate upward from the line with the slope 0.6, but no such behavior is seen for PIB.

The molecular weight dependence of g is shown in Figure 3.13. It can be seen that g stays at about 0.28 up to $M_w \sim 2 \times 10^5$ and then gradually increases to 0.45 - 0.50 with increasing M_w. This behavior of g is quite similar to what is shown for PS in the region of M_w above 10^5 in Figure 3.6.

Equation 2.12 indicates that if g is equal to 1/3 regardless of M_w, its third term vanishes and hence $(Kc/R_0)^{1/2}$ varies linearly with c up to a relatively high concentration at which the fourth term becomes important. The g values for both PS and PIB in Figures 3.6 and 3.13 change gradually from 0.25 to 0.5 as M_w increases from 2×10^4 to 10^7. This behavior implies that, to a good approximation, g may be taken as 1/3 over a molecular weight range of practical interest, and thus explains why the square-root plot has been successful in evaluating M_w and A_2 for the systems PS + benzene and PIB + cyclohexane.

On the other hand, the linearity of the square-root plot for osmotic pressure invokes a value of about 1/4 for g. The present g values for the two polymers

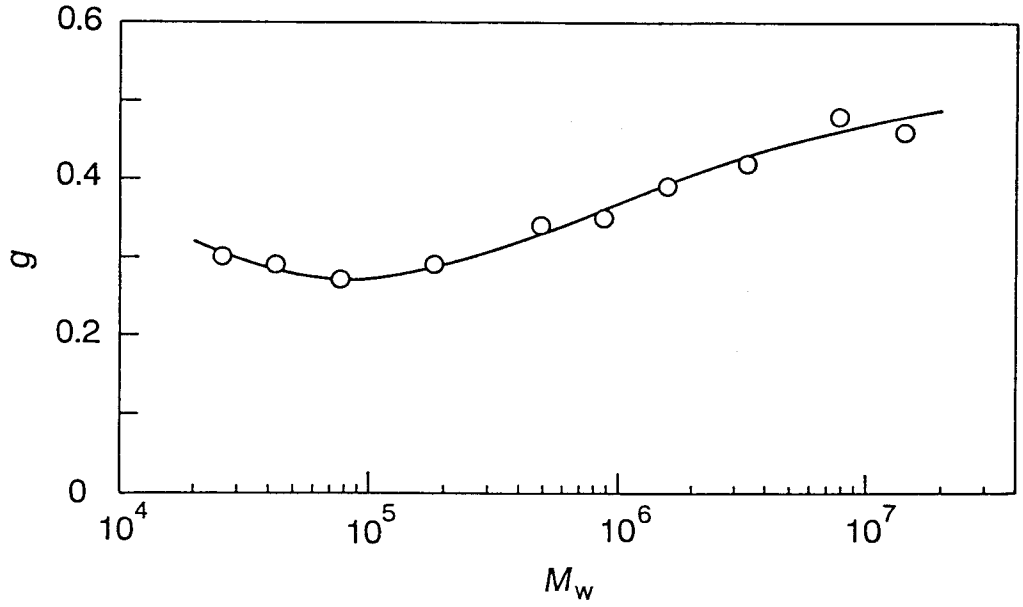

Figure 3.13 Molecular weight dependence of g for PIB in cyclohexane at 25°C.

are close to 1/4 in a range of M_w from 2 x 10^4 to 5 x 10^5, where osmometry is considered suitable for molecular weight determination. Hence, they substantiate Krigbaum and Flory's early proposal[19] that this type of plot should be useful for analyzing osmotic pressure data.

The values of $\langle S^2 \rangle_z$ for PIB in cyclohexane are plotted double-logarithmically against M_w in Figure 3.14, together with those of Matsumoto et al.[35] Our

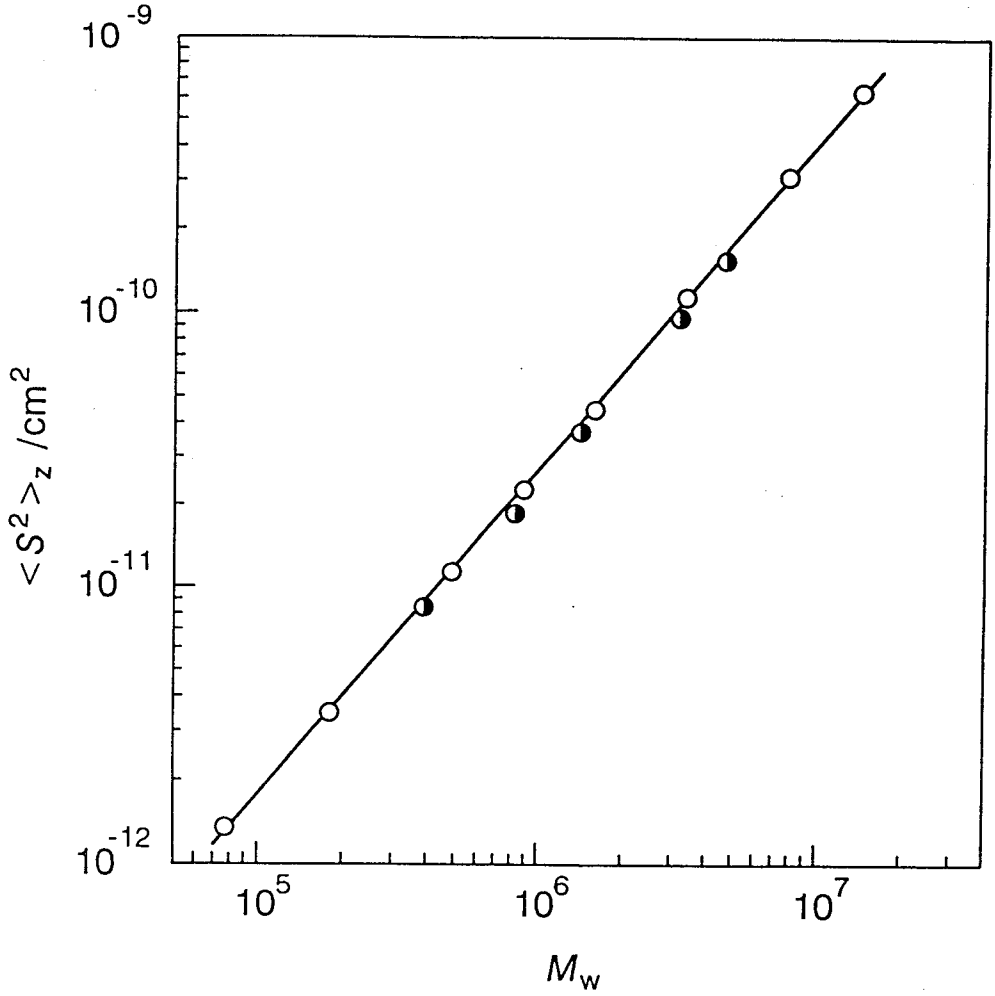

Figure 3.14 Molecular weight dependence of $\langle S^2 \rangle_z$ for PIB in cyclohexane at 25°C: (○) this work; (◑) Matsumoto et al.[35]

data points follow a straight line with slope 1.19 (± 0.01) throughout the entire range of M_w indicated. This slope agrees with that determined for PS in benzene by Miyaki et al.[33,38] (see Figure 3.7). The data points of Matsumoto et al. come below our data, but the slope 1.17 they obtained does not differ much from ours.

III.4 Discussion

Interpenetration Function

The second virial coefficient is usually discussed in terms of the interpenetration function Ψ defined by[2]

$$\Psi = \frac{A_2 M^2}{4\pi^{3/2} N_A \langle S^2 \rangle^{3/2}} \qquad (3.1)$$

Typical studies on this function, theoretical and experimental, made before 1970 and those in the last two decades are summarized in Yamakawa's book[2] and Fujita's,[3] respectively.

Although Ψ for PS in benzene has already been investigated by Yamamoto et al.,[36] Fukuda et al.,[37] and Miyaki et al.[33,38] in relation to the two-parameter theory, we here discuss it together with that for PIB

in cyclohexane. In Figure 3.15, our data of Ψ, the unfilled circles for PS in benzene and the unfilled squares for PIB in cyclohexane, are plotted against the cube of the radius expansion factor α_S defined by

$$\alpha_S = \langle S^2 \rangle^{1/2} / \langle S^2 \rangle_0^{1/2} \qquad (3.2)$$

where $\langle S^2 \rangle_0^{1/2}$ denotes the value of $\langle S^2 \rangle^{1/2}$ in the theta state. In calculating α_S, Miyaki's relation[33,38] $\langle S^2 \rangle_{0z} = 8.8 \times 10^{-18} M_w$ (cm^2) for PS (in cyclohexane at 34.5°C) and Matsumoto's relation[35] $\langle S^2 \rangle_{0z} = 9.52 \times 10^{-18} M_w$ (cm^2) for PIB (in isoamyl isovalerate at 22.1°C) were used. The figure includes the previous Ψ data (the filled circles with pips) of Yamamoto et al., Fukuda et al., Miyaki et al., and Sato et al.[26] for PS in benzene and those (the filled squares) of Matsumoto et al.[35] for PIB in cyclohexane.

All the data points except the filled squares essentially fall on a single solid curve as indicated. This is consistent with the prediction from two-parameter theory that Ψ should be a universal function of α_S^3. The asymptotic value of Ψ for infinitely large α_S may be estimated to be 0.22 ± 0.02. The filled squares deviate upward from the solid curve. This deviation reflects the small differences in both A_2 and

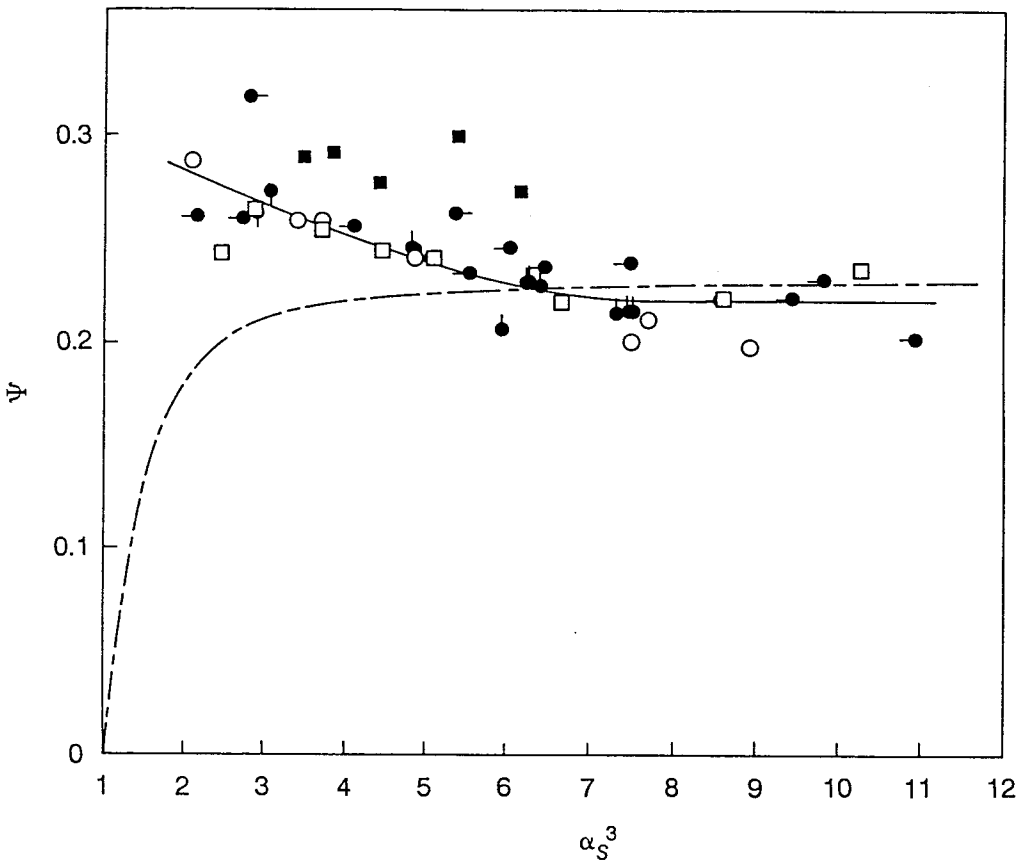

Figure 3.15 Plots of Ψ vs. α_S^3 for PS in benzene (○ , this work; ● , Yamamoto et al.;[36] ● , Fukuda et al.;[37] ● , Miyaki et al.;[38] ●, Sato et al.[26]) and PIB in cyclohexane (□ , this work; ■ , Matsumoto et al.[35]). The dot-dash line represents the Barrett theory.[39]

$\langle S^2 \rangle_z$ between our data and Matsumoto's, observed in Figures 3.11 and 3.14.

By combining perturbation calculations and computer simulation data, Barrett[39] and Domb and Barrett[55] constructed the following interpolation formulas for Ψ and α_S, respectively:

$$\Psi = \frac{z_2}{\alpha_S^3} (1 + 14.3 z_2 + 57.3 z_2^2)^{-0.2} \qquad (3.3)$$

$$\alpha_S^2 = [1 + 10 z_2 + (70\pi/9 + 10/3) z_2^2 + 8\pi^{3/2} z_2^3]^{2/15}$$

$$\times [0.933 + 0.067 \exp(-0.85 z_2 - 1.39 z_2^2)] \qquad (3.4)$$

Here, z_2 is the excluded-volume parameter defined by

$$z_2 = \left(\frac{3}{2\pi b^2}\right)^{3/2} \beta_2 n^{1/2} \qquad (3.5)$$

In this equation, b is the segment length and n the number of segments in one chain. The dot-dash line in Figure 3.15 represents eq 3.3 combined with eq 3.4. The agreement between this and solid curves is satisfactory for α_S^3 larger than 6. Equation 3.3, when

combined with the asymptotic relation $\alpha_S^2 = 1.53z^{5/2}$ derived from computer simulation data,[38,56] yields an asymptotic Ψ of 0.235, which is close to the above estimate 0.22 ± 0.02.

However, as α_S^3 decreases, the dot-dash line declines to zero, while the experimental curve rises (note that Ψ of any two-parameter theory decreases to zero as α_S^3 approaches unity[2,3]). This serious discrepancy has already been observed not only for PS in benzene[33] but also for poly(D-β-hydroxybutyrate) in trifluoroethanol.[57,58] The present PIB data give additional evidence for it. As pointed out by Fujita and Norisuye,[59] this discrepancy may be ascribed primarily to the fact that eq 3.3 with eq 3.4 predicts a molecular weight dependence of A_2 weaker than that represented by $A_2 \propto M_w^{-0.2}$, while the experimental A_2 for PIB (that for PS as well) has a stronger dependence. It should be added that in contrast to the dot-dash line sharply declining to zero, Ψ for low molecular weight PS in toluene rises first gradually and then sharply as α_S^3 approaches unity.[7,10]

Reduced Third Virial Coefficient

Theories of g for flexible chains were worked out first by Stockmayer and Casassa[24] and later by Koyama[40]

and by Yamakawa[41] in the framework of two-parameter theory, i.e., in the binary cluster approximation. The last author obtained g by combining his approximate closed expression for A_3 with the Casassa-Markovitz theory[60] for A_2. According to these two-parameter theories, g is a universal function of z_2/α_S^3. Knoll et al.,[42] des Cloizeaux and Noda,[43] and Douglas and Freed[44] calculated g for a good solvent system on the basis of the first-order ε expansion in renormalization group methods.

Table III-3 summarizes the asymptotic values of g predicted by the two-parameter and renormalization group theories. The value by the Stockmayer-Casassa theory agrees with that for rigid spheres and is not very different from that by the Koyama theory. We note that these two theories are based on the smoothed-density model with essentially identical intermolecular potentials. The Yamakawa theory gives a value much larger than the others. The renormalization group values by Knoll et al. and by des Cloizeaux and Noda come close to our experimental values of 0.45 - 0.50 for PS and PIB at $M_w \sim 10^7$ (see Figures 3.6 and 3.13). However, this agreement cannot be taken literally until g is calculated up to a higher order in ε.

Regarding the behavior of g at finite molecular

Table III-3

Theoretically Predicted Asymptotic Values of the Reduced Third Virial Coefficient g

Authors	Model or Method	g
Stockmayer-Casassa[24]	Smoothed Density	0.625
Koyama[40]	Smoothed Density	0.704
Yamakawa[41]	Differential Equation	1.333
Knoll-Schäfer-Witten[42]	Renormalization Group	0.44
des Cloizeaux-Noda[43]	Renormalization Group	0.435
Douglas-Freed[44]	Renormalization Group	0.277

weights, the renormalization group calculations made so far fail to explain why g depends on M_w as has been found in the present work. On the other hand, the two-parameter theories of the three groups mentioned above all predict g to increase monotonically with increasing molecular weight, in agreement with our data except those for M_w below 10^5.

In Figure 3.16, the values of g for PS in benzene and PIB in cyclohexane are plotted versus α_S^3. For fractions whose $\langle S^2 \rangle_z$ data are unavailable, we have estimated α_S by extrapolating the empirical relations

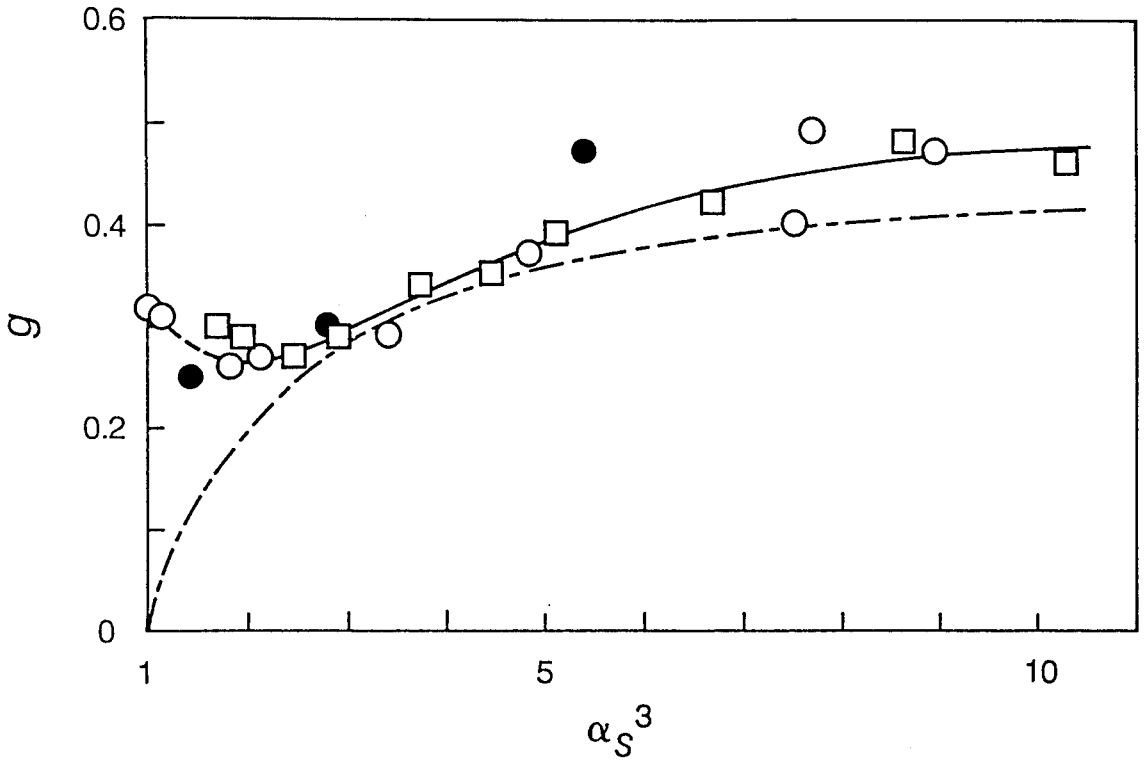

Figure 3.16 Plots of g vs. α_S^3 for PS in benzene (○ , this work; ● , Sato et al.[26]) and PIB in cyclohexane (□ ; this work). Dot-dash line, Stockmayer-Casassa's theory.[24]

$\alpha_S^2 = 0.167 M_w^{0.19}$ for PS[33] and $\alpha_S^2 = 0.206 M_w^{0.19}$ for PIB; the latter was obtained from the data in Figure 3.14 and the $\langle S^2 \rangle_{0z}$ data of Matsumoto et al.[35] Because of the extrapolation, the abscissa values below 2 may not be very accurate, but their accuracy is immaterial in the present discussion. The plotted points for the two systems approximately form a single composite curve, at least, in the region of α_S^3 above 2, as indicated by a solid line. This finding satisfies the requirement of the two-parameter theory.

The dot-dash line in the Figure 3.16 represents the g vs. α_S^3 relation predicted by Stockmayer and Casassa,[24] who combined their theory for g (as a functions of z_2/α_S^3) with the Flory equation[61] for α_S, i.e., $\alpha_S^5 - \alpha_S^3 = 2.60 z_2$. This line comes close to the solid curve for α_S^3 larger than 2. However, as α_S approaches unity, it sharply declines to zero, while the experimental g stays at about 0.3 or even goes up after passing through a shallow minimum. This sharp contrast is similar to what has been observed for Ψ.

As was shown by Miyaki and Fujita,[62] the original Flory equation used by Stockmayer and Casassa is a good approximation to either PS in benzene or PIB in cyclohexane for $\alpha_S^3 > 2$, so that the observed agreement

between the solid and dot-dash curves in Figure 3.16 may be taken as that in g itself. However, this agreement must be due to a compensation of the errors in both A_2 and A_3 that the Stockmayer-Casassa smoothed-density theory involves, because the Flory-Krigbaum theory[63] for A_2 based on the same smoothed-density model fails to describe A_2 for flexible polymers. In other words, the Stockmayer-Casassa theory should be invalid for A_3, though it almost quantitatively explains the ratios of A_3 to $A_2{}^2M_w$ for the two typical flexible polymers in the region of $\alpha_S{}^3$ above 2. The same argument applies to the Koyama theory, which is essentially identical to the Stockmayer-Casassa theory. The Yamakawa theory gives g values that are too large.

In conclusion, none of the available theories can explain the observed molecular weight dependence of A_3 for PS in benzene and PIB in cyclohexane. Even qualitatively, there exists a serious discrepancy in g between our experiments and the two-parameter theory when α_S is approached to unity by lowering the molecular weight in a given good solvent. The discrepancy is similar to that in Ψ, indicating that the current two-parameter theory for A_3 overlooks something important, as is the case for A_2.

Chapter IV

Theta Solvent Systems

IV.1 Introduction

In this chapter, A_2 and A_3 for two theta solvent systems, PS in cyclohexane and in trans-decalin, are determined as functions of M_w and T. It is shown that A_3 for either system remains positive at Θ. Since this implies the breakdown of the binary cluster approximation at Θ, the A_2 data are used to test the available theories of A_2 based on the smoothed-density model[11] and the first-order cluster expansion,[12,15] both taking three-segment interactions into account.

IV.2 Results for Polystyrene in Cyclohexane

IV.2.1 Data Analysis

Figure 4.1 illustrates the concentration dependence of Kc/R_0 for PS fraction 4a-B in cyclohexane at the indicated temperatures. The curves fitting the data points at the respective T bend upward and appear to converge to a common ordinate intercept.

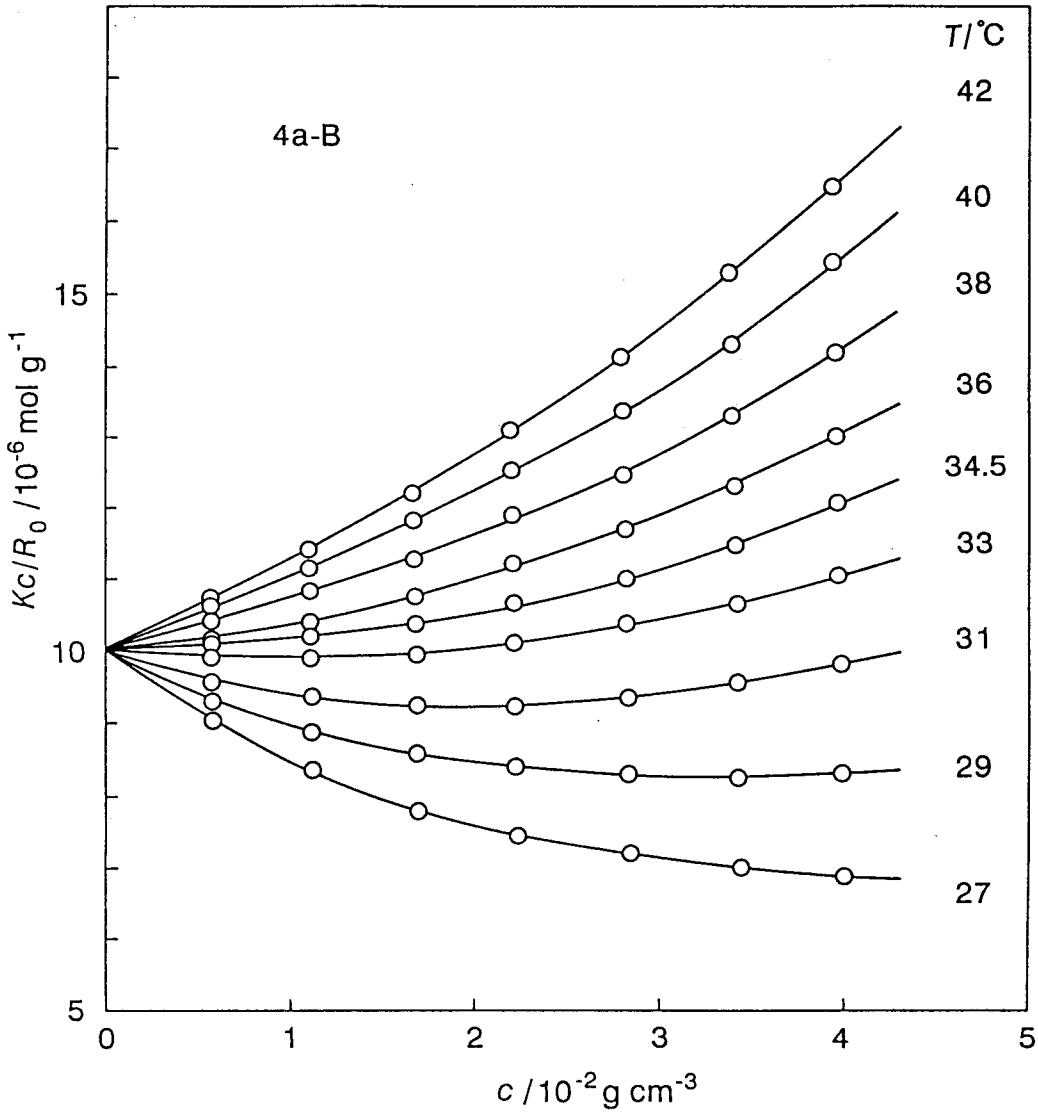

Figure 4.1 Concentration dependence of scattering intensity at zero angle for PS fraction 4a-B in cyclohexane at indicated temperatures.

The Bawn plots constructed from these data according eq 2.16 are shown in Figure 4.2. The plotted points at any T follow a straight line, whose intercept and slope may be equated to $2A_2$ and $3A_3$, respectively. Similar plots for six PS fractions 2b-B, F'4-B, 4a-B, F-40B, F80-B, and F288-B at a fixed T of 34.5°C are displayed in Figure 4.3. The values of A_2 and A_3 for the six fractions at different T are summarized in Tables IV-1 and IV-2, respectively.

With the A_2 and A_3 data for a given fraction at each T, the apparent molecular weight M_{app} defined by eq 2.17 was calculated as a function of c. Figure 4.4 shows that the resulting plots of M_{app} vs. c for the six fractions at 34.5°C are horizontal and permit unambiguous determination of M_{app} at infinite dilution, i.e., M_w of the respective fractions. The values of M_w obtained at 34.5°C agreed with those at other temperatures within ± 1% for any fractions. Thus, only those at 34.5°C are presented in both Tables IV-1 and IV-2. We note that the M_w values in cyclohexane agree with those in benzene within ± 2.5%, especially within ± 1% for fractions 4a-B, F-40B, and F80-B (see Table III-1).

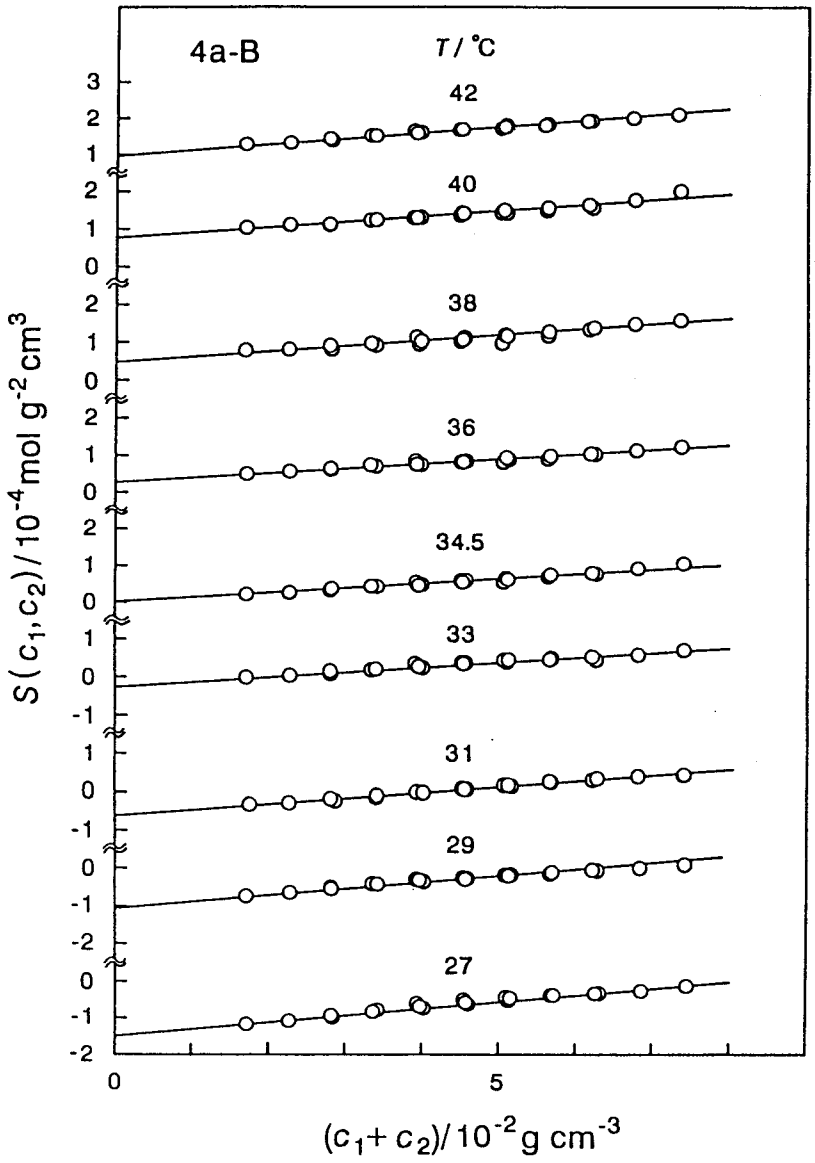

Figure 4.2 Bawn plots constructed from the data in Figure 4.1.

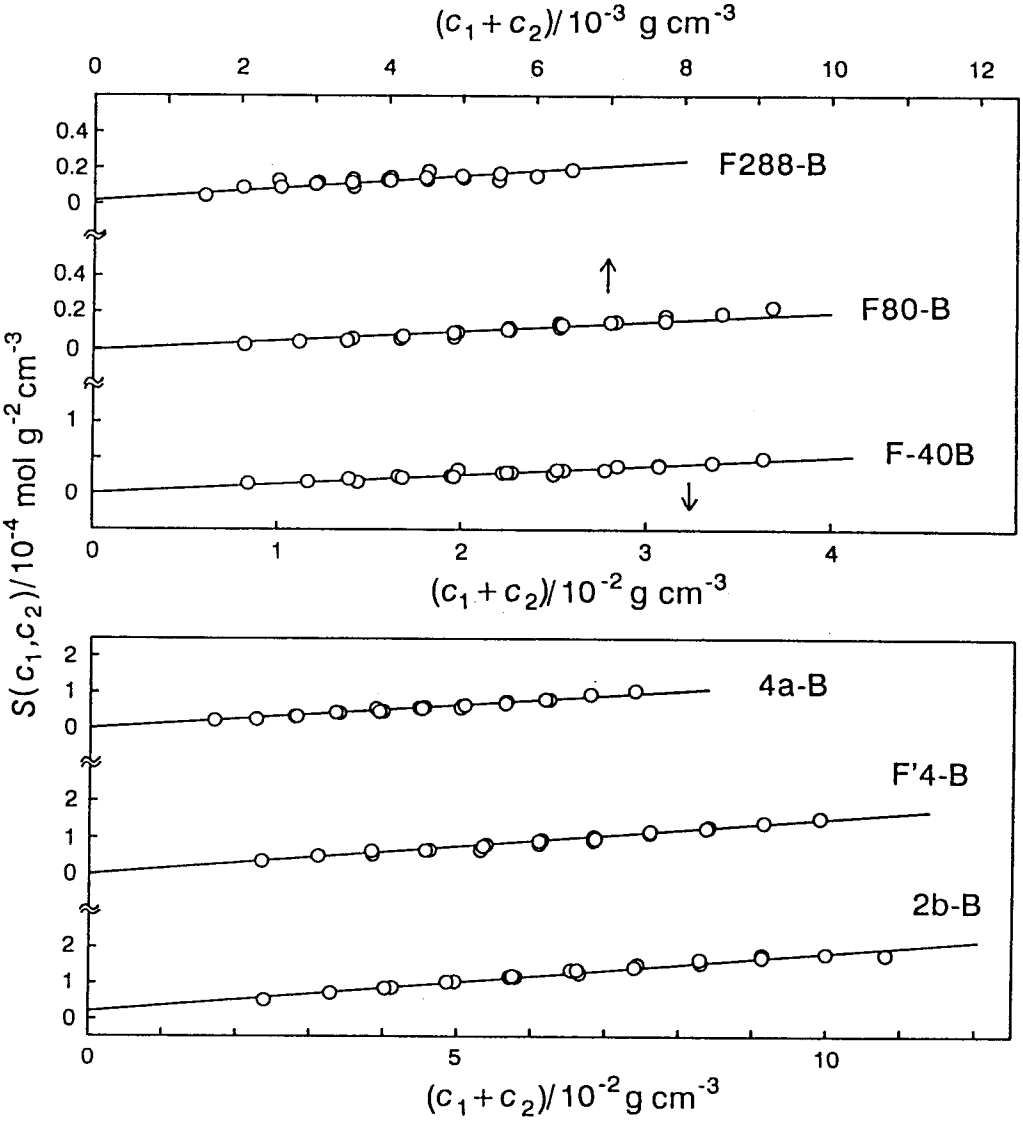

Figure 4.3 Bawn plots for the indicated PS fractions in cyclohexane at 34.5°C.

Table IV-1

Values of A_2 for Polystyrene Fractions in Cyclohexane at Different Temperatures

	$A_2/10^{-5}$ mol g^{-2} cm^3					
T/°C	2b-B M_w = 2.07 x 10^4	F'4-B M_w = 5.07 x 10^4	4a-B M_w = 9.97 x 10^4	F-40B M_w = 37.3 x 10^4	F80-B M_w = 84.3 x 10^4	F288-B M_w = 300 x 10^4
27.0	-7.5	-7.4	-7.5	-6.5	——	——
29.0	-5.1	-5.0	-5.4	-4.0	-4.5	——
31.0	-2.9	-3.1	-3.1	-2.4	-2.6	-2.4
33.0	-0.7	-1.4	-1.3	-0.7	-0.8	-0.7
34.5	1.0	0	0	0	0	0.2
36.0	2.6	1.1	1.4	1.3	1.0	0.9
38.0	4.6	2.1	2.5	2.7	2.1	1.9
40.0	6.3	3.6	3.9	3.7	3.3	2.5
42.0	7.5	5.0	4.9	4.7	4.1	3.2
45.0	——	6.3	——	——	——	4.1

Table IV-2

Values of A_3 for Polystyrene Fractions in Cyclohexane at Different Temperatures

	$A_3/10^{-4}$ mol g^{-3} cm^6					
T/°C	2b-B M_w = 2.07 x 10^4	F'4-B M_w = 5.07 x 10^4	4a-B M_w = 9.97 x 10^4	F-40B M_w = 37.3 x 10^4	F80-B M_w = 84.3 x 10^4	F288-B M_w = 300 x 10^4
27.0	6.4	6.0	6.2	7.0	——	——
29.0	5.8	5.7	5.8	5.0	9.7	——
31.0	5.8	5.4	5.0	4.8	8.7	12
33.0	5.6	5.3	4.2	3.4	6.7	10
34.5	5.4	5.0	4.3	4.2	7.1	9
36.0	4.8	5.3	4.3	3.8	7.3	10
38.0	5.1	5.9	4.9	3.5	7.9	10
40.0	5.2	6.1	4.9	4.1	9.0	15
42.0	5.4	6.0	5.4	4.7	9.9	16
45.0	——	7.5	——	——	——	20

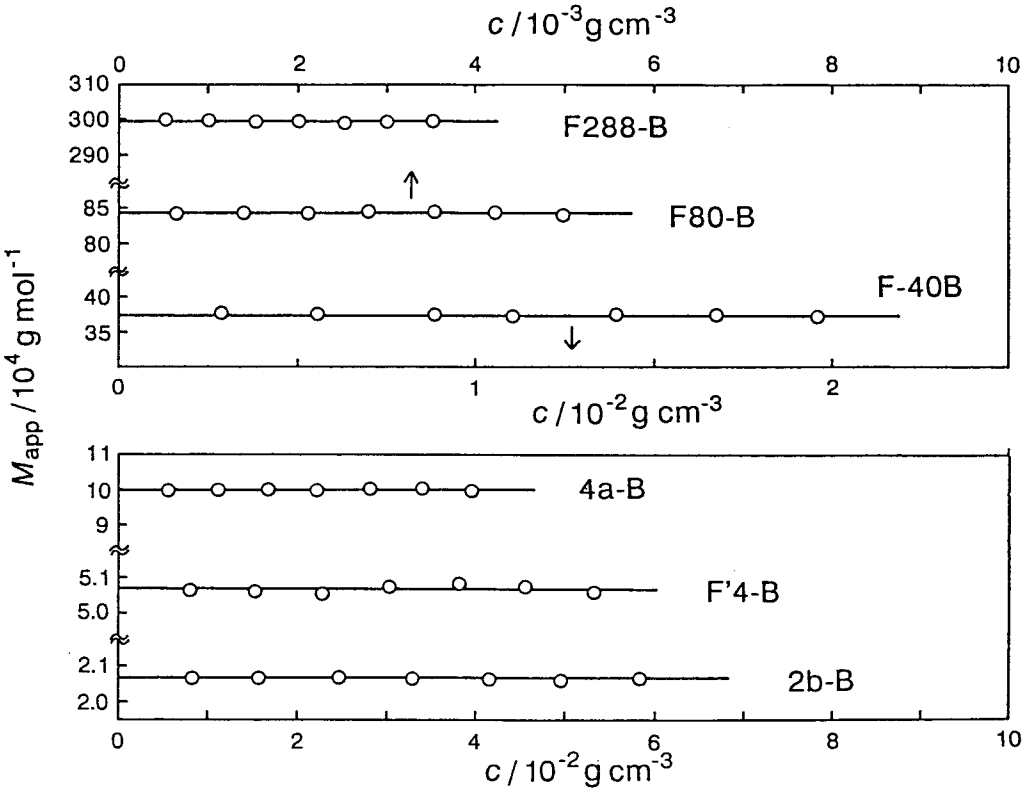

Figure 4.4 Plots of M_{app} vs. c for the indicated PS fractions in cyclohexane at 34.5°C.

IV.2.2 Second Virial Coefficient and Theta Temperature

Figure 4.5 depicts the temperature dependence of A_2 for the indicated PS fractions in cyclohexane. Except for the lowest molecular weight fraction 2b-B, A_2 becomes zero at 34.5°C (± 0.03°C); the graphically estimated A_2 value for F288-B is 2 x 10^{-6} mol g^{-2} cm^3, but it cannot be distinguished from zero within experimental uncertainties. This is in accord with Miyaki et al.,[33,38] who showed that A_2 of PS in cyclohexane vanishes at the same T of 34.5°C for M_w ranging from 1.9 x 10^5 to 5.6 x 10^7. Thus, it seems reasonable to conclude that above $M_w \sim 5 \times 10^4$, Θ for the PS + cyclohexane system is virtually independent of molecular weight. This disagrees with the finding of Vink,[31] whose osmotic pressure data for the same system showed that Θ appreciably increases as the molecular weight is lowered from 4.1 x 10^5 to 3.7 x 10^4.

Recently, Huber and Stockmayer[7] found that A_2 for low molecular weight PS ($M_w \lesssim 10^4$) in cyclohexane at 35°C is positive and markedly increases with decreasing M_w (in their work, this temperature is the theta point for high molecular weight samples). Similar trends

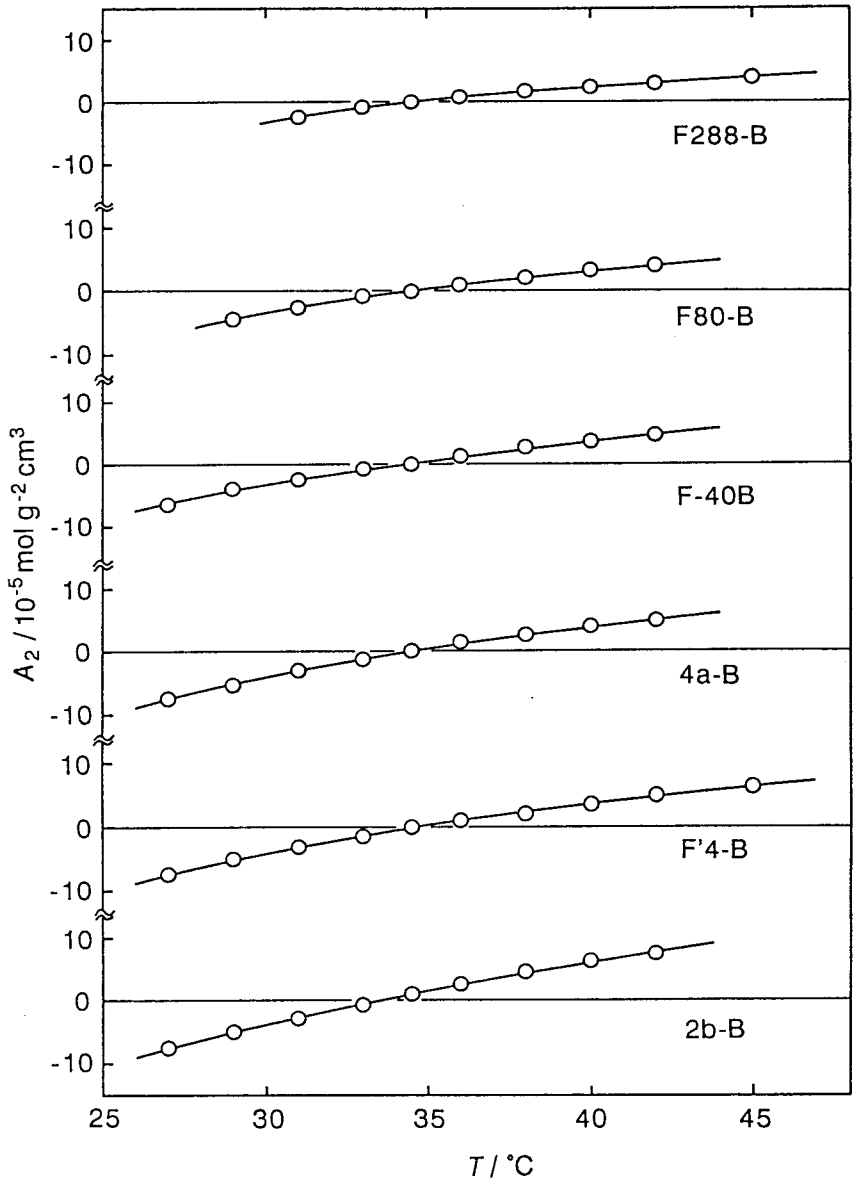

Figure 4.5 Temperature dependence of A_2 for the indicated PS fractions in cyclohexane.

were reported by Konishi et al.[8] for PS in cyclohexane at 34.5°C and by Tamai et al.[9] for poly(methyl methacrylate) in acetonitrile at the theta temperature 44.0°C. Our positive A_2 value for the lowest molecular weight fraction 2b-B at 34.5°C is consistent with these results for PS in cyclohexane.

IV.2.3 Third Virial Coefficient

The temperature dependence of A_3 is shown in Figure 4.6. Importantly, A_3 for any fraction remains nonzero at Θ. This reveals the breakdown of the two-parameter theory for A_3 near the theta point; the theory predicts that A_2 and A_3 simultaneously vanish when the binary cluster integral becomes zero.[2] The curve for each fraction is nearly parabolic with a broad minimum around 34.5°C, and the minimum becomes very shallow as M_w decreases. This molecular weight dependent variation in A_3 with T is probably the first finding and awaits some theoretical interpretation.

The highest polymer concentration studied for a given sample in cyclohexane is 2 - 4 times higher than that investigated for benzene solutions. In benzene solutions, distinct downward curvatures were observed in Bawn plots when the measurement was extended to such

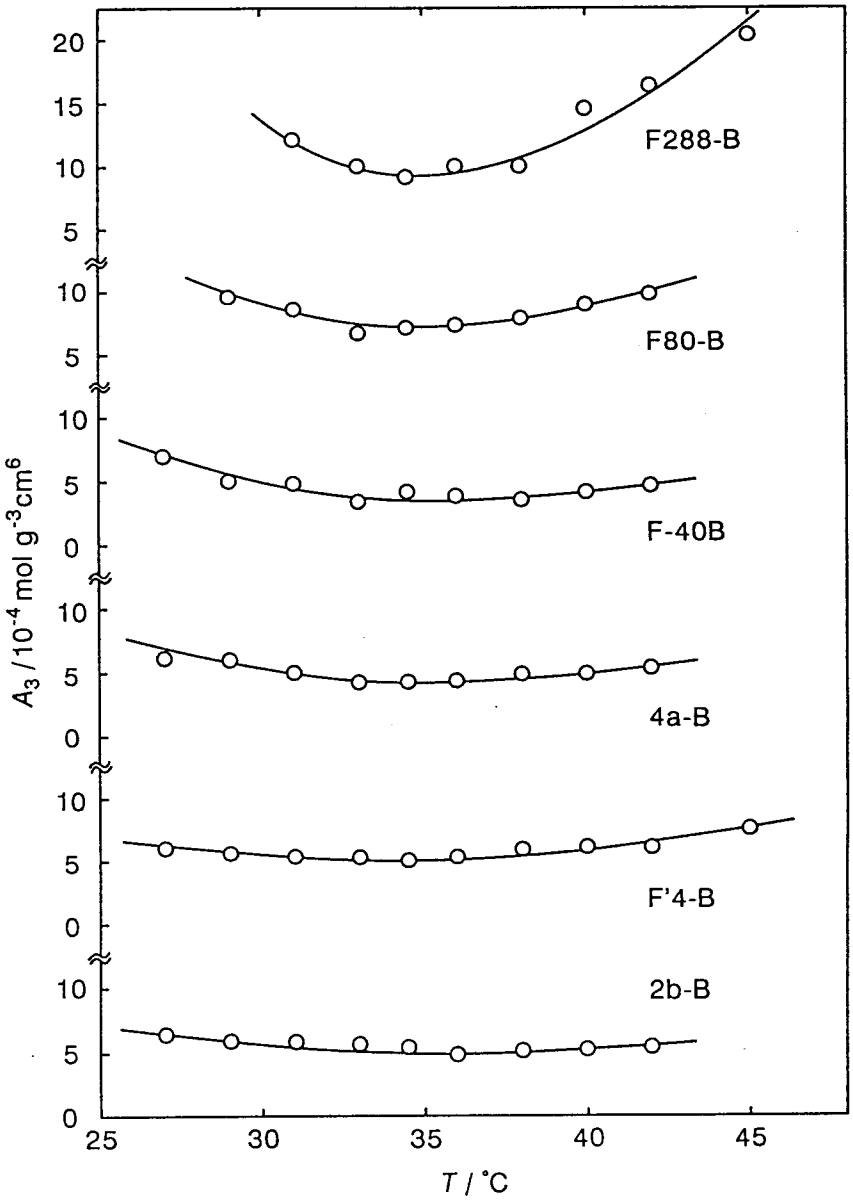

Figure 4.6 Temperature dependence of A_3 for the indicated PS fractions in cyclohexane.

high concentrations. On the other hand, any Bawn plots for cyclohexane solutions show no discernible curvature, suggesting that in poor solvents, the second and third virial terms dominate $[(Kc/R_0) - (1/M_w)]$ over a wider concentration range than in good solvents. The fourth virial contributions to the $S(c_1, c_2)$ vs. $c_1 + c_2$ and $[(Kc/R_0) - (1/M_w)]/c$ vs. c relations are different (compare eqs 2.14 and 2.16), and hence the linearity of the former plot does not necessarily ensure that Kc/R_0 at Θ contains no substantial A_4 contribution in the range of c studied. This point is discussed in the following using the data presented in Figure 4.3.

When $A_2 = 0$, it follows from eq 2.11 that

$$Q \equiv [(Kc/R_0) - (1/M_w)]/c^2$$

$$= 3A_3 + 4A_4 c + \ldots \qquad (A_2 = 0) \qquad (4.1)$$

Equation 4.1 indicates that Q is essentially independent of c if it is dominated by A_3 in the concentration range considered; we note that this equation is applicable when an accurate M_w is known in advance. Figure 4.7 shows the plots of Q vs. c constructed from the Kc/R_0 data in cyclohexane at 34.5°C and the M_w data

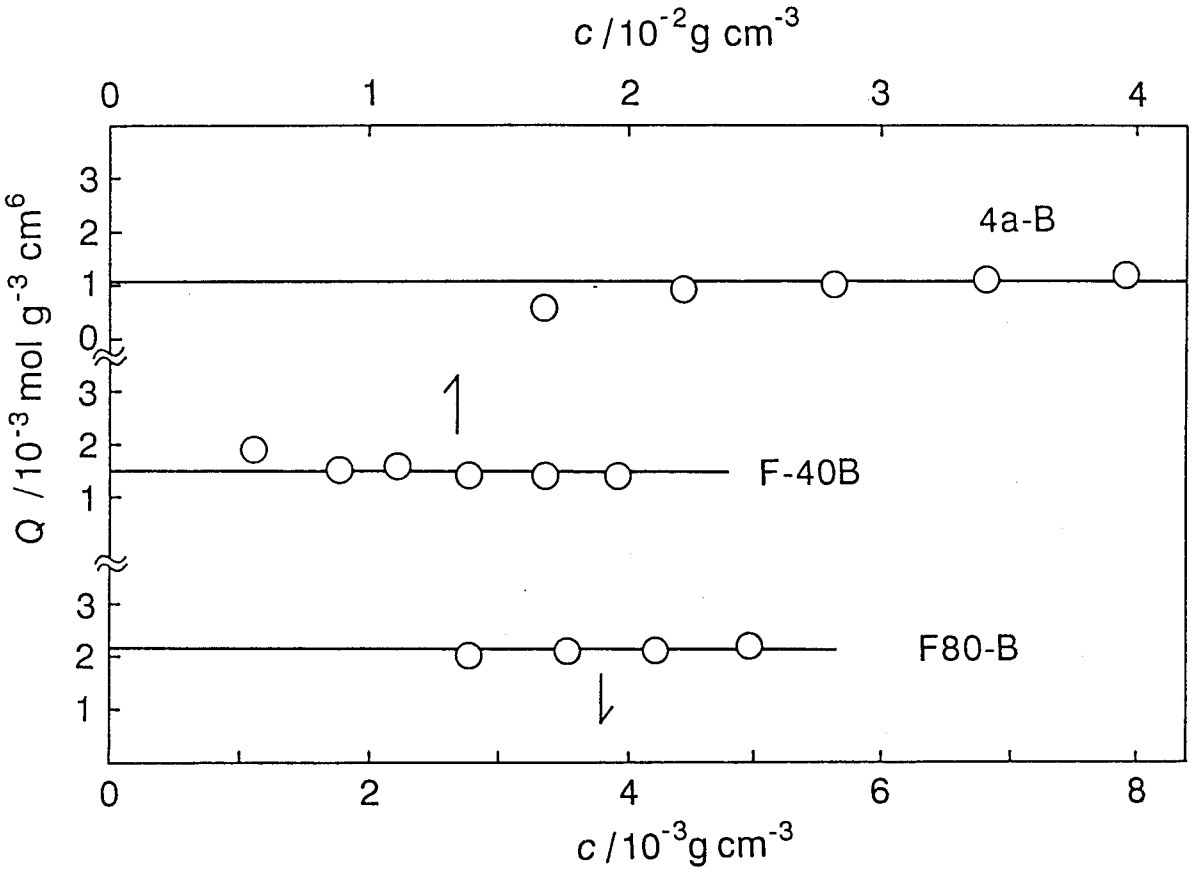

Figure 4.7 Plots of Q vs. c for the indicated PS fractions in cyclohexane at the theta point.

in benzene for three fractions 4a-B, F-40B, and F80-B whose M_w values in the two solvents agreed within ± 1%. We have omitted intensity data at low c where Kc/R_0 is not removed from the input value of $1/M_w$ by more than 1%. All the plotted points except two at the lowest c for fractions 4a-B and F-40B fall on horizontal lines for the respective fractions, yielding A_3 of 4×10^{-4}, 5×10^{-4}, and 7×10^{-4} mol g^{-3} cm^6 for fractions 4a-B, F-40B, and F80-B, respectively; the deviations of the two points from the lines are probably immaterial, since the differences between Kc/R_0 and $1/M_w$ values for them are only about 2%. The substantial agreement of these A_3 values with those at 34.5°C in Table IV-2, along with the observed c-independent behavior of Q, convinces us that A_4 has a negligible contribution to Kc/R_0 when the Bawn plot is linear.

IV.2.4 Some Remarks

With the experimental relation $\langle S^2 \rangle_0 = 8.8 \times 10^{-18} M_w$ cm^2 reported by Miyaki et al.[33,38] for polystyrene in cyclohexane at 34.5°C, the overlap concentration c^* defined by[3] $c^* = 3M_w/(4\pi N_A \langle S^2 \rangle_0^{3/2})$ was estimated for each fraction. The calculated c^* values were 20 - 30% higher than the highest concentrations studied for

three fractions F'4-B, 4a-B, and F-40B and 2 - 3 times higher than those for others. Thus, we find that at least for these three fractions the concentration dependence of $[(Kc/R_0) - (1/M_w)]$ in cyclohexane at 34.5°C is determined substantially by A_3 only over a wide range of c from 0 to $0.7c^*$.

Nonetheless, there is a low concentration region in which Kc/R_0 at Θ is unaffected by A_3. For example, Kc/R_0 calculated for fraction 4a-B with the M_w and A_3 values at 34.5°C in Table IV-2 stays equal to $1/M_w$ within 1% up to as high a c as 8.8×10^{-3} g cm^{-3} ($= 0.18c^*$). Such c-independent behavior of Kc/R_0 yielding $A_2 = 0$ is just what is usually observed in theta solvents. In this connection, it should be noticed in Figure 4.1 that Θ for the fraction 4a-B appears to be not at 34.5°C but at 33°C owing to the compensation of negative A_2 and positive A_3 in the range of c between 1×10^{-2} and 2×10^{-2} g cm^{-3}. Hence, Θ may be underestimated if light scattering data at relatively high c are analyzed by the conventional Kc/R_0 vs. c plot.

IV.3 Results for Polystyrene in trans-Decalin

IV.3.1 Second Virial Coefficient and Theta Temperature

Analyses of light scattering data for PS fractions in trans-decalin in a temperature region from 13 to 55°C are presented in Figures 4.8 through 4.11. The numerical results for A_2 and A_3 are summarized in Tables IV-3 and IV-4, respectively, along with those for M_w at 21°C. We again note that the M_w values at this temperature agree with those not only at other T in the same solvent but also in benzene (Table III-1) and cyclohexane (Table IV-1) within experimental errors.

Figure 4.12 shows the temperature dependence of A_2 for the indicated fractions. The theta point for each fraction was determined from the intersection between the line for $A_2 = 0$ and the solid line fitting the data points. The values of Θ thus obtained as a function of M_w are shown by unfilled circles in Figure 4.13; bars attached to the circles represent the experimental uncertainty. In contrast with the M_w-independence of Θ in cyclohexane for $M_w \gtrsim 5 \times 10^4$, Θ in trans-decalin increases approximately from 21 to 23°C as M_w decreases

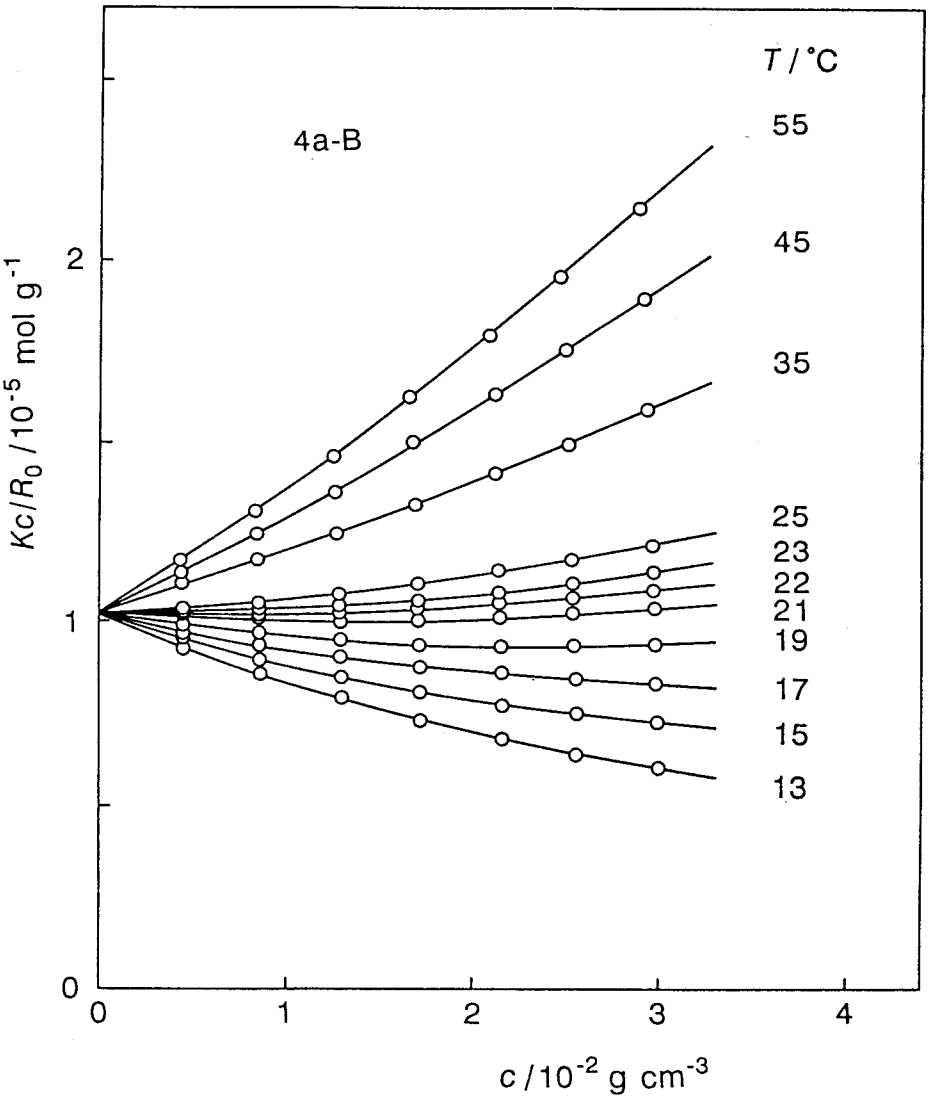

Figure 4.8 Concentration dependence of scattering intensity at zero angle for PS fraction 4a-B in trans-decalin at indicated temperatures.

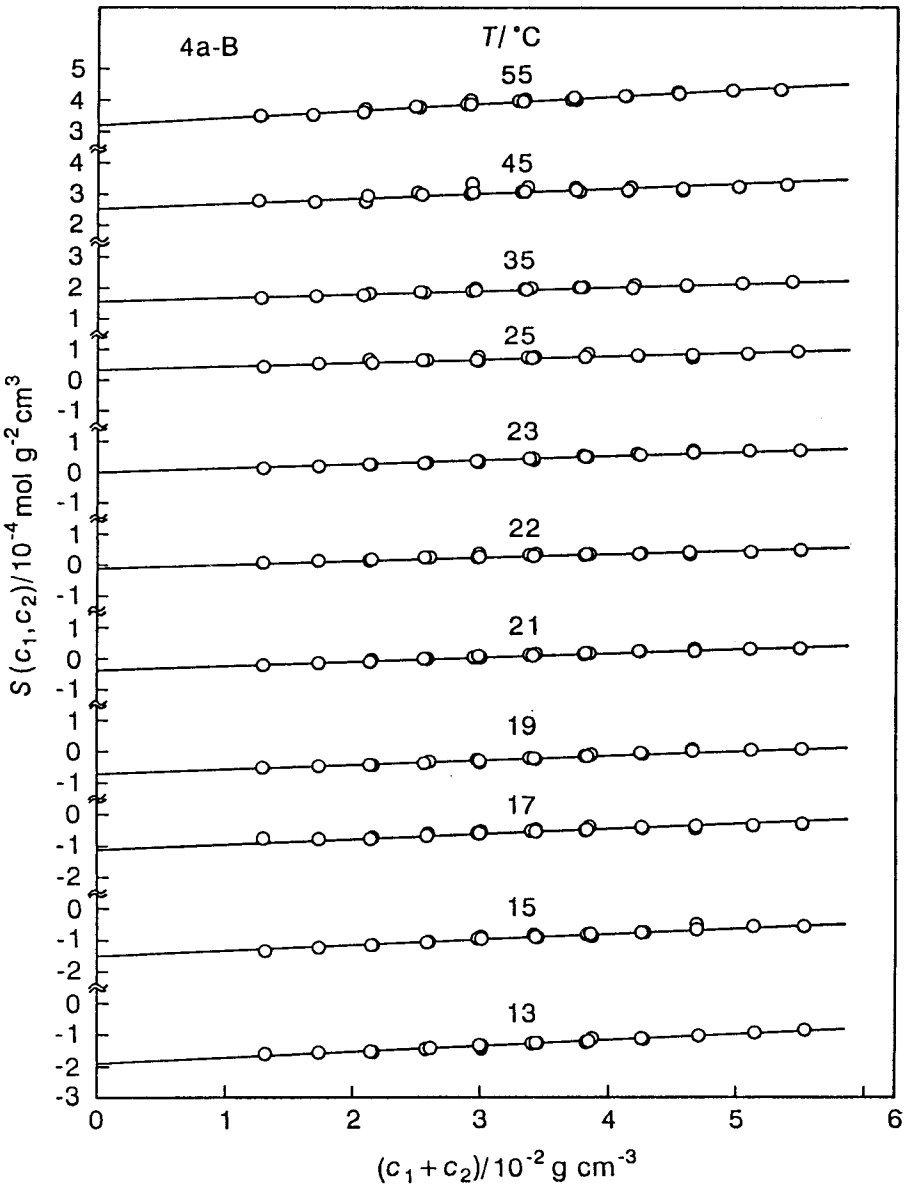

Figure 4.9 Bawn plots constructed from the data in Figure 4.8.

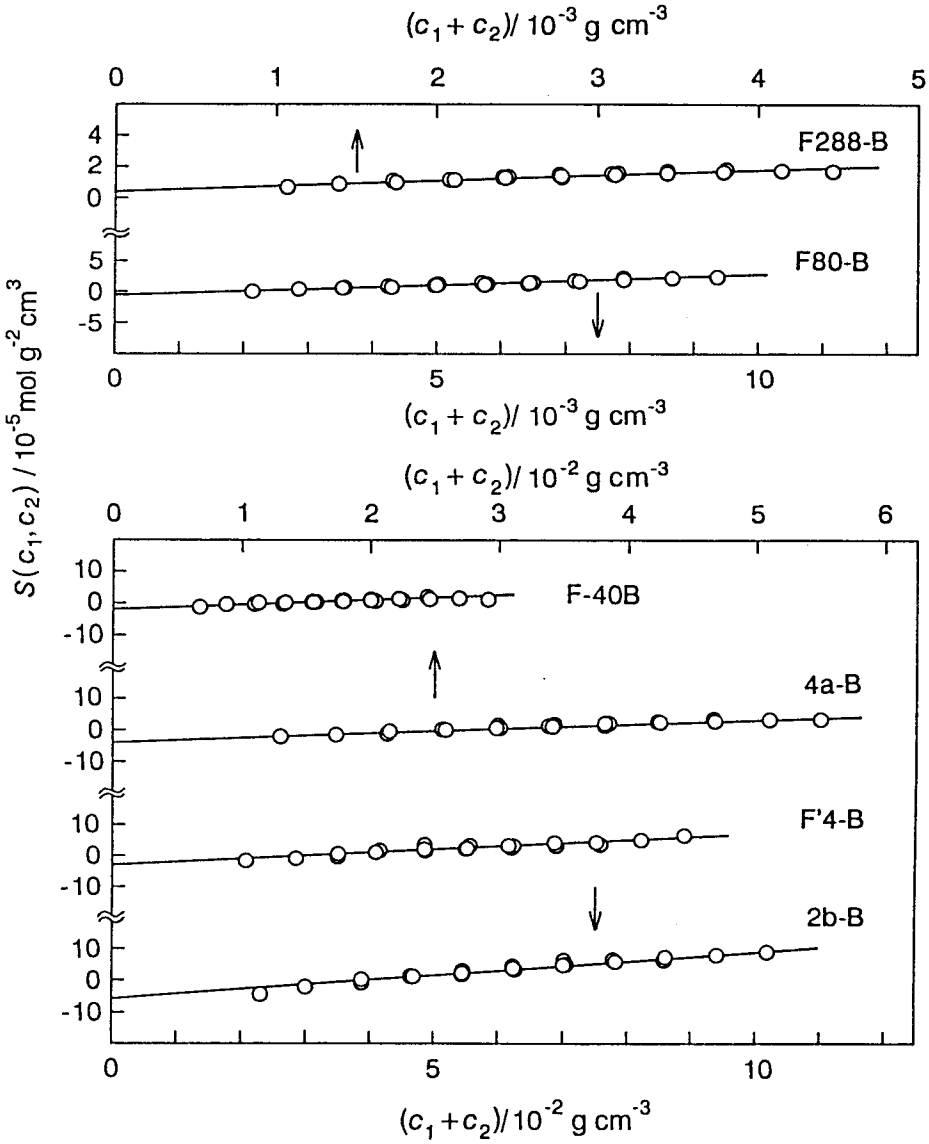

Figure 4.10 Bawn plots for the indicated PS fractions in trans-decalin at 21.0°C.

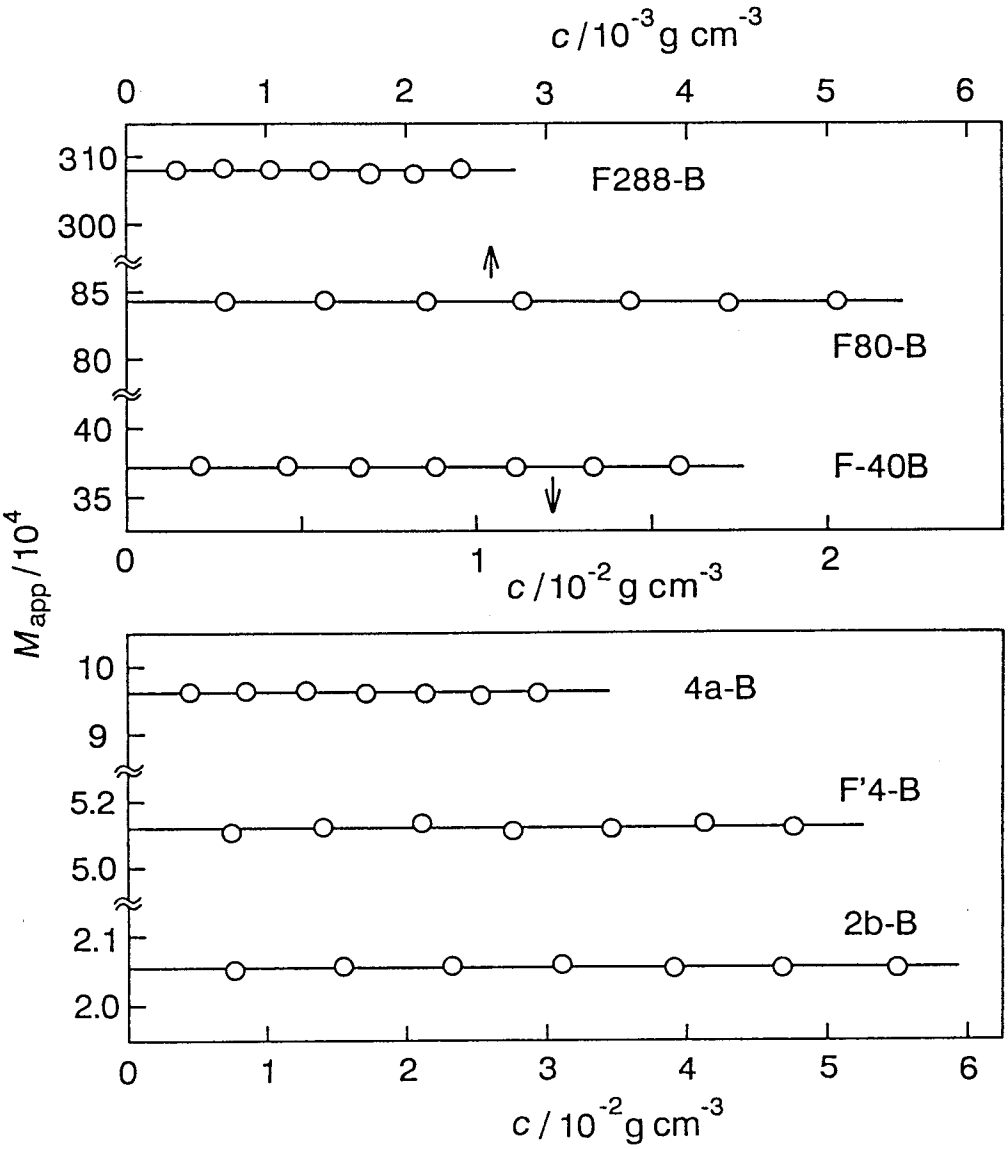

Figure 4.11 Plots of M_{app} vs. c for the indicated PS fractions in trans-decalin at 21.0°C.

Table IV-3

Values of A_2 for Polystyrene Fractions in trans-Decalin at Different Temperatures

	$A_2/10^{-5}$ mol g^{-2} cm^3					
$T/^{o}C$	2b-B M_w = 2.06 x 10^4	F'4-B M_w = 5.12 x 10^4	4a-B M_w = 9.62 x 10^4	F-40B M_w = 37.2 x 10^4	F80-B M_w = 84.3 x 10^4	F288-B M_w = 308 x 10^4
13.0	——	-11.0	-9.5	——	——	——
15.0	-11.4	-7.9	-7.6	-7.0	——	——
17.0	-8.2	-5.5	-5.6	-4.5	-3.8	-3.0
19.0	-5.3	-3.0	-3.5	-2.5	-1.7	-1.0
21.0	-3.0	-1.6	-2.0	-1.0	-0.3	0.2
22.0	-1.5	——	-0.5	——	——	——
23.0	0	-0.1	0	0.2	1.0	1.4
25.0	1.5	1.3	1.7	1.5	2.2	2.3
35.0	9.0	8.0	7.8	7.0	6.6	5.0
45.0	14.8	13.5	12.7	11.0	9.2	7.1
55.0	19.5	18.5	16.0	14.5	11.1	8.9

Table IV-4

Values of A_3 for Polystyrene Fractions in trans-Decalin at Different Temperatures

	$A_3/10^{-4}$ mol g^{-3} cm^6					
T/°C	2b-B M_w = 2.06 x 10^4	F'4-B M_w = 5.12 x 10^4	4a-B M_w = 9.62 x 10^4	F-40B M_w = 37.2 x 10^4	F80-B M_w = 84.3 x 10^4	F288-B M_w = 308 x 10^4
13.0	——	6.3	6.1	——	——	——
15.0	7.5	5.3	5.9	8.0	——	——
17.0	5.9	4.4	5.5	6.1	16	17
19.0	4.9	3.7	4.7	4.4	10	14
21.0	5.0	3.3	4.7	4.4	10	12
22.0	4.4	——	3.7	——	——	——
23.0	3.9	3.9	4.3	4.6	11	12
25.0	3.8	3.8	3.8	4.4	11	11
35.0	4.5	5.0	3.9	5.2	11	28
45.0	5.4	5.6	5.6	6.7	21	39
55.0	6.7	5.7	7.7	8.6	26	48

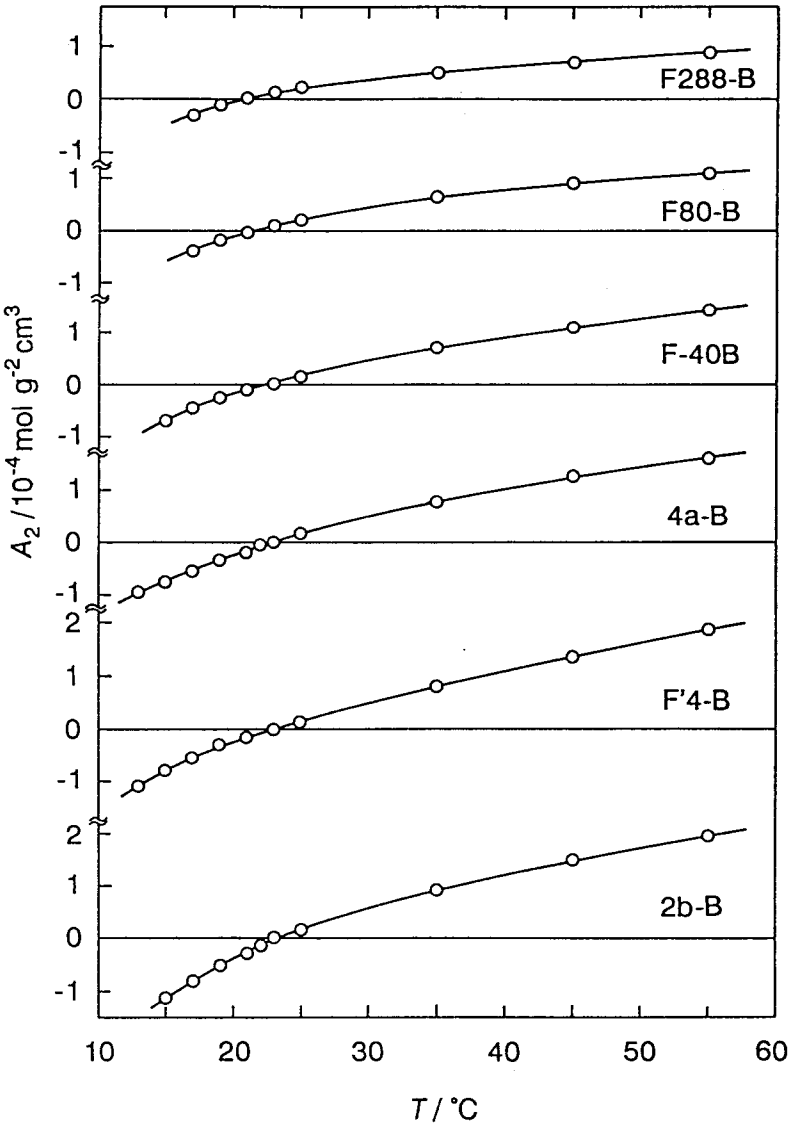

Figure 4.12 Temperature dependence of A_2 for the indicated PS fractions in trans-decalin.

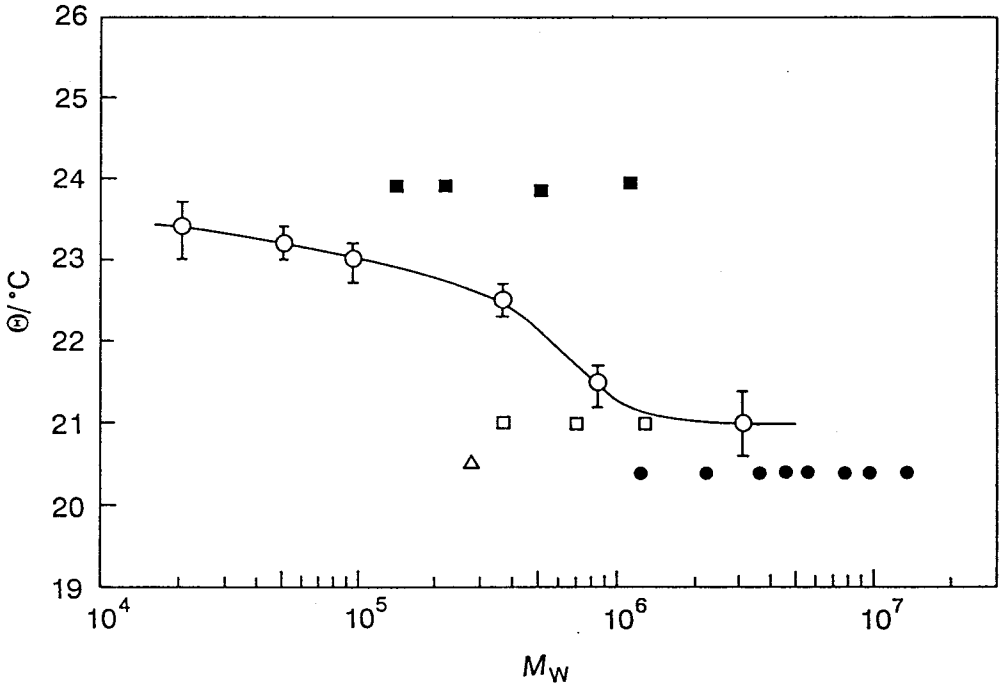

Figure 4.13 Molecular weight dependence of Θ for PS in trans-decalin: (○ with error bars) this work; (■) Inagaki et al.;[65] (●) Fukuda et al.;[37] (△) Nose and Chu;[66] (□) Konishi et al.[64]

from 10^6 to 10^5. This finding is striking, in that Θ for any flexible polymer has long been believed to be independent of molecular weight unless M_w is too low. In the following, we compare in detail our Θ data in trans-decalin with those reported by previous workers.[37,64-66]

The literature data for Θ, all obtained by use of the conventional linear or square-root plot (see eqs 2.11 and 2.12), are shown by different marks in Figure 4.13. Though Berry[52] determined Θ of a PS sample to be 21.3°C, his datum is not included here, because the molecular weight of the sample is not given. It can be seen that the Θ values by different groups are at variance, being in the range 20.4 - 24°C. On the basis of our experience, we estimate the experimental uncertainty of Θ to be $\pm$ 0.5°C. Taking this uncertainty into account, we can say that our Θ data are in rather good agreement with those of Fukuda et al.[37] (the filled circles) and Konishi et al.[64] (the unfilled squares) for M_w above 8 x 10^5 but closer to those of Inagaki et al.[65] (the filled squares) for M_w below 4 x 10^5.

Fukuda et al.[37] found that Θ for Pressure Chemical's (PC's) sample is higher by 3°C than that for their own anionically prepared PS samples shown in

Figure 4.13. They attributed this to a possible but unknown difference in microstructure between the two kinds of sample. However, this interpretation is not conclusive, since for cyclohexane solutions these authors observed no difference in Θ between the samples. It should be noted that our Θ of about 23°C for PC's samples 2b-B and 4a-B ($M_w \sim 2 \times 10^4$ and 10^5) in the figure agrees essentially with that for Tosoh's sample F'4-B ($M_w \sim 5 \times 10^4$). Interestingly, this Θ value is very close to 23.4°C for PC's sample determined by Fukuda et al. from light scattering, though the molecular weight of the sample of these authors is not given.

Nose and Chu's Θ value[66] (the unfilled triangle in Figure 4.13) was determined at relatively high c of 2×10^{-3} to 2×10^{-2} g cm^{-3}. As remarked in section IV.2.4, a conventional plot at such high c leads to an appreciably low Θ unless A_2 is estimated separately from A_3, as was done in the present work (see below for A_3 values at Θ). The discrepancy between our Θ (22.5°C) and Konishi et al.'s (21°C)[64] at $M_w \sim 4 \times 10^5$ in Figure 4.13 remains to be seen. The two Θ values ought to agree with each other, since the scattering data of the latter group were taken at sufficiently low c for Tosoh's sample F-40, the same as our F-40B in its

origin. In passing, we determined Θ for the same sample F-40 (M_w = 3.71 x 10^5) as Konishi et al.'s from additional light scattering measurements to be 22.0°C, which is slightly higher than Konishi et al.'s value but agrees substantially with 22.5 (± 0.2)°C for our fractionated sample F-40B.

In Appendix A, it is shown that the intrinsic viscosity [η] in trans-decalin at 21°C (Θ for high molecular weight samples) varies as $M_w^{1/2}$ and that below $M_w \sim 4 \times 10^5$, [η] values at 21 and 23°C are approximately the same. Thus, the Gaussian behavior of [η] is observed at 21°C down to $M_w \sim 2 \times 10^4$ despite the fact that Θ for $M_w < 10^5$ is about 23°C. In other words, Θ for the PS + trans-decalin system would erroneously be concluded to be 21°C regardless of M_w, if it were determined only for samples with M_w higher than 8 x 10^5.

IV.3.2 Third Virial Coefficient

Figure 4.14 shows the temperature dependence of A_3 for the indicated fractions in trans-decalin. The general features of the curves are very similar to those for cyclohexane solutions in Figure 4.6, and in

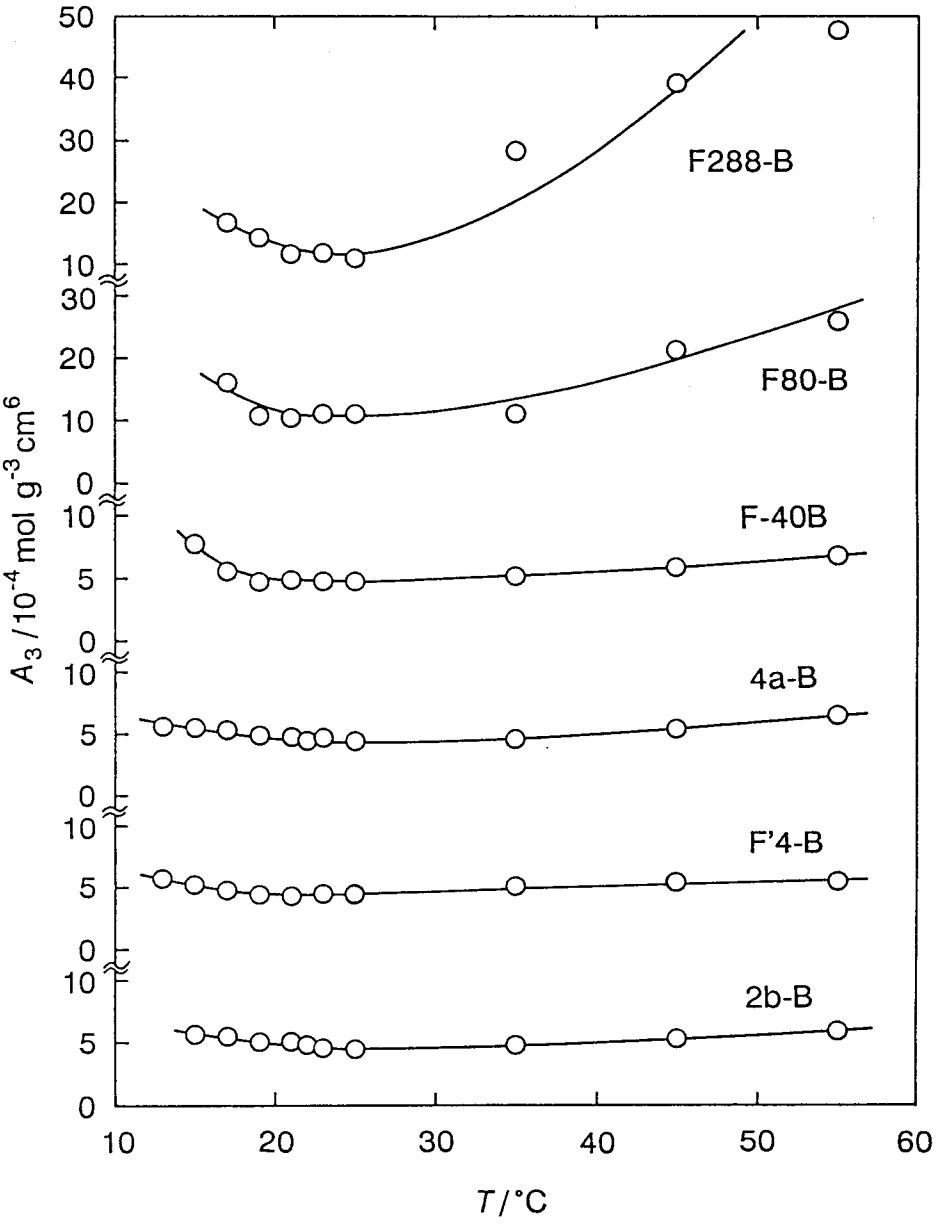

Figure 4.14 Temperature dependence of A_3 for the indicated PS fractions in trans-decalin.

particular, A_3 in trans-decalin also remains positive at any T encompassing Θ.

IV.4 Discussion

A_3 at the theta point

The molecular weight dependence of A_3 for PS in cyclohexane at 34.5°C and in trans-decalin at 21.0°C is shown in Figure 4.15, along with that for PS in benzene at 25°C.

Although the temperatures of 34.5°C for cyclohexane and 21.0°C for trans-decalin are the theta points for high molecular weight samples, i.e., not always equal to Θ for low molecular weight ones, the indicated A_3 data in the two solvents may be equated to $A_3(\Theta)$ (those at Θ) within experimental errors, because A_3 very near Θ is insensitive to T as shown in Figures 4.6 and 4.14.

The two sets of data for $A_3(\Theta)$ in Figure 4.15 happen to be almost superimposed on a single curve, which is essentially horizontal with $A_3(\Theta) \sim 4.5 \times 10^{-4}$ mol g^{-3} cm^6 for $2 \times 10^4 \lesssim M_w \lesssim 5 \times 10^5$ and appears to rise with increasing M_w for $M_w \gtrsim 5 \times 10^5$. We note, however, that no much emphasis can be put on this upswing of $A_3(\Theta)$ at high M_w since our light scattering

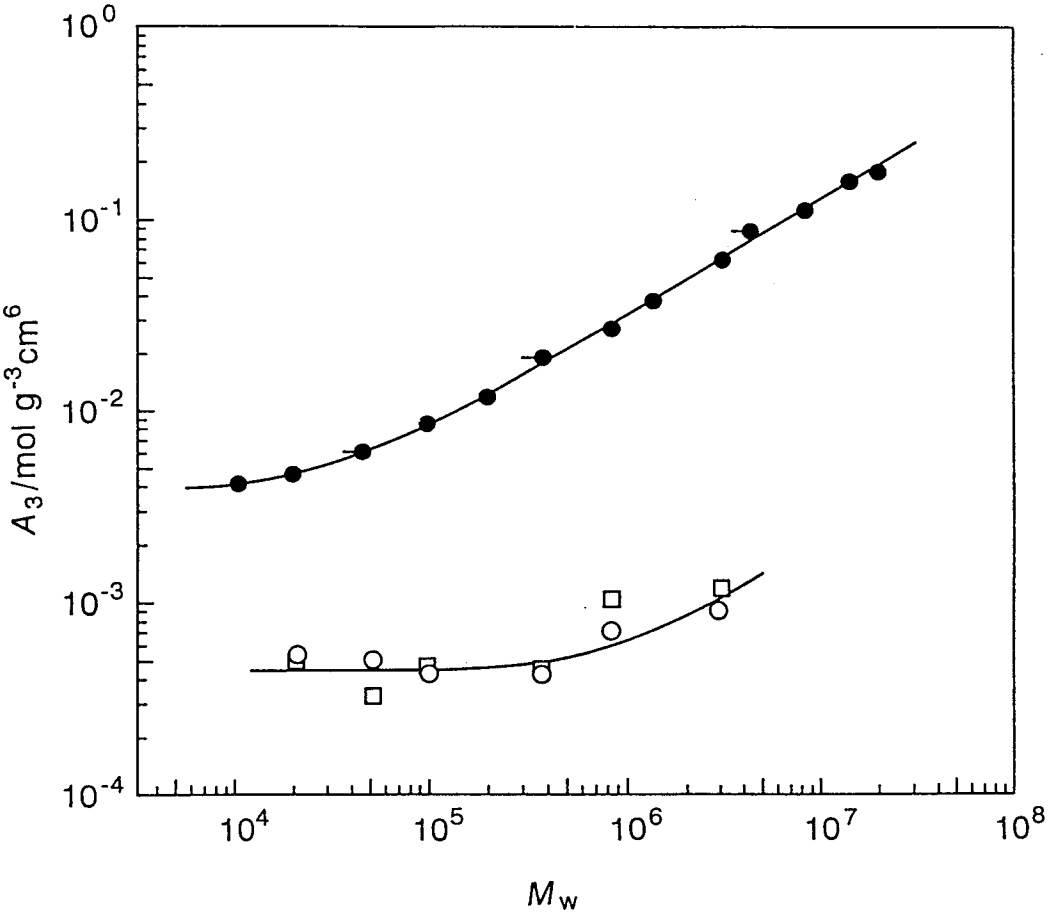

Figure 4.15 Molecular weight dependence of A_3 for PS in cyclohexane at 34.5°C (○), in trans-decalin at 21.0°C (□), and in benzene at 25°C (●): (-●) data of Sato et al.[26] for PS in benzene at 25°C.

measurements on high molecular weight fractions were confined to low-concentration regions in which $S(c_1, c_2)$ values in the Bawn plot are not removed much from zero (see Figures 4.3 and 4.10). It is important to observe in Figure 4.15 that the $A_3(\Theta)$ values are one or two orders of magnitude smaller than those in the good solvent benzene at any M_w.

Since A_3 near Θ remains positive in both cyclohexane and trans-decalin, it is mandatory to take three-body segment interactions into consideration in discussing A_3 near the theta point. In the following, we compare the present data with the first-order perturbation theory[15,18] for A_3 formulated with the ternary cluster integral β_3 incorporated, i.e.,

$$A_3 = \frac{N_A{}^2 n^3}{3M^3} (\beta_3 + \text{orders in } \beta_2\beta_3,\ \beta_3{}^2, \text{ and } \beta_2{}^3)$$

$$= \frac{N_A{}^2}{3} \left(\frac{4\pi \langle S^2 \rangle_0}{M}\right)^3 (z_3 + \ldots) \qquad (4.2)$$

where

$$z_3 = \left(\frac{3}{2\pi b^2}\right)^3 \beta_3 \qquad (4.3)$$

According to eq 4.2, A_3 is independent of M when

both β_2 and β_3 are vanishingly small. This is consistent with the behavior of $A_3(\Theta)$ observed for $M_w \lesssim 4 \times 10^5$ in Figure 4.15. If as was proposed by Cherayil et al.,[15] eq 4.2 is applied to the $A_3(\Theta)$ data in this molecular weight region, a value of $4 (\pm 1) \times 10^{-45}$ cm^6 is obtained for β_3 in both cyclohexane and trans-decalin. This value in turn yields $z_3 \sim 0.003$ in cyclohexane and $z_3 \sim 0.005$ in trans-decalin when use is made of the $\langle S^2 \rangle_0 - M_w$ relation of Miyaki et al.[33,38] for the former and that of Konishi et al.[64] for the latter. These z_3 values may be considered essentially the same within the uncertainty in their determination; the difference between them arises from that in b between the two solvents (0.74nm in cyclohexane and 0.68nm in trans-decalin).

Very recently, Chen and Berry[67] showed that $Kc/R_0 - 1/M_w$ for a PS sample ($M_w = 8.6 \times 10^5$) in cyclohexane at Θ increases almost linearly with c^2 in a concentration region roughly from $0.7c^*$ to $4c^*$. They took this finding as evidence for the nonvanishing of $A_3(\Theta)$ and estimated z_3 at Θ to be 0.0045, using the experimental $A_3(\Theta)$ and eq 4.2. This z_3 value is close to our estimate 0.003 in the same solvent.

Molecular Weight Dependence of A_2 near the Theta Point

From the foregoing discussion, it is evident that β_3 for PS in either cyclohexane or trans-decalin cannot be ignored near the theta point. In this subsection, we compare the A_2 data in cyclohexane at 34.5°C and trans-decalin at 21.0°C with the currently available theories[11,12,15] which take β_3 into account.

The first-order perturbation theory[12,15] for A_2 is written in the form

$$A_2 = \frac{N_A n^2}{2M^2} \{\beta_2 + \frac{4}{\sigma^{1/2}}(\frac{3}{2\pi b^2})^{3/2} \beta_3[1 - 2(\frac{\sigma}{n})^{1/2}]$$

$$+ \text{orders in } \beta_2^2,\ \beta_2\beta_3, \text{ and } \beta_3^2\} \qquad (4.4)$$

where σ is a cut-off parameter which approximately represents a minimum number of consecutive segments necessary for the formation of a loop in one chain; it should be much smaller than n. We note that the $n^{-1/2}$ term in the braces of eq 4.4 is not affected by the stiffness or non-Gaussian nature of short chains (see Appendix B).

Equation 4.4 indicates that the theta state for sufficiently long chains, signified by Θ_∞ in the ensuing presentation, is attained by compensation of

negative β_2 and positive $4\sigma^{-1/2}(3/2\pi b^2)^{3/2}\beta_3$ values provided both β_2 and β_3 are vanishingly small. Thus, under this condition, $A_2(\Theta_\infty)$ (A_2 at Θ_∞) is represented by

$$A_2(\Theta_\infty) = -\frac{4N_A n^2}{M^2}\left(\frac{3}{2\pi b^2}\right)^{3/2}\frac{\beta_3}{n^{1/2}} \qquad (4.5)$$

which predicts that $A_2(\Theta_\infty)$ varies as $-1/n^{1/2}$. This is in line with results from computer simulations.[68-71]

Figure 4.16 compares the experimental $A_2(\Theta_\infty)$ values for PS in cyclohexane (the unfilled circles) and trans-decalin (the squares) with the solid curve computed from eq 4.5 for $\beta_3 = 4 \times 10^{-45}$ cm^6 (estimated above from A_3) and $b = 0.7$ nm; the Θ_∞ values in cyclohexane and trans-decalin have been taken as 34.5 and 21.0°C, respectively. The figure includes Huber and Stockmayer's data[7] (the filled circles) in cyclohexane (in their case, $\Theta_\infty = 35$°C). The solid curve comes fairly close to the data points in trans-decalin for $M_w \gtrsim 10^5$. However, its decline with decreasing molecular weight is incompatible with the cyclohexane points, which stay zero down to $M_w \sim 5 \times 10^4$ and then sharply go up. The discrepancy occurs whatever value may be taken for β_3, as may be seen from eq 4.5. We therefore conclude that the first-order perturbation

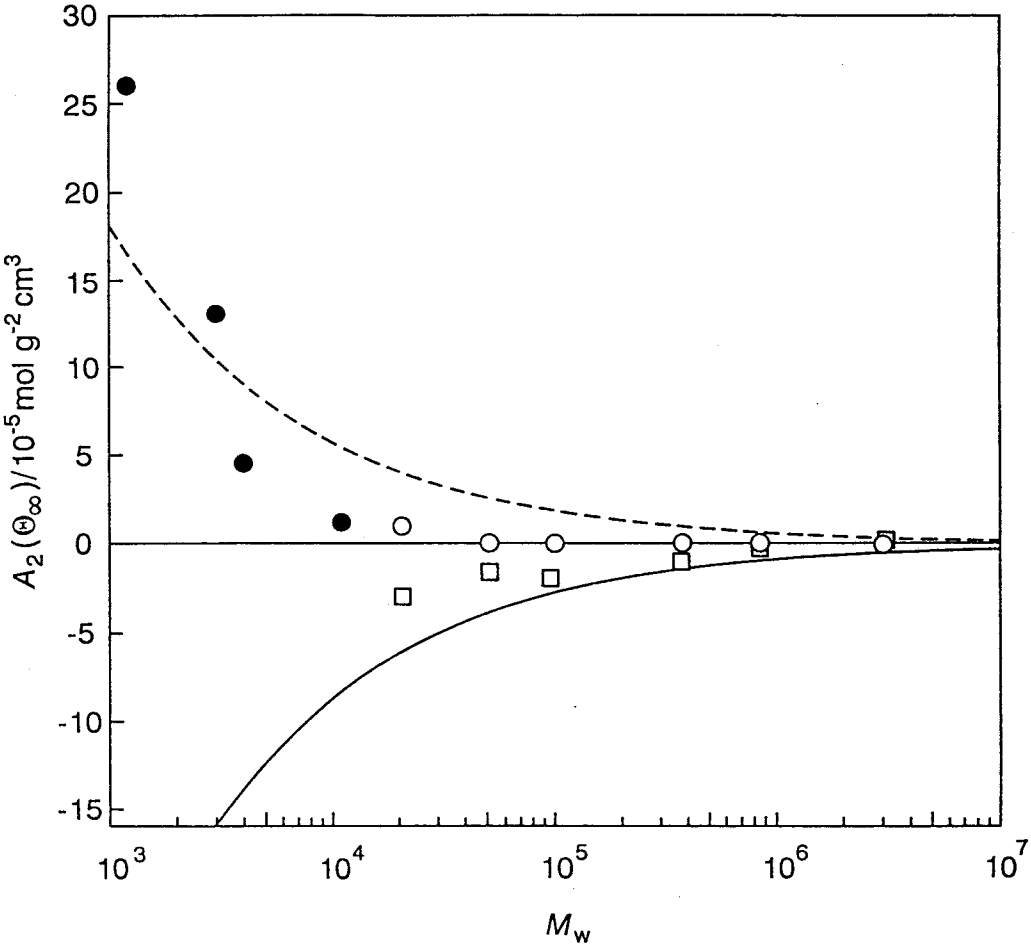

Figure 4.16 Molecular weight dependence of A_2 for PS in trans-decalin at 21.0°C (□) and in cyclohexane at 34.5°C (○). The filled circles represents the data of Huber and Stockmayer[7] for PS in cyclohexane. The solid curve is computed from eq 4.5 and the dashed one, from eq 4.6 (see the text).

theory fails to give a consistent explanation for the observed M_w-dependence of $A_2(\Theta_\infty)$ in cyclohexane and that in trans-decalin.

Huber and Stockmayer[7] found that the upswing of the experimental $A_2(\Theta_\infty)$ in cyclohexane at low M_w in Figure 4.16 can be explained qualitatively by the smoothed-density theory of Orofino and Flory[11] for A_2. Near Θ, this theory (see eq 5.12 in Chapter V) is written in the form

$$A_2 = \frac{N_A n^2}{2M^2} \{\beta_2 + 3^{3/2}(\frac{3}{2\pi b^2})^{3/2} \frac{\beta_3}{n^{1/2}} + \ldots \} \qquad (4.6)$$

which indicates that the condition for Θ_∞ is given by $\beta_2 = 0$ and hence that $A_2(\Theta_\infty)$ varies as $1/n^{1/2}$ (compare with eq 4.5). The dashed line in Figure 4.16 represents the theoretical value of $A_2(\Theta_\infty)$ computed from eq 4.6 with $\beta_2 = 0$ for the same β_3 and b values as above. Though its rise with a decrease in molecular weight is consistent with the cyclohexane data, the curve begins to deviate appreciably from zero at as high a molecular weight as 3×10^6, and moreover it contradicts the data in trans-decalin in which $A_2(\Theta_\infty)$ decreases with lowering M_w.

Apart from the above comparisons between theory and experiment, the discrepancy between the perturba-

tion and smoothed-density theories themselves cannot be overlooked. It is serious, in that the two types of theory give different explanations of Θ_∞ unless β_3 happens to be zero: The condition for Θ_∞ is given by $\beta_2 + 4(3/2\pi b^2)^{3/2}\beta_3/\sigma^{1/2} = 0$ in the perturbation theory, while it is given by $\beta_2 = 0$ in the smoothed-density theory. In the next chapter, we show that the Orofino-Flory theory[11] is incorrect for nonzero β_3 and that a correct treatment of the smoothed-density model leads to an expression consistent with the first-order perturbation calculation. Thus, Huber and Stockmayer's explanation mentioned above has no theoretical base.

In short, the first-order perturbation theory is the only one that is currently reliable for A_2 very near Θ, but as shown above, it fails to explain consistently our $A_2(\Theta_\infty)$ data. Second and higher order calculations on A_2 and A_3 may be worth trying. However, we deem it necessary to find a certain physical factor in addition to β_3, overlooked in the current polymer solution theory. The reason is that the observed opposite M_w-dependencies of $A_2(\Theta_\infty)$ in cyclohexane and trans-decalin seem difficult to explain on the basis of essentially the same $A_3(\Theta)$ values and hence approximately the same β_3 or z_3 values in the

two solvents. As shown in Appendix B, the stiffness of polymer chains does not affect $A_2(\Theta_\infty)$ to first order. At present, we are unable to say what the factor is.

Appendix A

Intrinsic Viscosity of PS in trans-Decalin

Intrinsic viscosities $[\eta]$ for six PS fractions in trans-decalin at 21 and 23°C were determined, using a conventional capillary viscometer of the Ubbelohde type. The results are shown in the form of log $[\eta]$ vs. log M_w in Figure A.1, in which the unfilled and filled circles refer to 21 and 23°C (i.e., the theta temperature for high and low molecular weight fractions), respectively. The unfilled circles are fitted accurately by a straight line having the slope 0.5 expected for Gaussian chains, i.e., for long flexible chains in the theta state. The filled circles fall on the same line for $M_w < 4 \times 10^5$ and deviate upward from it for $M_w > 8 \times 10^5$. Thus, $[\eta]$ is virtually unaffected by the temperature difference of 2°C if M_w is lower than 4×10^5. It is instructive to notice that without precise Θ data in this M_w region, Θ for the PS + trans-decalin system might be concluded to be 21°C regardless of M_w.

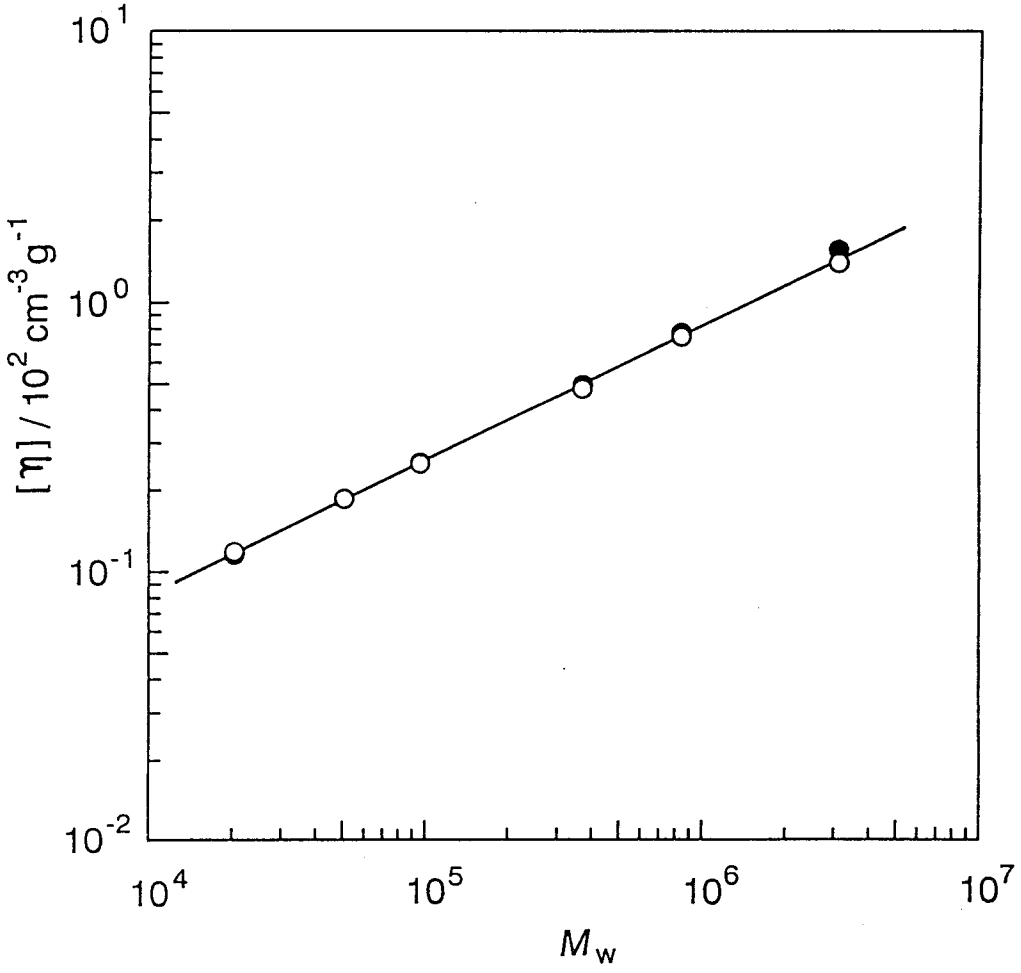

Figure A.1 Molecular weight dependence of intrinsic viscosity for PS in trans-decalin at 21°C (○) and 23°C (●). The indicated straight line has a slope of 0.5.

Appendix B

Perturbation Calculation of A_2 for Wormlike Chains

Equation 4.4 is based on the Gaussian chain model valid for infinitely long chains. Thus, we ought to examine whether the $n^{-1/2}$ term in it is affected by chain stiffness. To this end, with the Kratky-Porod wormlike chain,[72] a typical model for stiff polymers, we perform a first-order perturbation calculation on A_2 in this appendix.

This model chain is characterized by two parameters, the contour length L of the chain and Kuhn's segment length λ^{-1}. The latter is just twice the persistence length of the chain and a direct measure of stiffness associated with chain bending. Following Yamakawa and Stockmayer,[73] we use a wormlike bead model, i.e., an array of n beads, each being separated by spacing b along the chain contour. In this model, L is equal to nb, and the interaction between two beads and that among three beads (two belonging to one chain and the rest belonging to the other chain) are represented by β_2 and β_3, respectively.

For simplicity, we assume b to equal λ^{-1} and measure every contour distance in units of λ^{-1}, so

that the reduced contour length $\lambda L = n$. Then, A_2 near Θ is expressed as

$$A_2 = \frac{N_A n^2}{2M_2} \{\beta_2 + \frac{2\beta_3}{nb^3} \int_0^n (n - t) G(0; t)\, dt + \ldots\} \tag{B-1}$$

where t denotes the reduced contour distance between two beads belonging to one of the two interacting chains and $G(0; t)$, the ring-closure probability, i.e., the distribution function representing the probability of contact of the two beads separated by t along the chain contour. Yamakawa and Stockmayer[73] evaluated this function to be

$$G(0; t) = (\frac{3}{2\pi})^{3/2} g_0(t) \tag{B-2}$$

where

$$g_0(t) = \begin{cases} \frac{C_0}{t} e^{-A/t} (1 + C_1 t) & (t \leqq 0.96093) \\ \frac{1}{t^{3/2}} (1 - \frac{5}{8t} - \frac{79}{640 t^2}) & (t > 0.96093) \end{cases} \tag{B-3}$$

with $C_0 = 1504.9$, $C_1 = -0.81242$, and $A = 7.0266$.

Substituting of eq B-2 with eq B-3 into eq B-1, followed by integration, gives

$$A_2 = \frac{N_A n^2}{2M^2} \{\beta_2 + (\frac{3}{2\pi b^2})^{3/2} \beta_3 [3.160 - \frac{8}{n^{1/2}} + O(\frac{1}{n})] + \ldots \} \qquad (B\text{-}4)$$

Comparison with eq 4.4 shows that the $n^{-1/2}$ term in eq 4.4 for Gaussian chains is unaffected by chain stiffness. Note that if σ is taken to be 1.602, the two equations coincide with each other up to the order $n^{-1/2}$.

Chapter V

Remarks on Smoothed-Density Theories for Flexible Chains with Three-Segment Interactions

V.1 Introduction

As discussed in the preceding chapter, the Orofino-Flory (OF) smoothed-density theory[11] for A_2 is inconsistent with the first-order perturbation calculation[12,15] unless the ternary cluster integral β_3 happens to be zero. This inconsistency was pointed out first by Yamakawa[12] about 25 years ago, but its origin has been left unexplored. Tanaka[14] presented a mean-field theory for A_2 (based on the smoothed-density sphere model) taking β_3 into account, and qualitatively explained the molecular weight-independent behavior[4-6] of A_2 below Θ. However, the Tanaka theory is essentially equivalent to the OF theory and hence inconsistent with the perturbation calculation. Yamakawa[12] also showed a similar inconsistency to exist in the end-distance expansion factor α_R defined by $\alpha_R^2 = \langle R^2\rangle/\langle R^2\rangle_0$, with $\langle R^2\rangle$ and $\langle R^2\rangle_0$ being the mean-square end-to-end distances in the perturbed and unperturbed

states, respectively.

In this chapter, we investigate the origin of these inconsistencies between the smoothed-density and first-order perturbation theories, confining ourselves to infinitely long chains. First, we calculate A_2 using the smoothed-density model but taking into account chain connectivity which is ignored in the OF theory. Then, a similar calculation is made on α_R^2. The results demonstrate that the neglect of chain connectivity in the OF theories for both A_2 and α_R^2 is responsible for the above-mentioned inconsistencies. We also examine the validity of the uniform expansion approximation[2] to α_R^2 near Θ, by carrying out a second-order perturbation calculation.

V.2 Second Virial Coefficient

We consider two identical, long flexible chains of molecular weight M each of which is Gaussian in the unperturbed state. Given an average intermolecular potential V_{12} as a function of the distance S_{12} between the centers of mass of the two chains, A_2 may be expressed by[11]

$$A_2 = \frac{N_A}{2M^2} \int \{1 - \exp[-V_{12}(S_{12})/k_B T]\} dS_{12} \qquad (5.1)$$

Taking two- and three-segment interactions into account, we may express V_{12} in the smoothed-density model as[2]

$$V_{12}(S_{12})/k_BT = \beta_2 \sum_{i_1=1}^{n} \sum_{i_2=1}^{n} \int P_{i_1}(s) P_{i_2}(s - S_{12}) ds$$

$$+ 2\beta_3 \sum_{i_1=1}^{n} \sum_{j_1=i_1+1}^{n} \sum_{i_2=1}^{n} \int P_{i_1 j_1}(s,s) P_{i_2}(s - S_{12}) ds \qquad (5.2)$$

Here, $P_{i_1}(s)$ [or $P_{i_2}(s)$] denotes the distribution function for the distance vector s of segment i_1 in chain 1 (or segment i_2 in chain 2) from the center of mass, and $P_{i_1 j_1}(s,s)$, the bivariate distribution function representing the probability that a pair of segments i_1 and j_1 in chain 1 are located at s.

We consider no intramolecular excluded-volume effect. Then, the distribution functions $P_{0 i_1}(s)$ and $P_{0 i_1 j_1}(s,s)$ in the unperturbed state are obtained by the standard method[2] as

$$P_{0 i_1}(s) = (3/2\pi \langle S_{i_1}{}^2 \rangle_0)^{3/2} \exp(-3s^2/2\langle S_{i_1}{}^2 \rangle_0) \qquad (5.3)$$

$$P_{0 i_1 j_1}(s,s) = [3/2\pi b^2(j_1 - i_1)]^{3/2}(3/2\pi \langle D_{i_1 j_1}{}^2\rangle_0)^{3/2}$$

$$\times \exp(-3s^2/2\langle D_{i_1 j_1}{}^2\rangle_0)$$

$$(\text{for } j_1 > i_1) \qquad (5.4)$$

where

$$\langle S_{i_1}{}^2\rangle_0 = \frac{nb^2}{3}\left(1 - \frac{3i_1}{n} + \frac{3i_1{}^2}{n^2}\right) \qquad (5.5)$$

$$\langle D_{i_1 j_1}{}^2\rangle_0 = \frac{nb^2}{3}\left[1 - \frac{3j_1}{n} + \frac{3j_1{}^2}{n^2} - \frac{3(j_1{}^2 - i_1{}^2)(j_1 + i_1)}{4n^3}\right] \qquad (5.6)$$

The segment density distribution function $\sum_{i_1} P_{0 i_1}(s)$ may be replaced in a good approximation[2] by

$$\sum_{i_1} P_{0 i_1}(s) = n(3/2\pi\langle S^2\rangle_0)^{3/2} \exp(-3s^2/2\langle S^2\rangle_0) \qquad (5.7)$$

with $\langle S^2\rangle_0 = nb^2/6$. To evaluate $\sum_{i_1<j_1} P_{0 i_1 j_1}(s,s)$ we introduce a cut-off parameter σ which approximately represents a minimum number of consecutive segments necessary for the formation of a loop in one chain, so that $i_1 \leq j_1 - \sigma$. With this parameter, $\sum P_{0 i_1 j_1}(s,s)$ for very large n may be evaluated first by integration over i_1 by part and then by use of the above Gaussian

approximation to $\sum_{j_1} P_{0j_1}(s)$ (i.e., eq 5.7 with the sum replaced by an integral). The result thus obtained reads

$$\sum_{i_1<j_1} P_{0i_1j_1}(s,s) = \frac{2n^{5/2}}{6^{3/2}\sigma^{1/2}} \left(\frac{3}{2\pi\langle S^2\rangle_0}\right)^3 \exp\left(-\frac{3s^2}{2\langle S^2\rangle_0}\right)$$

$$(n^{1/2} >> \sigma^{1/2} > 1) \qquad (5.8)$$

Substitution of eqs 5.7 and 5.8, together with a similar expression for $P_{0i_2}(s - S_{12})$, into eq 5.2, followed by integration, yields

$$V_{12}(S_{12})/k_BT = 3^{3/2}[z_2 + 4(\frac{n}{\sigma})^{1/2}z_3] \exp(-3S_{12}^2/4\langle S^2\rangle_0) \qquad (5.9)$$

where z_2 and z_3 are the excluded-volume parameters defined by eqs 3.5 and 4.3, respectively. The integral in eq 5.1 with eq 5.9 is approximately evaluated by the OF procedure[11] to give

$$A_2 = \frac{16\pi N_A\langle S^2\rangle_0^{3/2}}{3^{3/2}M^2} \ln\left[1 + \frac{3^{3/2}\pi^{1/2}}{4}(z_2 + 4(\frac{n}{\sigma})^{1/2}z_3)\right] \qquad (5.10)$$

for positive or small negative A_2. If intramolecular

excluded-volume effect is introduced by invoking the uniform expansion approximation,[2] $\langle S^2\rangle_0^{3/2}$, z_2, and z_3 in this expression are replaced by $\langle S^2\rangle_0^{3/2}\alpha^3$, z_2/α^3, and z_3/α^6, respectively, with α being an expansion factor.

When $z_2 + 4(n/\sigma)^{1/2}z_3$ is much smaller than unity, eq 5.10 gives

$$A_2 = \frac{N_A n^2}{2M^2}\left[\beta_2 + \frac{4}{\sigma^{1/2}}\left(\frac{3}{2\pi b^2}\right)^{3/2}\beta_3 + \ldots\right] \qquad (5.11)$$

which conforms to eq 4.4 for infinite n, i.e., to the first-order perturbation calculation. Equation 4.4 can be derived from eq 5.1 with eqs 5.2 through 5.6 (or even by use of the Gaussian approximation for ΣP_{0i_1}). Either eq 5.10 or 5.11 indicates that Θ_∞ is the temperature at which $\beta_2 + 4\sigma^{-1/2}(3/2\pi b^2)^{3/2}\beta_3 = 0$.

If $P_{0i_1j_1}(s,s)$ is approximated by $P_{0i_1}(s)P_{0j_1}(s)$ and if eq 5.7 is used, V_{12} is obtained as

$$V_{12}(S_{12})/k_BT = 3^{3/2}[z_2\exp(-3S_{12}^2/4\langle S^2\rangle_0) + 8z_3\exp(-S_{12}^2/\langle S^2\rangle_0)]$$

This is the OF potential and leads to the OF expression[11] (without intramolecular excluded volume):

$$A_2 = \frac{16\pi N_A \langle S^2 \rangle_0^{3/2}}{3^{3/2} M^2} \ln\left[1 + \frac{3^{3/2}\pi^{1/2}}{4}(z_2 + 3^{3/2} z_3)\right] \qquad \text{(OF)} \quad (5.12)$$

Note that the parameters X_1 and X_2 in eq 17 of ref 11 are equal to $3^{3/2}z_2$ and $8 \cdot 3^{3/2}z_3$, respectively.[12] In the vicinity of Θ, eq 5.12 gives eq 4.6.

The OF equation 5.12 differs from eq 5.10 in the ternary cluster term. Apparently, this discrepancy results from the above replacement of $P_{0 i_1 j_1}(s, s)$ by $P_{0 i_1}(s) P_{0 j_1}(s)$. Thus, we find that the inconsistency of the OF theory with the first-order perturbation calculation arises from this factorization approximation, i.e., ignoring the effect of chain connectivity on the probability of segment collision in one of the two interacting chains. This allows us to conclude that the vanishing of β_2 cannot be regarded as the theta condition for long chains unless β_3 happens to be zero.

V.3 End-Distance Expansion Factor

As mentioned in section V.1, the smoothed-density[11] and perturbation[12] theories for α_R are also inconsistent. The former leads to

$$\alpha_R^2 = 1 + d_1 z_2 + d_2 z_3 + \ldots \quad \text{(smoothed-density)} \tag{5.13}$$

with d_1 and d_2 being positive constants, while the latter is shown to give for large n

$$\alpha_R^2 = 1 + \frac{4}{3}\left[z_2 + 4\left(\frac{n}{\sigma}\right)^{1/2} z_3\right] + \ldots \quad \text{(perturbation)} \tag{5.14}$$

Thus, apart from the numerical constants, the two expressions differ again in the molecular weight dependence of ternary cluster term.

The end-to-end distance of a smoothed-density chain may be calculated from[2]

$$\langle R^2 \rangle = \left(\int R^2 P_0(R)\ e^{-V(R)/k_B T}\, dR\right) \Big/ \left(\int P_0(R)\ e^{-V(R)/k_B T}\, dR\right) \tag{5.15}$$

using the unperturbed distribution function $P_0(R)$ for the end-to-end vector R and the intramolecular poten-

tial $V(\boldsymbol{R})$ given, respectively, by

$$P_0(\boldsymbol{R}) = (3/2\pi nb^2)^{3/2} \exp(-3R^2/2nb^2) \qquad (5.16)$$

$$V(\boldsymbol{R})/k_B T = \beta_2 \sum_{i<j} \int P_{ij}(\boldsymbol{s}, \boldsymbol{s} \mid \boldsymbol{R})\, d\boldsymbol{s} + \beta_3 \sum_{i<j<k} \int P_{ijk}(\boldsymbol{s}, \boldsymbol{s}, \boldsymbol{s} \mid \boldsymbol{R})\, d\boldsymbol{s} \qquad (5.17)$$

In eq 5.17, $P_{ij}(\boldsymbol{s}, \boldsymbol{s} \mid \boldsymbol{R})$ denotes the conditional probability density of finding both segments i and j at distance $\boldsymbol{s}$ from the center of mass under the condition that the end-to-end vector of the chain is fixed to $\boldsymbol{R}$; $P_{ijk}(\boldsymbol{s}, \boldsymbol{s}, \boldsymbol{s} \mid \boldsymbol{R})$ is self-explanatory. We evaluated these functions first in the unperturbed state (see ref 2 for the procedure) and then transformed them to those in the perturbed state using the uniform expansion approximation. The result thus obtained for $V(\boldsymbol{R})$ is written as

$$\frac{V(\boldsymbol{R})}{k_B T} = \frac{z_2}{\alpha_R^3} \sum_{i<j} \frac{n}{[(j-i)(n-j+i)]^{3/2}} \times \exp\left[-\frac{3(j-i)R^2}{2nb^2\alpha_R^2(n-j+i)}\right] + \frac{z_3}{\alpha_R^6} \sum_{i<j<k} \frac{n^{3/2}}{[(k-j)(j-i)(n-k+i)]^{3/2}}$$

$$\times \exp\left[-\frac{3(k-i)R^2}{2nb^2\alpha_R^2(n-k+i)}\right] \qquad (5.18)$$

In passing, we note that there hold the relations $\int P_{0ij}(s,s|R)ds = P_0(0_{ij}|R)$ and $\int P_{0ijk}(s,s,s|R)ds = P_0(0_{ij},0_{ik}|R)$, with $P_0(0_{ij}|R)$, for example, being the conditional distribution function for the contact of segments i and j under the condition of fixed R.

Using the Hermans-Overbeek[74] approximation after substitution of eqs 5.16 and 5.18 into eq 5.15, we get

$$\alpha_R^5 - \alpha_R^3 = z_2 \sum_{i<j} \frac{n}{(j-i)^{1/2}(n-j+i)^{5/2}} \times \exp\left[-\frac{3(j-i)}{2(n-j+i)}\right] + \frac{z_3}{\alpha_R^3} \sum_{i<j<k} \frac{n^{3/2}(k-i)}{[(j-i)(k-j)]^{3/2}(n-k+i)^{5/2}} \times \exp\left[-\frac{3(k-i)}{2(n-k+i)}\right] \qquad (5.19)$$

which in turn gives

$$\alpha_R^5 - \alpha_R^3 = \left(\frac{2\pi}{3}\right)^{1/2}\left[z_2 + 4\left(\frac{n}{\sigma}\right)^{1/2}\frac{z_3}{\alpha_R^3}\right] \qquad (5.20)$$

When α_R is close to unity, this equation agrees with

eq 5.14 excepting the slight difference between the numerical constants $(2\pi/3)^{1/2}$ (in eq 5.20) and 4/3 (in eq 5.14); this difference is due to the Hermans-Overbeek approximation. Equation 5.20 differs in the z_3 term from the OF type equation:[11]

$$\alpha_R^5 - \alpha_R^3 = d_1 z_2 + d_2 \frac{z_3}{\alpha_R^3} \qquad \text{(OF type)} \qquad (5.21)$$

The latter can be derived when $P_{ij}(s,s \mid R)$ and $P_{ijk}(s,s,s \mid R)$ in eq 5.17 are approximated by $P_i(s \mid R)P_j(s \mid R)$ and $P_i(s \mid R)P_j(s \mid R)P_k(s \mid R)$, respectively. Thus, it may be concluded that, as is the case with A_2, the factorization approximation is responsible for the discrepancy between the z_3 terms of the OF and perturbation equations and that the OF type theories for A_2 and α_R are incorrect unless $\beta_3 = 0$.

V.4 Discussion

We have shown that chain connectivity plays a crucial role in the ternary cluster terms of A_2 and α_R^2. As may be seen from eq 5.19, a pair of segments (i and j or j and k) close to each other contributes primarily to the z_3 term in eq 5.20; this is also the case with A_2 (see eq 5.4). Since a chain portion

consisting of a small number of segments may not be fully perturbed, the uniform expansion approximation invoked in deriving eq 5.20 is likely to be invalid for the ternary cluster term of α_R at least near Θ. If $j - i$ and $k - j$ segments are unperturbed for j between i and $i + t$ and between $k - t$ and k (for $k - i > 2t$) and if $n^{1/2} >> t^{1/2} >> \sigma^{1/2}$, it can be shown that z_3 replaces z_3/α_R^3 in eq 5.20. This suggests that α_R near Θ should read

$$\alpha_R^5 - \alpha_R^3 = \frac{4}{3}Z \tag{5.22}$$

where

$$Z = z_2 + 4\left(\frac{n}{\sigma}\right)^{1/2} z_3 \tag{5.23}$$

In eq 5.22, we have replaced the numerical coefficient $(2\pi/3)^{1/2}$ by 4/3. In the vicinity of $\alpha_R = 1$, this equation gives $\alpha_R^2 = 1 + (4/3)Z - (8/3)Z^2 + \ldots$, whereas eq 5.20 leads to $\alpha_R^2 = 1 + (4/3)Z - (8/3)Z^2 - (32/3)(n/\sigma)^{1/2} z_3 Z + \ldots$ if the coefficient $(2\pi/3)^{1/2}$ is again replaced with 4/3. Hence, the difference between these equations appears in the second and higher orders of z_3 in the expansion.

To confirm the relevance of eq 5.22 near Θ, we

have made a second-order perturbation calculation of α_R^2 for an infinitely long chain (see Appendix C), with the result that

$$\alpha_R^2 = 1 + \frac{4}{3}Z - (\frac{16}{3} - \frac{28}{27}\pi)Z^2 + \ldots \qquad (5.24)$$

This expression is in line with the Z-expansion of eq 5.22, leading to the conclusion that the uniform expansion approximation is invalid near Θ. This should also be the case for A_2.

Equations 5.22 and 5.24 are formally identical, respectively, to the modified Flory equation (eq 5.22 with $Z = z_2$) and the z_2 expansion of α_R^2 (eq 5.24 with $Z = z_2$), both in the binary cluster approximation (see ref 2). If, as often assumed in the vicinity of Θ, β_2 varies linearly with $1/T$ while β_3 is independent of T,[3] the relation $Z = \text{const } M^{1/2}(1 - \Theta/T)$ holds in a fixed solvent at temperatures close to Θ. It is also formally equivalent to the relation $z_2 = \text{const } M^{1/2}(1 - \Theta/T)$ (in the binary cluster approximation) that is often assumed in discussing polymer properties very near Θ.[2,3,52] As T is removed from Θ, however, the relation $Z = \text{const } M^{1/2}(1 - \Theta/T)$ should become inadequate and z_3 in eq 5.23 may be expected to approach z_3/α_R^3 eventually.

As discussed by de Gennes[75] and Ptitsyn,[76] the Orofino-Flory type equation 5.21 for α_R (or more correctly for α_S) predicts a coil-globule transition to occur in a single chain far below Θ, provided that $d_2 z_3$ is larger than a certain positive value. However, this prediction is no longer correct, since the theory ignores the effect of chain connectivity on segment density distribution. For $\alpha_R \ll 1$, our equation 5.20 gives $\alpha_R{}^3 = -4(n/\sigma)^{1/2} z_3/z_2$, which is independent of molecular weight. This result is incompatible with the prevailing notion[77,78] that a long flexible chain should collapse to a globule far below Θ. Probably, we should take into account segment interactions higher than the ternary one to discuss the dimensions of a collapsed coil. Sanchez's theory[79] incorporates such interactions but neglects chain connectivity.

In conclusion, the factorization approximation to segment density distribution functions associated with three-segment interactions is responsible for the inconsistency of the OF smoothed-density theories for A_2 and α_R with the first-order perturbation calculations. Thus, the OF theories or similar mean-field theories[14,75,76] retain no valid place near Θ unless β_3 is zero.

Appendix C

Second-Order Perturbation Calculation of α_R^2 for an Infinitely Long Flexible Chain

When both β_2 and β_3 are vanishingly small, the cluster expansion method[2] allows the distribution function $P(R)$ to be written

$$P(R) = P_0(R) + \beta_2 \sum_{i<j} Q_0(R,0_{ij}) + \beta_3 \sum_{i<j<k} Q_0(R,0_{ij},0_{jk})$$

$$- \beta_2^2 \sum_{\substack{i<j \\ i<k}} \sum_{k<s} Q_0(R,0_{ij},0_{ks})$$

$$- \beta_2\beta_3 \sum_{i<j} \sum_{s<t<u} Q_0(R,0_{ij},0_{st},0_{tu})$$

$$- \beta_3^2 \sum_{\substack{i<j<k \\ i<s}} \sum_{s<t<u} Q_0(R,0_{ij},0_{jk},0_{st},0_{tu})$$

$$+ O(\beta_2^3, \beta_2^2\beta_3, \beta_2\beta_3^2, \beta_3^3) \qquad \text{(C-1)}$$

where

$$Q_0(R,0_{ij},0_{st},0_{tu}) = P_0(R)P_0(0_{ij},0_{st},0_{tu})$$

$$- P_0(R,0_{ij},0_{st},0_{tu}) + P_0(R,0_{ij})P_0(0_{st},0_{tu})$$

$$+ P_0(R,0_{st},0_{tu})P_0(0_{ij})$$

$$- 2P_0(R)P_0(0_{ij})P_0(0_{st},0_{tu}) \qquad \text{(C-2)}$$

$$Q_0(R,0_{ij},0_{jk},0_{st},0_{tu}) = P_0(R)P_0(0_{ij},0_{jk},0_{st},0_{tu})$$

$$- P_0(R,0_{ij},0_{jk},0_{st},0_{tu}) + P_0(R,0_{ij},0_{jk})P_0(0_{st},0_{tu})$$

$$+ P_0(R,0_{st},0_{tu})P_0(0_{ij},0_{jk})$$

$$- 2P_0(R)P_0(0_{ij},0_{jk})P_0(0_{st},0_{tu}) \qquad \text{(C-3)}$$

and the other Q_0's are given in ref 2 or 12; the subscript 0 attached to each function refers to the unperturbed state.

The distribution functions in eqs C-2 and C-3 were evaluated by the Wang-Uhlenbeck-Fixman theorem.[2] The results allow α_R^2 for large n to be expressed as

$$\alpha_R^2 = 1 + (4/3)[z_2 + 4(n/\sigma)^{1/2}z_3] - C_1 z_2^2 - Iz_2 z_3$$

$$- Jz_3^2 + \ldots \qquad \text{(C-4)}$$

Here,

$$I = 2(I_1 + I_2 + I_3) + I_4 + 2I_5 + I_6 \qquad \text{(C-5)}$$

$$J = J_1 + J_2 + 2J_3 + 2J_4 + J_5 + 2J_6 + J_7 \qquad \text{(C-6)}$$

$$I_p = \frac{1}{n^{3/2}} \sum_{i,j,s,t,u} \{E_p - \frac{j - i + u - s}{[(j - i)(t - s)(u - t)]^{3/2}}\}$$

$$(p = 1 - 6) \qquad \text{(C-7)}$$

$$J_p = \frac{1}{n} \sum_{i,j,k,s,t,u} \{F_p - \frac{k - i + u - s}{[(j - i)(k - j)(t - s)(u - t)]^{3/2}}\}$$

$$(p = 1 - 7) \qquad \text{(C-8)}$$

and $C_1 = (\frac{16}{3} - \frac{28}{27}\pi)$;[2] we note that the factor 2 in eqs C-5 and C-6 arises from identical contributions from different cases of relative positions of segments in the chain and that E_p and F_p come from the first two terms on the right-hand sides of eqs C-2 and C-3. The expressions for E_p and F_p are so lengthy that we here present only those contributing to I_p and J_p in the limit of $n = \infty$, along with the restrictions on the sums in eqs C-7 and C-8. They are

$$E_2 = \frac{(j - i)(t - s)(u - j + s - i) - (u - t)(j - s)^2}{(u - t)^{3/2}[(j - i)(t - s) - (j - s)^2]^{5/2}}$$

$$(i < s < j < t < u)$$

$$E_3 = \frac{(j-t)(u-j)(u-s) + (s-i)(u-t)(u-i)}{(t-s)^{3/2}[(u-t)(j-i-t+s) - (j-t)^2]^{5/2}}$$

$(i < s < t < j < u)$

$$E_4 = \frac{j-i}{[(t-s)(u-t)(j-i-u+s)]^{3/2}}$$

$(i < s < t < u < j)$

$$E_5 = \frac{u-s}{[(j-i)(u-t)(t-s-j+i)]^{3/2}}$$

$(s < i < j < t < u)$

$$F_2 = \frac{(k-j)(t-s)(u+s-i-k) - (k-s)^2(j-i+u-t)}{[(j-i)(u-t)]^{3/2}[(k-j)(t-s) - (k-s)^2]^{5/2}}$$

$(i < j < s < k < t < u)$

$$F_3 = \frac{(k-t)(u-k)(j-i+u-s) + (s-j)(u-t)(u-i)}{[(j-i)(t-s)]^{3/2}[(k-j-t+s)(u-t) - (k-t)^2]^{5/2}}$$

$(i < j < s < t < k < u)$

$$F_4 = \frac{k-i}{[(j-i)(t-s)(u-t)(k-j+s-u)]^{3/2}}$$

$(i < j < s < t < u < k)$

$$F_7 = \frac{(j-t)[(s-i)(k-i)+(u-k)(u-i)]+(s-i)(u-k)(u-i)}{[(k-j)(t-s)]^{3/2}[(u-t-k+j)(j-i-t+s)-(j-t)^2]^{5/2}}$$

$$(i < s < t < j < k < u)$$

After lengthy calculations, we obtain for infinite n

$$I_2 = I_3 = 8(1 - \frac{7\pi}{27})(\frac{n}{\sigma})^{1/2}$$

$$I_4 = 2I_5 = \frac{16}{3}(\frac{n}{\sigma})^{1/2}$$

$$J_2 = J_3 = J_7 = 16(1 - \frac{7\pi}{27})(\frac{n}{\sigma})$$

$$J_4 = \frac{32}{3}(\frac{n}{\sigma})$$

Upon substitution into eqs C-5 and C-6, these expressions yield $I = 8C_1(n/\sigma)^{1/2}$ and $J = 16C_1(n/\sigma)$, so that we arrive at eq 5.24.

Chapter VI

Summary and Conclusions

This thesis has dealt with A_2 and A_3 for polystyrene (PS) and polyisobutylene (PIB), typical linear flexible polymers, in good and theta solvents and with the related theories. The main results and conclusions are summarized below.

Good Solvent Systems (Chapter III)

The second and third virial coefficients for PS in benzene and PIB in cyclohexane, both at 25°C, were determined by light scattering as functions of M_w, using the plot of Bawn et al.,[23] the most reliable method among the currently available ones. We also determined $\langle S^2 \rangle_z$ for the two good solvent systems. In both systems, A_3 varies as $M_w^{0.6}$ for $M_w \gtrsim 10^5$. This exponent 0.6 is the asymptotic value predicted by the two-parameter theory. On the other hand, A_2 exhibits the predicted asymptotic behavior[2] ($A_2 \propto M_w^{-0.2}$) only at very high M_w, i.e., $M_w \gtrsim 10^7$ for PS and $M_w \gtrsim 3 \times 10^6$ for PIB.

The interpenetration functions Ψ (see eq 3.1) for the two systems are almost superimposed when plotted against the cube of the radius expansion factor, α_S^3, being consistent with the prediction from the two-parameter theory. For $\alpha_S^3 \gtrsim 7$, Ψ stays at 0.22 $\pm$ 0.02, which is close to the asymptotic value 0.235 predicted by Barrett's theory[39] (the latest two-parameter theory) for large α_S^3. However, with a decrease in α_S^3 below 7, the experimental curve gradually rises, whereas Barrett's theoretical curve or those from any other two-parameter theories decline[2,3] toward zero.

For either system, the reduced third virial coefficient g defined by $A_3/A_2^2 M_w$ depends on M_w; as M_w increases, it increases to 0.45 - 0.50 after passing through a shallow minimum of about 0.25 at $M_w \sim 10^5$. When plotted against α_S^3, the values of g for PS and PIB also form a composite curve, as required by the two-parameter theory. For $\alpha_S^3 > 2$, this experimental relation is reasonably well described by the two-parameter theory of Stockmayer and Casassa[24] based on the smoothed-density model. However, the agreement is due primarily to the cancellation of theoretical defects involved in A_2 and A_3. Further, as α_S^3 approaches unity, the theoretical g goes to zero, while the exper-

imental g slightly increases. This discrepancy is similar to what is observed for Ψ, indicating that something important is overlooked in the two-parameter theories of both A_2 and A_3 in good solvents.

Theta Solvent Systems (Chapters IV and V)

Two theta solvent systems, PS in cyclohexane and in trans-decalin, were studied and their A_2 and A_3 were determined as functions of M_w and temperature T. The curve of A_3 vs. T for each fraction in either solvent is nearly parabolic with a broad minimum around the theta point Θ where A_2 vanishes, and the minimum becomes very shallow as M_w decreases. Importantly, A_3 remains positive at Θ, being about 4.5×10^{-4} mol g^{-3} cm^6 for $2 \times 10^4 \lesssim M_w \lesssim 4 \times 10^5$ in both systems. This positive A_3 reveals the breakdown of the two-parameter theory at Θ, since the theory predicts that A_2 and A_3 simultaneously vanish at this temperature.

The theta point for PS in cyclohexane is 34.5°C down to $M_w \sim 5 \times 10^4$ and tends to lower as M_w is further decreased, while in trans-decalin, it increases from 21 to 23°C when M_w is lowered below 4×10^5. Thus, A_2 at Θ_∞ (Θ for sufficiently high molecular weight samples) is positive below $M_w \sim 2 \times 10^4$ in

cyclohexane and negative below $M_w \sim 4 \times 10^5$ in trans-decalin. The Orofino-Flory smoothed-density theory[11] taking into account three-segment interactions is consistent with the former finding. On the other hand, the first-order perturbation theory[12,15] incorporating such interactions almost quantitatively explains the latter finding. In other words, neither theory can explain consistently the observed behavior of A_2 for PS in the two theta solvents.

The two types of theory mentioned above are inconsistent with each other and give different interpretations of Θ_∞, the concept most basic to polymer solution studies. Thus, the origin of this serious inconsistency was investigated in this work (Chapter V). It is shown that the factorization approximation to segment density distribution functions, invoked in the Orofino-Flory smoothed-density theory, is responsible for the inconsistency and that a proper treatment of those distribution functions leads to a result consistent with the first-order perturbation calculation. Thus, unless three-segment interactions are negligible, the Orofino-Flory theory widely accepted and appreciated so far retains no valid place. Its prediction of the coil-globule transition in a single chain far below Θ has no theoretical significance.

To sum up, this thesis work has revealed serious shortcomings of the current theories of polymer virial coefficients. In good solvents, the two-parameter theory appears to work well only for long chains. This suggests that for such chains binary interactions predominate over ternary ones. On the other hand, in theta solvents, the two-parameter theory breaks down regardless of chain length, and consideration of three segment interaction is mandatory. We wish to emphasize from the experimental point of view that the present work has established a procedure of accurately determining A_2 and A_3 in theta solvents as well as in good solvents.

References

1. P. J. Flory, *Principle of Polymer Chemistry*, Cornell University Press, Ithaca, New York, 1953.
2. H. Yamakawa, *Modern Theory of Polymer Solutions*, Harper & Row, New York, 1971.
3. H. Fujita, *Polymer Solutions*, Elsevier, Amsterdam, 1990.
4. Z. Tong, S. Ohashi, Y. Einaga, and H. Fujita, The Second Virial Coefficient of Monodisperse Polystyrene in Cyclohexane below the Theta Point, *Polym. J.*, 15, 835 - 843 (1983).
5. N. Takano, Y. Einaga, and H. Fujita, Phase Equilibrium in the Binary System Polyisoprene + Dioxane, *Polym. J.*, 17, 1123 - 1130 (1985).
6. R. Perzynski, M. Delsanti, and M. Adam, Experimental Study of Polymer Interactions in a Bad Solvent, *J. Phys. (Paris)*, 48, 115 - 124 (1987).
7. K. Huber and W. H. Stockmayer, Osmotic Second Virial Coefficient and Two-Parameter Theories, *Macromolecules*, 20, 1400 - 1402 (1987).
8. T. Konishi, T. Yoshizaki, T. Saito, Y. Einaga, and H. Yamakawa, Mean-Square Radius of Gyration of Oligo- and Polystyrenes in Dilute Solutions,

Macromolecules, 23, 290 - 297 (1990).

9. Y. Tamai, T. Konishi, Y. Einaga, M. Fujii, and H. Yamakawa, Mean-Square Radius of Gyration of Oligo- and Poly(methylmethacrylate)s in Dilute Solutions, *Macromolecules*, 23, 4067 - 4075 (1990).

10. K. Huber, S. Bantle, P. Lutz, and W. Burchard, Hydrodynamic and Thermodynamic Behavior of Short-Chain Polystyrene in Toluene and Cyclohexane at 34.5°C, *Macromolecules*, 18, 1461 - 1467 (1985).

11. T. A. Orofino and P. J. Flory, Relationship of the Second Virial Coefficient to Polymer Chain Dimensions and Interaction Parameters, *J. Chem. Phys.*, 26, 1067 - 1076 (1957).

12. H. Yamakawa, Three-Parameter Theory of Dilute Polymer Solutions, *J. Chem. Phys.*, 45, 2606 - 2617 (1966).

13. T. Oyama and Y. Oono, Three-Body Intrachain Collisions in a Single Polymer Chain, *J. Phys. Soc. Japan*, 42, 1348 - 1354 (1977).

14. F. Tanaka, Theory of the Second Virial Coefficients in Polymeric Solutions below the Theta Temperature, *J. Chem. Phys.*, 82, 4707 - 4714 (1985).

15. B. J. Cherayil, J. F. Douglas, and K. F. Freed, Effect of Residual Interactions on Polymer

Properties near the Theta Point, *J. Chem. Phys.*, 83, 5293 - 5310 (1985).

16. B. Duplantier, Geometry of Polymer Chains near the Theta-Point and Dimensional Regularization, *J. Chem. Phys.*, 86, 4233 - 4244 (1987).

17. G. Allegra and F. Ganazzori, Chain Configurations and Dynamics in the Gaussian Approximation, *Adv. Chem. Phys.*, 75, 265 - 348 (1989).

18. B. H. Zimm, Application of the Methods of Molecular Distribution to Solutions of Large Molecules, *J. Chem. Phys.*, 14, 164 - 179 (1946).

19. W. R. Krigbaum and P. J. Flory, Statistical Mechanics of Dilute Polymer Solutions. IV. Variation of the Osmotic Second Coefficient with Molecular Weight, *J. Am. Chem. Soc.*, 75, 1775 - 1784 (1953).

20. T. Ohta and Y. Oono, Conformation Space Renormalization Theory of Semidilute Polymer Solutions, *Phys. Lett.*, 89A, 460 - 464 (1982).

21. L. Schäfer, Osmotic Pressure of Dilute and Semidilute Polymer Solutions: A Comparison between a New Calculation and Old Experiments, *Macromolecules*, 15, 652 - 660 (1982).

22. R. Kniewske and W. M. Kulicke, Study on the Molecular Weight Dependence of Dilute Solution Proper-

ties of Narrowly Distributed Polystyrene in Toluene and in the Unperturbed State, *Makromol. Chem.*, **184**, 2173 - 2186 (1983).

23. C. E. H. Bawn, R. F. J. Freeman, and A. R. Kamaliddin, High Polymer Solutions Part II. — The Osmotic Pressures of Polystyrene Solutions, *Trans. Faraday Soc.*, **46**, 862 - 872 (1950).

24. W. H. Stockmayer and E. F. Casassa, The Third Virial Coefficient in Polymer Solutions, *J. Chem. Phys.*, **20**, 1560 - 1566 (1952).

25. E. F. Casassa and W. H. Stockmayer, Thermodynamic Properties of Dilute Solutions of Polymethyl Methacrylate in Butanone and in Nitroethane, *Polymer*, **3**, 53 - 69 (1962).

26. T. Sato, T. Norisuye, and H. Fujita, Second and Third Virial Coefficients for Binary Polystyrene Mixtures in Benzene, *J. Polym. Sci.: Part B: Polym. Phys.*, **25**, 1 - 17 (1987).

27. P. J. Flory and H. Daoust, Osmotic Pressures of Moderately Concentrated Polymer Solutions, *J. Polym. Sci.*, **25**, 429 - 440 (1957).

28. P. J. Flory, Thermodynamics of High Polymer Solutions, *J. Chem. Phys.*, **10**, 51 - 61 (1942).

29. M. L. Huggins, Solutions of Long Chain Compounds, *J. Chem. Phys.*, **9**, 440 (1941).

30. W. R. Krigbaum and D. O. Geymer, Thermodynamics of Polymer Solutions. The Polystyrene - Cyclohexane System near the Flory Theta Temperature, *J. Am. Chem. Soc.*, 81, 1859 - 1868 (1959).

31. H. Vink, Precision Measurements of Osmotic Pressure in Concentrated Polymer Solutions - II, *Europ. Polym. J.*, 10, 149 - 156 (1974).

32. H. G. Elias, Theta Solvents, in *Polymer Handbook Third Ed.*, J. Brundrup and E. H. Immergut, Eds., Wiley-Interscience, New York, 1989.

33. Y. Miyaki, Dilute Solutions of Polystyrene over a Very Wide Range of Molecular Weight, Ph. D. Thesis, Osaka University, 1981.

34. H. Murakami, T. Norisuye, and H. Fujita, Ultracentrifugal Evaluation of Chemical Potentials for the System Poly(chloroprene) - Methyl Ethyl Ketone, *Polym. J.*, 7, 248 - 258 (1975).

35. T. Matsumoto, N. Nishioka, and H. Fujita, Excluded-Volume Effects in Dilute Polymer Solutions. IV. Polyisobutylene, *J. Polym. Sci.: A-2*, 10, 23 - 42 (1972).

36. A. Yamamoto, M. Fujii, G. Tanaka, and H. Yamakawa, More on the Analysis of Dilute Solution Data: Polystyrenes Prepared Anionically in Tetrahydrofuran, *Polym. J.*, 2, 799 - 811 (1971).

37. M. Fukuda, M. Fukutomi, Y. Kato, and T. Hashimoto, Solution Properties of High Molecular Weight Polystyrene, *J. Polym. Sci.: Polym. Phys. Ed.*, **12**, 871 - 890 (1974).

38. Y. Miyaki, Y. Einaga, and H. Fujita, Excluded-Volume Effects in Dilute Polymer Solutions. 7. Very High Molecular Weight Polystyrene in Benzene and Cyclohexane, *Macromolecules*, **11**, 1180 - 1186 (1978).

39. A. J. Barrett, Second Osmotic Virial Coefficient for Linear Excluded Volume Polymers in the Domb-Joice Model, *Macromolecules*, **18**, 196 - 200 (1985).

40. R. Koyama, Theory of Dilute Polymer Solutions, *J. Chem. Phys.*, **27**, 234 - 239 (1957).

41. H. Yamakawa, Third Virial Coefficient of Polymer Solutions, *J. Chem. Phys.*, **42**, 1764 - 1771 (1965).

42. A. Knoll, L. Schäfer, and T. A. Witten, The Thermodynamic Scaling Function of a Polymer Solution, *J. Phys. (Paris)*, **42**, 767 - 781 (1981); see ref 21.

43. J. des Cloizeaux and I. Noda, Osmotic Pressure of Long Polymers in Good Solvents at Moderate Concentrations: A Comparison between Experiments and Theory, *Macromolecules*, **15**, 1505 - 1507 (1982).

44. J. F. Douglas and K. F. Freed, Renormalization and

the Two-Parameter Theory. 2. Comparison with Experiment and Other Two-Parameter Theories, *Macromolecules*, 18, 201 - 211 (1985).

45. Gj. Deželić and J. Vavra, Angular Dependence of the Light Scattering in Pure Liquids, *Croat. Chem. Acta*, 38, 35 - 47 (1966).

46. D. N. Rubingh and H. Yu, Characterization of Stiff Chain Macromolecules. Poly(n-hexyl isocyanate) in n-Hexane, *Macromolecules*, 9, 681 - 685 (1976).

47. Th. G. Scholte, Determination of Thermodynamic Parameters of Polymer-Solvent Systems from Sedimentation-Diffusion Equilibrium in the Ultracentrifuge, *J. Polym. Sci.: A-2*, 8, 841 - 868 (1970).

48. G. V. Schulz and M. Hoffmann, Scheinbares und Partielles Spezifisches Volumen von Polystyrol und Polymethylmethacrylat in Organischen Lösungsmitteln, *Makromol. Chem.*, 23, 220 - 232 (1957).

49. Z. Tong, Y. Einaga, T. Kitagawa, and H. Fujita, Phase Equilibrium in Polymer-Polymer-Solvent Ternary Systems. 4. Polystyrene + Polyisobutylene in Cyclohexane and in Benzene, *Macromolecules*, 22, 450 - 457 (1989).

50. B. H. Zimm, The Scattering of Light and the Radial Distribution Function of High Polymer Solutions,

J. Chem. Phys., **16**, 1093 - 1116 (1948).

51. T. Norisuye and H. Fujita, The Third Virial Coefficient for Linear Flexible Polymers, *Chemtracts*, in press.

52. G. C. Berry, Thermodynamic and Conformational Properties of Polystyrene. I. Light-Scattering Studies on Dilute Solutions of Linear Polystyrenes, *J. Chem. Phys.*, **44**, 4550 - 4564 (1966).

53. T. Kitagawa, J. Sadanobu, and T. Norisuye, Chain Stiffness and Excluded-Volume Effects in Dilute Polymer Solutions. Poly(isophthaloyl-trans-2,5-dimethylpiperazine), *Macromolecules*, **23**, 602 - 607 (1990).

54. L. J. Fetters, N. Hadjichristidis, J. S. Lindner, J. W. Mays, and W. W. Wilson, Transport Properties of Polyisobutylene in Dilute Solution, *Macromolecules*, **24**, 3127 - 3135 (1991).

55. C. Domb and A. J. Barrett, Universality Approach to the Expansion Factor of a Polymer Chain, *Polymer*, **17**, 179 - 184 (1976).

56. M. Lax, A. J. Barrett, and C. Domb, Polymer Chain Statistics and Universality I, *J. Phys. A: Math. Gen.*, **11**, 361 - 374 (1978); A. J. Barrett and C. Domb, Statistical Properties of a Polymer Chain in the Two-Parameter Approximation, *Proc. Roy.*

Soc. London, **A376**, 361 - 375 (1981).

57. Y. Miyaki, Y. Einaga, T. Hirosye, and H. Fujita, Solution Properties of Poly(D-β-hydroxybutyrate). 2. Light Scattering and Viscosity in Trifluoroethanol and Behavior of Highly Expanded Polymer Coils, *Macromolecules*, **10**, 1356 - 1364 (1977).

58. T. Hirosye, Y. Einaga, and H. Fujita, Excluded-Volume Effects in Dilute Polymer Solutions. VIII. Poly(D,L-β-methyl β-propiolactone) in Several Solvents and Reanalysis of Data on Poly(D-β-hydroxybutyrate), *Polym. J.*, **11**, 819 - 826 (1979).

59. H. Fujita and T. Norisuye, Molecular Weight Dependence of the Second Virial Coefficient for Linear Flexible Polymers in Good Solvents, *Macromolecules*, **18**, 1637 - 1638 (1985).

60. E. F. Casassa and H. Markovitz, Statistical Thermodynamics of Polymer Solutions. I. Theory of the Second Virial Coefficient for a Homogeneous State, *J. Chem. Phys.*, **29**, 493 - 503 (1958).

61. P. J. Flory, The Configuration of Real Polymer Chains, *J. Chem. Phys.*, **17**, 303 - 310 (1949).

62. Y. Miyaki and H. Fujita, Excluded-Volume Effects in Dilute Polymer Solutions. 11. Tests of the Two-Parameter Theory for Radius of Gyration and Intrinsic Viscosity, *Macromolecules*, **14**, 742 - 746

(1981).

63. P. J. Flory and W. R. Krigbaum, Statistical Mechanics of Dilute Polymer Solutions. II, *J. Chem. Phys.*, 18, 1086 - 1094 (1950).

64. T. Konishi, T. Yoshizaki, and H. Yamakawa, On the "Universal Constants" ρ and Φ of Flexible Polymers, *Macromolecules*, 24, 5614 - 5622 (1991).

65. H. Inagaki, H. Suzuki, M. Fujii and T. Matsuo, Note on Experimental Tests of Theories for the Excluded Volume Effect in Polymer Coils, *J. Phys. Chem.*, 70, 1718 - 1726 (1966).

66. T. Nose and B. Chu, Static and Dynamical Properties of Polystyrene in trans-Decalin. 1. NBS 705 Standard Near Θ Conditions, *Macromolecules*, 12, 590 - 599 (1979).

67. S. -J. Chen and G. C. Berry, Moderately Concentrated Solutions of Polystyrene: 4. Elastic and Quasi-Elastic Light Scattering at the Flory Theta Temperature, *Polymer*, 31, 793 - 804 (1990).

68. M. Janssens and A. Bellemans, On the Osmotic Second Virial coefficient of Polymer Solutions, *Macromolecules*, 9, 303 - 307 (1976).

69. A. Baumgätner, Statics and Dynamics of the Freely Jointed Polymer Chain with Lennard-Jones Interaction, *J. Chem. Phys.*, 72, 871 - 879 (1980).

70. W. Bruns, The Ideal and the Pseudoideal State of Macromolecules: A Comparison, *Macromolecules*, **17**, 2826 - 2830 (1984).

71. H. Yato and H. Okamoto, Vanishing of the Chain Length Dependence of the Second Virial Coefficient Zero Point for Lattice Polymers, *Macromolecules*, **23**, 3459 - 3463 (1990).

72. O. Kratky and G. Porod, Röntgenuntersuchung Gelöster Fadenmoleküle, *Rec. Trav. Chim.*, **68**, 1106 - 1122 (1949).

73. H. Yamakawa and W. H. Stockmayer, Statistical Mechanics of Wormlike Chains. II. Excluded Volume Effects, *J. Chem. Phys.*, **57**, 2843 - 2854 (1972).

74. J. J. Hermans and J. Th. G. Overbeek, The Dimensions of Charged Long Chain Molecules in Solutions Containing Electrolytes, *Rec. Trav. Chim.*, **67**, 761 - 776 (1948).

75. P. G. de Gennes, Collapse of a Polymer Chain in Poor Solvents, *J. Phys. Lett. (Paris)*, **36**, L55 - L57 (1975).

76. O. B. Ptitsyn, A. K. Kron, and Yu. Ye. Eizner, The Models of the Denaturation of Globular Proteins. I. Theory of Globula-Coil Transitions in Macromolecules, *J. Polym. Sci., Part C*, **16**, 3509 - 3517 (1968).

77. W. H. Stockmayer, Problems of the Statistical Thermodynamics of Dilute Polymer Solutions, *Makromol. Chem.*, 35, 54 - 74 (1960).

78. C. Williams, F. Brochard, and H. L. Frisch, Polymer Collapse, *Ann. Rev. Phys. Chem.*, 32, 433 - 451 (1981).

79. I. C. Sanchez, Phase Transition Behavior of the Isolated Polymer Chain, *Macromolecules*, 12, 980 - 988 (1979).

List of Abbreviations and Symbols

PIB	polyisobutylene
PS	polystyrene
A_2	second virial coefficient
$A_2(\Theta_\infty)$	second virial coefficient at the theta point Θ_∞ for sufficiently high molecular weight samples
A_3	third virial coefficient
$A_3(\Theta)$	third virial coefficient at the theta point Θ
A_4	fourth virial coefficient
b	segment length
c, c_1, c_2	polymer mass concentration
c^*	overlap polymer mass concentration
g	reduced third virial coefficient defined by eq 1.3
$G(0; t)$	probability of contact of the two beads separated by the contour distance t along the contour of a wormlike chain
$I_{\theta,\mathrm{Uv}}$	scattering intensity measured at a scattering angle θ with a vertically oriented polarizer and no analyzer
k_B	Boltzmann constant

K	light-scattering optical constant defined by eq 2.9
L	contour length of a chain
M	molecular weight of a monodisperse polymer
M_{app}	apparent molecular weight defined by eq 2.17
M_n	number-average molecular weight
M_v	viscosity-average molecular weight
M_w	weight-average molecular weight
n	refractive index of a solution (Chapter II) or segment number in a chain (Chapters III, IV, and V)
n_b	refractive index of benzene
Δn	excess refractive index
N_A	Avogadro constant
$P(\theta)$	intramolecular scattering factor
$P(R)$	distribution function of the end-to-end distance R
$P_0(R)$	$P(R)$ for an unperturbed chain
$P_0(R_{ij}, 0_{kl}, \ldots, 0_{uv})$	multivariate distribution function for segment distances $R_{ij}, R_{kl}, \ldots, R_{uv}$ where 0_{kl}, for example, signifies that $R_{kl} = 0$.
$P_{i_1}(s)$	distribution function of the distance s between the center of mass and i_1th segment in a chain 1

$P_{0i_1}(s)$ $P_{i_1}(s)$ in the unperturbed state

$P_{i_1j_1}(s,s)$

bivariate probability density of finding i_1th and j_1th segments of a chain 1 at distance s from the center of mass

$P_{ij}(s,s|R)$, $P_{ijk}(s,s,s|R)$

conditional probability density of finding ith and jth or ith, jth, and kth segments of a chain at distance s from the center of mass under the condition that the end-to-end distance R is fixed.

$P_{0ij}(s,s|R)$, $P_{0ijk}(s,s,s|R)$

$P_{ij}(s,s|R)$ or $P_{ijk}(s,s,s|R)$ in the unperturbed state

Q $\equiv [(Kc/R_0) - (1/M_w)]/c^2$

$Q_i(\theta)$ $(i = 2.3)$

intermolecular interference factor associated with i polymer chains

$R_{b,Uu}$ Rayleigh ratio of benzene at 90° for unpolarized light

$R_{\theta,Uv}(c)$ reduced scattering intensity measured at scattering angle θ for a solution of concentration c with a vertically oriented polarizer and no analyzer

R_θ excess scattering intensity at scattering angle θ defined by $R_{\theta,Uv}(c) - R_{\theta,Uv}(0)$

R_0 R_θ at zero scattering angle

R end-to-end vector of a chain

R_{ij} distance vector between segments i and j

$\langle S^2 \rangle$ mean-square radius of gyration

$\langle S^2 \rangle_z$ z-average mean-square radius of gyration

$\langle S^2 \rangle_0$ $\langle S^2 \rangle$ in the unperturbed state

$\langle S^2 \rangle_{0z}$ $\langle S^2 \rangle_z$ in the unperturbed state

$S(c) \equiv [(Kc/R_0) - (1/M_w)]/c$

$$S(c_1, c_2) \equiv \frac{(Kc/R_0)_{c=c_2} - (Kc/R_0)_{c=c_1}}{c_2 - c_1}$$

S_{12} distance between the centers of mass of two chains

$\langle S_{i_1}^2 \rangle$ mean-square distance between the center of mass of a chain 1 and its i_1th segment

T temperature

$V(R)$ average intramolecular potential of mean force under the condition that the end-to-end vector is fixed to R

$V_{12}(S_{12})$ average intermolecular potential of mean force on two chains 1 and 2 under the condition that the distance between their centers of mass has a given value S_{12}

w	polymer weight fraction
$W(R_{12})$	potential of mean force acting on segments 1 and 2
z_2	excluded-volume parameter for binary segment interactions, defined by eq 3.5
z_3	excluded-volume parameter for ternary segment interactions, defined by eq 4.3
Z	effective excluded-volume parameter defined by eq 5.22
α	expansion factor
α_R	end-distance expansion factor
α_S	radius expansion factor
β_2	binary cluster integral
β_3	ternary cluster integral
ε	parameter in renormalization group methods
$[\eta]$	intrinsic viscosity
θ	scattering angle
Θ	theta temperature
Θ_∞	theta temperature for sufficiently long chains
λ	wavelength of light in scattering medium
λ_0	wavelength of light in vacuum
ρ	solution density
ρ_0	solvent density

ρ_u	depolarization ratio
σ	cut-off parameter
Φ	instrument constant of light scattering photometer
Ψ	interpenetration function defined by eq 3.1

List of Publications

Part of this thesis has been or will be published in the following papers

1. Third Virial Coefficient of Polystyrene in Benzene, Y. Nakamura, T. Norisuye, and A. Teramoto, *J. Polym. Sci: Part B: Polymer Physics*, **29**, 153 (1991).

2. Second and Third Virial Coefficients for Polystyrene in Cyclohexane near the Θ Point, Y. Nakamura, T. Norisuye, and A. Teramoto, *Macromolecules*, **24**, 4904 (1991).

3. Second and Third Virial Coefficients for Polyisobutylene in Cyclohexane, Y. Nakamura, K. Akasaka, K. Katayama, T. Norisuye, and A. Teramoto, *Macromolecules*, **25**, xxxx (1992).

4. Remarks on Smoothed-Density Theories for Flexible Chains with Three-Segment Interactions, T. Norisuye and Y. Nakamura, in preparation.

5. Second and Third Virial Coefficients for Polystyrene in trans-Decalin near the Θ Point, Y. Nakamura, T. Norisuye, and A. Teramoto, in preparation.